98-620

Direction Finding of Ionospheric Scattering Sources For Vortex Antenna System

by

Alex To, Max Wong, Yan Meng

Communication Research Laboratory

McMaster University

Hamilton, Ontario

Work performed for the Defence Research Establishment Ottawa

FINAL REPORT FOR RESEARCH
CONTRACT W7714-5-99925

Direction Finding of Ionospheric Scattering Sources For Vortex Antenna System

by

Alex To, Max Wong and Yan Meng

Communications Research Laboratory

McMaster University

Hamilton, Ontario

Canada L8S 4K1

Work performed for the
Defence Research Establishment Ottawa
Contract Scientific Authority: W.J.L. Read

105-03432/

Direction Finding (DF) of Ionospheric Scattering Source for Vortex Antenna System

Final Report

by

A.TO, K.M.WONG, Y.MENG
Communications Research Laboratory, McMaster University
Hamilton, Ont. L8S 4K1, CANADA

TITLE:	Direction Finding (DF) of Ionospheric Scattering Source for Vortex Antenna System
AUTHOR:	Alex K.H. TO Dr. K.M. WONG Dr. Y. MENG
NUMBER OF PAGES:	x, 125

Preface

Since the introduction of the Multiple Signals Classification (MUSIC) algorithm in 1980s, it has become the best known and the most widely investigated Direction Finding (DF) method in array signal processing. However, it is based on the assumption that the signals are generated (or reflected) by point sources and are propagated through a non-dispersive medium. Such an assumption is not valid in many practical situations. One example is high frequency (HF) radio communications through ionospheric scattering.

In the last few years, a library of HF measurement data has been collected by Defence Research Establishment in Ottawa (DREO) to investigate the ionospheric scattering problem. When MUSIC was applied to this data, the results were quite disappointing: the estimated angles exhibit large unacceptable fluctuations. On the other hand, the Advanced Signal Processing Group under the direction of Dr. K.M. Wong has recently developed several powerful methods to estimate the DOAs of dispersed signals. Among these methods, DISPARE I, DISPARE II, MUSIC DISC and BF DISC require moderate computation load which would make them appropriate for the HF task. Additionally, both theoretical calculations and computer simulations show that these methods give better estimates than MUSIC when dealing with dispersed signals.

Naturally, the most logical step was to study whether these newly developed DF methods could really solve the problem of estimating DOAs of ionospheric scattering signals. This report describes in details the theoretical background, the tests performed, the results obtained and the conclusions that were made.

Acknowledgement

We would like to express our sincere thanks to Mr. W. Read, who provided a list of data in Matlab format for our testing. He also gave us inspiring suggestions from time to time.

We would like to acknowledge the support from the Department of Electrical and Computer Engineering by providing the computing facilities. We would also like to acknowledge the financial support from DREO.

Contents

List of Tables viii

List of Figures x

1 Introduction **1**

1.1 Objective 1

1.2 Array Geometry 2

1.3 Input Data 3

1.4 Validity of the Input Data 4

1.5 Notation and Glossary 12

2 Signal Model and DF Methods **14**

2.1 Signal Model for Point Source 14

2.2 General Signal Model for Distributed Source 16

2.3 MUSIC 17

2.4 Effective Signal Dimension 19

2.4.1 Effective Signal Dimension and Notation 19

2.4.2 Approach to Estimate $\hat{M}_0$ 21

2.5 Dispersive Methods 22

2.5.1 DISPAREs 22

2.5.2 DISCs 24

3 Approximated Models and Direction Finding Approaches **26**

3.1 Approximated Models for Uniform Distribution 26

3.1.1 Model 1a: Dispersive Azimuth / Non-Dispersive Elevation 26

3.1.2 Model 1b: Dispersive Azimuth / Multiple Elevation Layers 29
3.1.3 Model 2: Multiple Points Approximation 30
3.2 Approaches for Estimating $\hat{\bar{\theta}}$ 32
3.2.1 Assume $\hat{\bar{\phi}} = \hat{\alpha}_\phi$ 32
3.2.2 Approach 1: 2-D Search on $\bar{\theta}$ and α_θ, Pre-determined $\hat{\alpha}_\phi$ 32
3.2.3 Approach 2: 2-D Search on $\bar{\theta}$ and α_θ, $\hat{\alpha}_\phi = \frac{1}{2}\hat{\alpha}_\theta$ 33
3.2.4 Approach 3: 1-D Search on $\bar{\theta}$ 34
3.3 Plots of Cost Function Values 36
3.4 Testing of Models and Approaches 49
3.4.1 Testing of the Approximated Signal Models 49
3.4.2 Testing of Approaches 55
3.4.3 Computation Load 58

4 Distribution Types and Combinations **59**
4.1 Distribution Types 59
4.2 Testing of Distribution Types 63
4.3 Combination of Dispersive Methods 70

5 Fine Tuning of Parameter Settings **73**
5.1 Grid Density 73
5.2 Effective Signal Dimension 76
5.2.1 Parameter Settings in Estimating $\hat{M}_0$ 76
5.2.2 Testing 77
5.3 Spread 90
5.3.1 Four Approaches to Estimate $\hat{\alpha}_\theta$ 90
5.3.2 Testing 92

6 Changing M and K **99**
6.1 Changing the Number of Sensors M 99
6.2 Changing the Number of Signals K 103
6.2.1 Narrower Passing Band 103
6.2.2 Changing K for MUSIC 106

6.2.3 Assume Multiple Signals for Dispersive Methods 110

7 Conclusion **113**

7.1 Achievement 113

7.2 The Best Achieved Results 115

7.3 Conclusion 124

List of Tables

1.1 Data Files 12

3.1 Settings and Results of Experiment 3.1 38
3.2 Model 1a, Approach 1 52
3.3 Model 1b, Approach 1 53
3.4 Model 2, Approach 1 54
3.5 Approach 2, Model 2 56
3.6 Approach 3, Model 2 57
3.7 cpu Time Required 58

4.1 Distribution Type 1 64
4.2 Distribution Type 2 65
4.3 Distribution Type 3 66
4.4 Distribution Type 4 67
4.5 Distribution Type 5 68
4.6 Distribution Type 6 69
4.7 Combination of Multiple Dispersive Methods 72

5.1 Grid Density Type 2 75
5.2 $\hat{M}_0$ Estimated from $\{\tilde{\lambda}\}$ 79
5.3 $\hat{M}_0$ Estimated from both $\{\hat{\lambda}\}$ and $\{\tilde{\lambda}\}$ 80
5.4 cp = 4 81
5.5 cp = 2 82
5.6 cp = 0 83

5.7 cv = 90% 84
5.8 cv = 85% 85
5.9 cv = 80% 86
5.10 $\hat{M}_0 = 2$ 87
5.11 $\hat{M}_0 = 4$ 88
5.12 $\hat{M}_0 = 6$ 89
5.13 $\hat{\alpha}_\theta$ Limited by $\hat{M}_0$ 93
5.14 $\hat{\alpha}_\theta$ Estimated from $\hat{m}_0$ 94
5.15 $\hat{\alpha}_\theta = 5^0$ 95
5.16 $\hat{\alpha}_\theta = 10^0$ 96
5.17 $\hat{\alpha}_\theta = 15^0$ 97
5.18 $\hat{\alpha}_\theta = 20^0$ 98

6.1 Number of Sensor $M = 10$ 101
6.2 Number of Sensor $M = 8$ 102
6.3 Narrower bandwidth, cv = 95% 104
6.4 Narrower bandwidth, cv = 90% 105
6.5 MUSIC, $K = 2$ 107
6.6 MUSIC, $K = 3$ 108
6.7 MUSIC, $K = 4$ 109
6.8 Dispersive Methods, $\hat{m}_0 = \hat{M}_0 - 1$ 111
6.9 Dispersive Methods, $\hat{m}_0 = \frac{\hat{M}_0}{2}$ 112

7.1 Comparison of the Best Achieved Results 116

List of Figures

1.1 Vortex Antenna Array Configuration 2
1.2 FFT Frequency Spectrums 5

2.1 Definitions of θ and ϕ 15

3.1 Frobenius Norm of Difference of Covariances 31
3.2 $\hat{\theta}$ and $\hat{\phi}$ from MUSIC 33
3.3 Eigenvalues at various $\bar{\theta}$ and α_θ 35
3.4 Plots of MUSIC Cost Function Values 39
3.5 Plots of DISPARE I Cost Function Values 41
3.6 Plots of DISPARE II Cost Function Values 43
3.7 Plots of MUSIC DISC Cost Function Values 45
3.8 Plots of BF DISC Cost Function Values 47

4.1 Weighting Functions for Different Distribution Types 62
4.2 Cost Function Values for Different Methods and Combinations 71

7.1 Plots of the Estimated Azimuth Angles 117

Chapter 1

Introduction

1.1 Objective

Currently, the Multiple Signals Classification (MUSIC) method is employed to estimate the Directions of Arrival (DOAs) of ionospheric scattering signals collected by the Vortex system. However, the estimated angles often exhibit large fluctuations, which is not desirable. One probable reason is that MUSIC (as well as other conventional Direction Finding methods) assumes a perfect reflection of the signal off the ionosphere (i.e. point source), which is far from being true.

The objective of this project is to use some newly developed parametric methods to estimate the DOAs of ionospheric scattering signals, with the hope that more consistent and accurate estimates can be achieved. Unless otherwise stated, we assume there is only one signal in the frequency band of interest. As such, we bypass the detection of the number of signals.

This is the final report for this project.

1.2 Array Geometry

The Vortex system consists of 12 antennas, 8 of which are shared with another High Frequency Direction Finding (HFDF) system. These 8 antennas are part of a circular ring of 24 antennas, but the 8 antennas are not evenly spaced around the ring. The 4 remaining antennas are outriggered to give the antenna system a larger aperture. The array geometry is illustrated in Figure 1.1.[1]

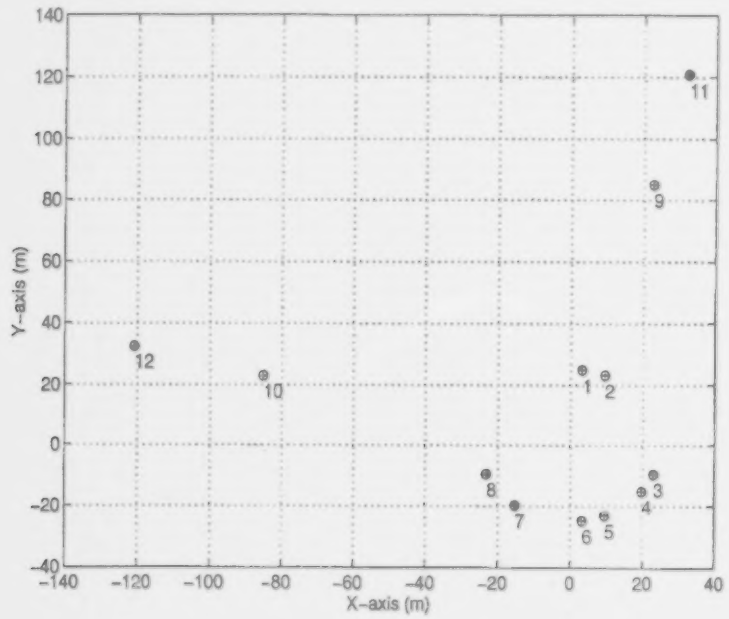

Figure 1.1: Vortex Antenna Array Configuration

The antenna plane (x-y plane) is parallel to the ground. The y-axis is aligning with the geographic North. The origin is at the centre of the 8-antenna circular ring.

[1]The array shown here is rotated by 90^0 from the one presented in the April report. We believe that this one is correct as it is derived directly from the MATLAB file.

1.3 Input Data

For each data collection, a calibration was also performed. The calibration consisted of measuring the phase and the amplitude differences among the 12 channels. However, it did not quantify the effects of antenna mislocations nor mutual coupling. In other words, the array manifold had not been measured.

A list of data was collected in March 1995. The data was analog down-converted and bandpass filtered, such that a Radio Frequency (RF) signal was converted to an Intermediate Frequency (IF) signal with a bandwidth of 3 kHz centered at 2.5 kHz. The analog IF signal was then digitized at a sampling rate of 10 kHz. The conversion was done on all 12 channels simultaneously. The digital data was stored in a real format (rather than an IQ format) on tapes for later off-line processing. This was the raw data we processed in this project.

The estimated covariance $\hat{\boldsymbol{R}}$ was computed from the raw data using the following approach:-

Step 1 Apply the Fast Fourier Transform (FFT) to the data to convert it from the time domain to the frequency domain.

Step 2 Zero all frequency data outside the band of interest: 1.0 kHz – 4.0 kHz.

Step 3 Multiply the data by the calibration matrix.

Step 4 Compute the estimated covariance matrix $\hat{\boldsymbol{R}}$ directly from the frequency domain data.

As the estimated covariance matrix $\hat{\boldsymbol{R}}$ was the only information required by the methods studied in this project, no conversion of the frequency domain data back to the time domain was required. Later on this report when we quote the cpu time spent by certain method, the time measurement starts after $\hat{\boldsymbol{R}}$ has been determined.

1.4 Validity of the Input Data

We were given with 27 data files. The filename format of the data files was "xxx_yn.mat". The first three letters "xxx" indicate the transmitter station (e.g. cfh means the signal was coming from Halifax). The letter "y" differentiates the data from different tape files (which were collected in different time). It starts with "a", and then "b", "c" and so on. The integer "n" locates the consecutive 64K samples block of the tape file. We received 3 consecutive data files derived from the original tape file vcs_a, and 4 consecutive data files for all other tape files. To simplify the notation, the name "xxx_y" was used to denote all the corresponding data files xxx_y1, xxx_y2 etc. of the same tape file.

Each data file contained 64K samples. Unless otherwise stated, we compute an $\hat{\boldsymbol{R}}$ based on an non-overlapping 8K samples block. As the sampling rate was 10 KHz, each $\hat{\boldsymbol{R}}$ was based on data collected within 1 second.

27 data files means that there are 216 sets of data. Of these 216 sets, 4 were corrupted: the frequency spectrum contained nothing except noise. The frequency spectrums of all data are shown in Fig.1.2(a)-(g). To simplify the figure, only the first spectrum of each tape file is bounded and scaled. The x-axis is in kHz and the y-axis is in normalized dB. "Normalized" means that the highest power is set to 0dB. All spectrums have the same scale. The invalid data sets are highlighted. All tests stated in this report used the 212 sets of uncorrupted data. We believe that such a trial size was large enough for estimation performance comparison purposes.

Table 1.1 lists the names and the transmitters of all the data files, as well as the locations of the corrupted data sets.

Figure 1.2: FFT Frequency Spectrums

(a) cfh_a

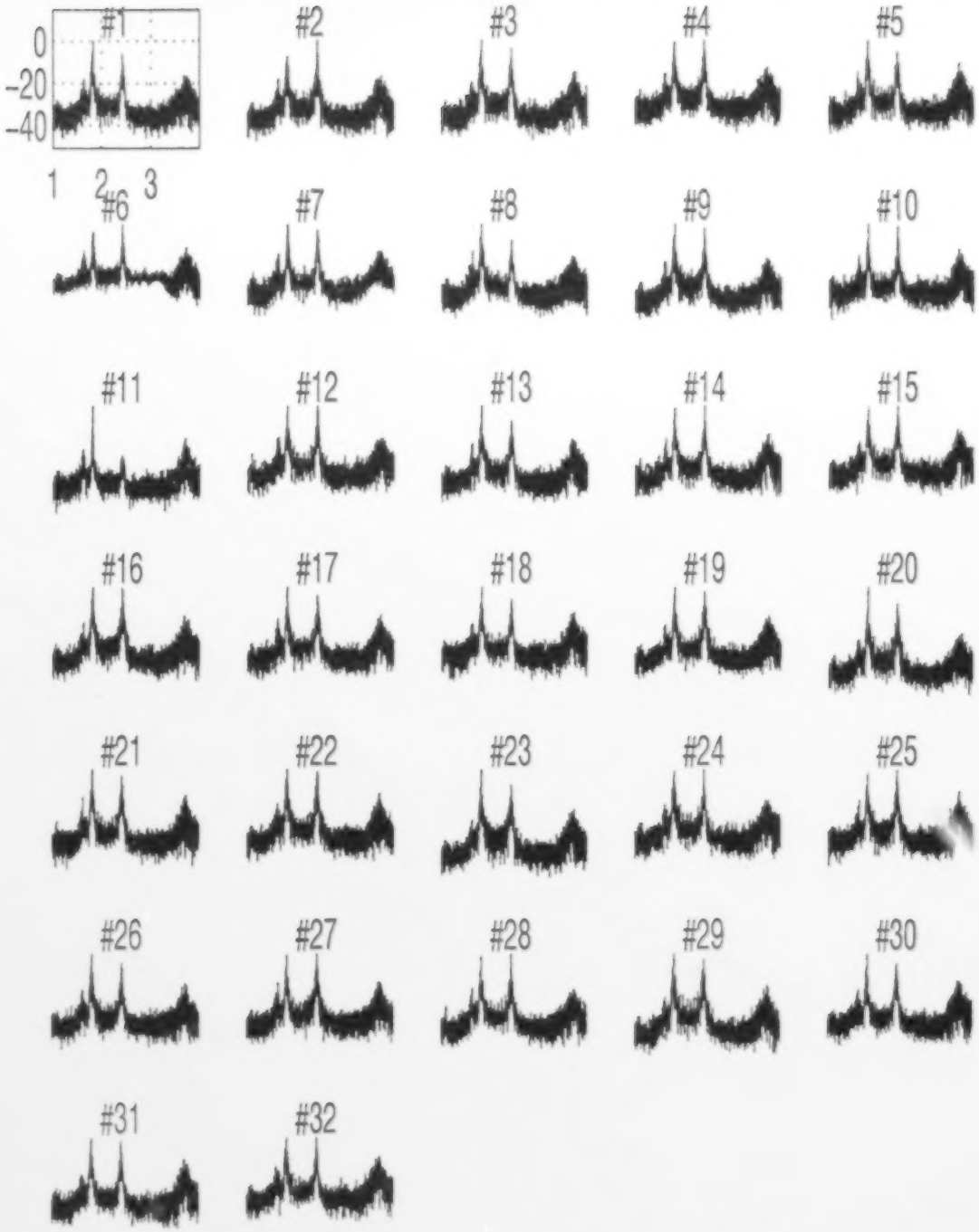

(b) iar_a

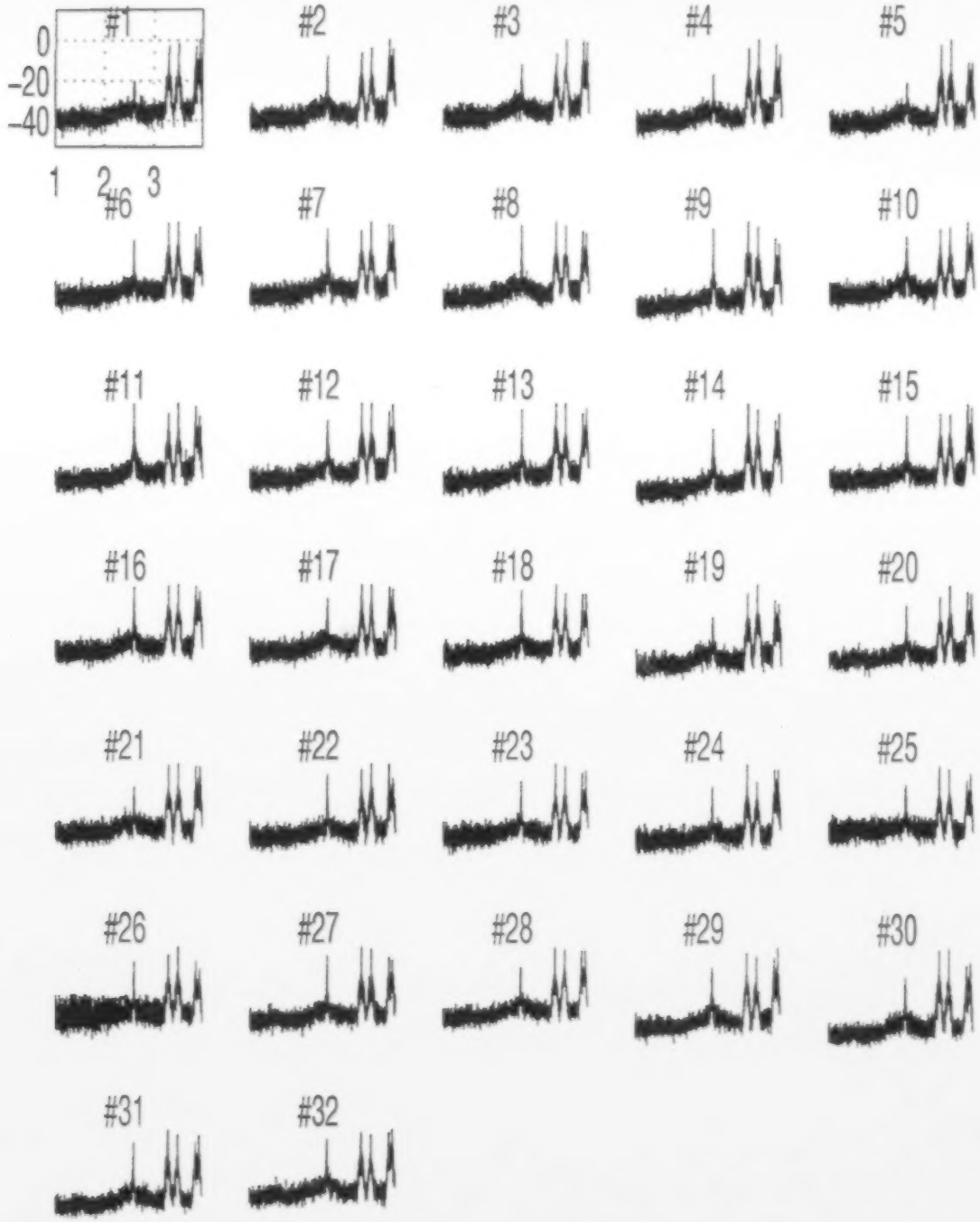
#1
0
-20
-40
1 2 3
#2
#3
#4
#5
#6
#7
#8
#9
#10
#11
#12
#13
#14
#15
#16
#17
#18
#19
#20
#21
#22
#23
#24
#25
#26
#27
#28
#29
#30
#31
#32

(c) vai_a

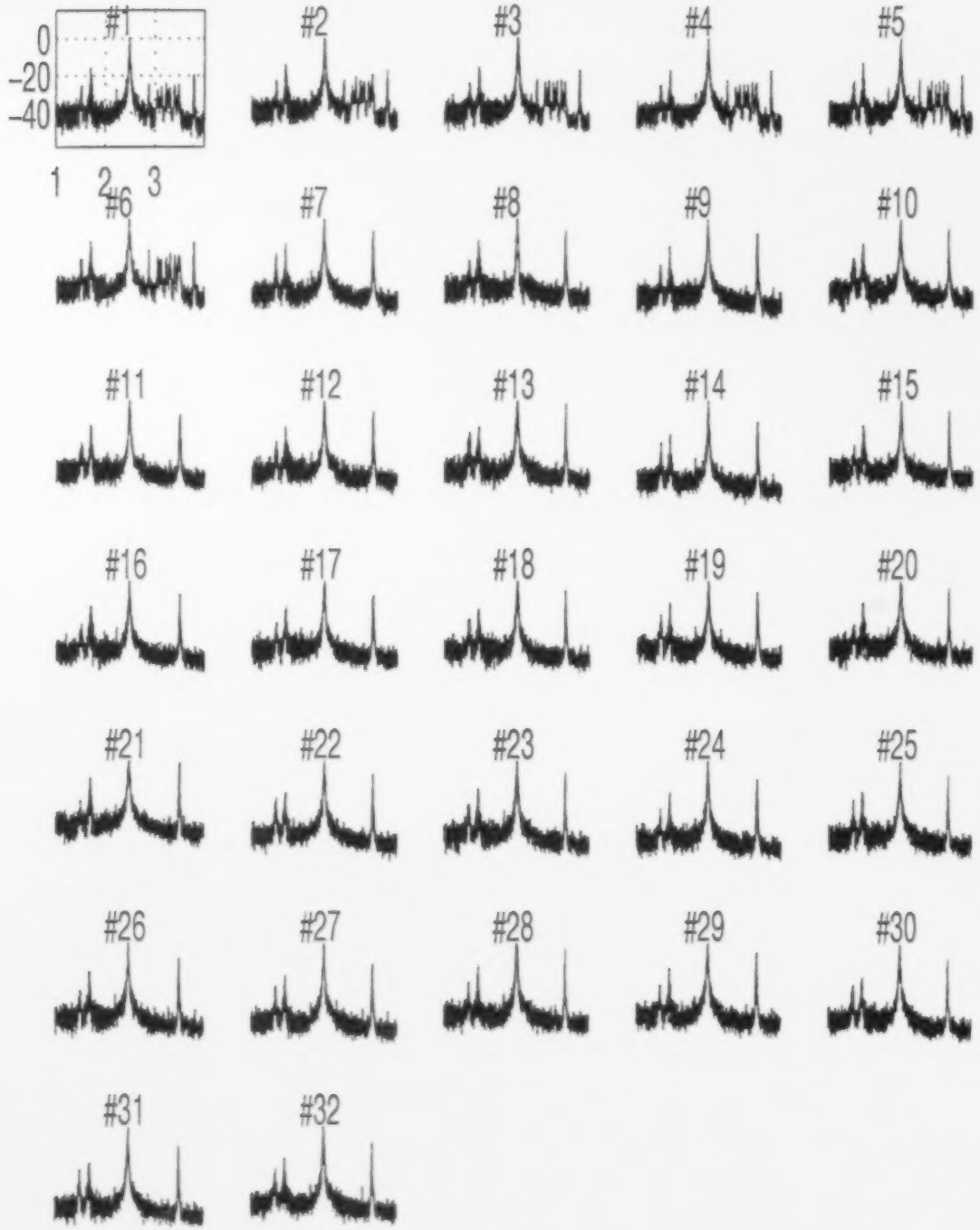
#1
0
-20
-40
1 2 3
#2
#3
#4
#5
#6
#7
#8
#9
#10
#11
#12
#13
#14
#15
#16
#17
#18
#19
#20
#21
#22
#23
#24
#25
#26
#27
#28
#29
#30
#31
#32

(d) vcs_a

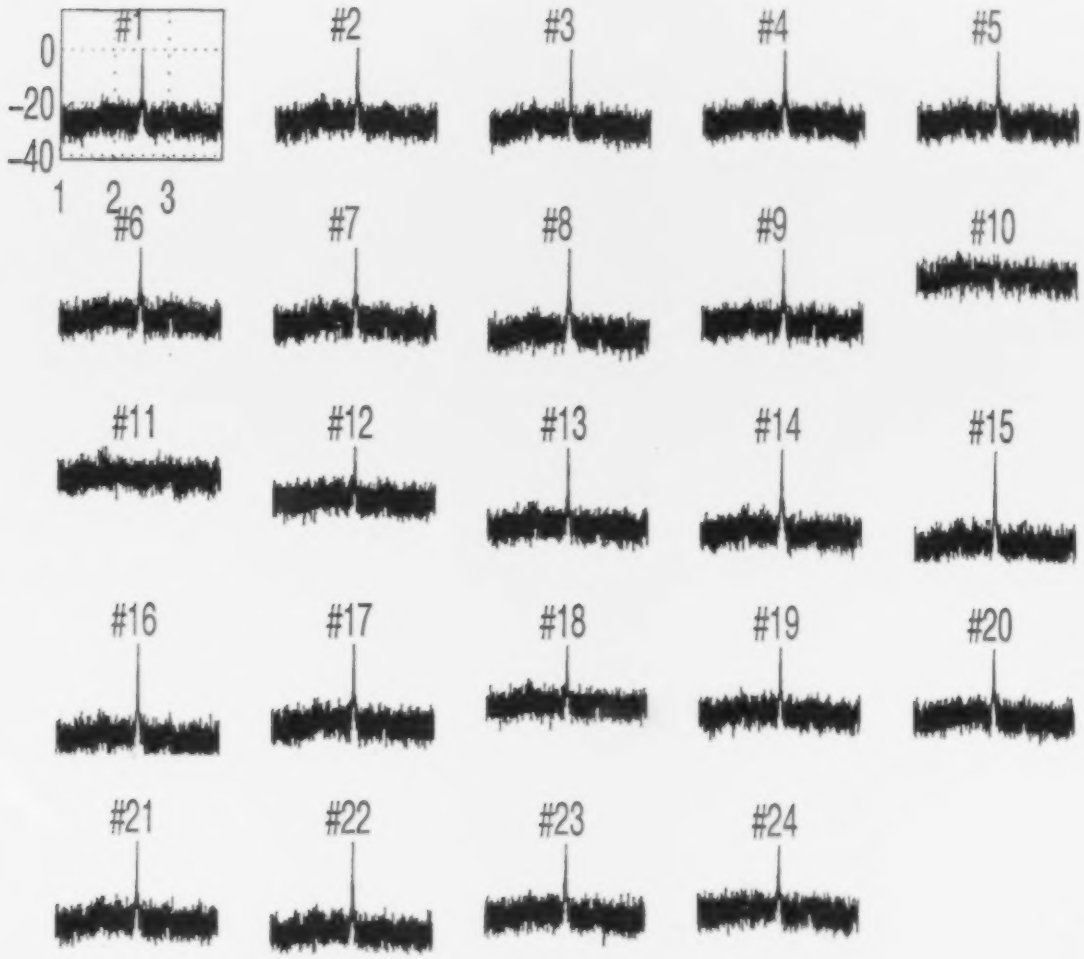

(e) vcs_b

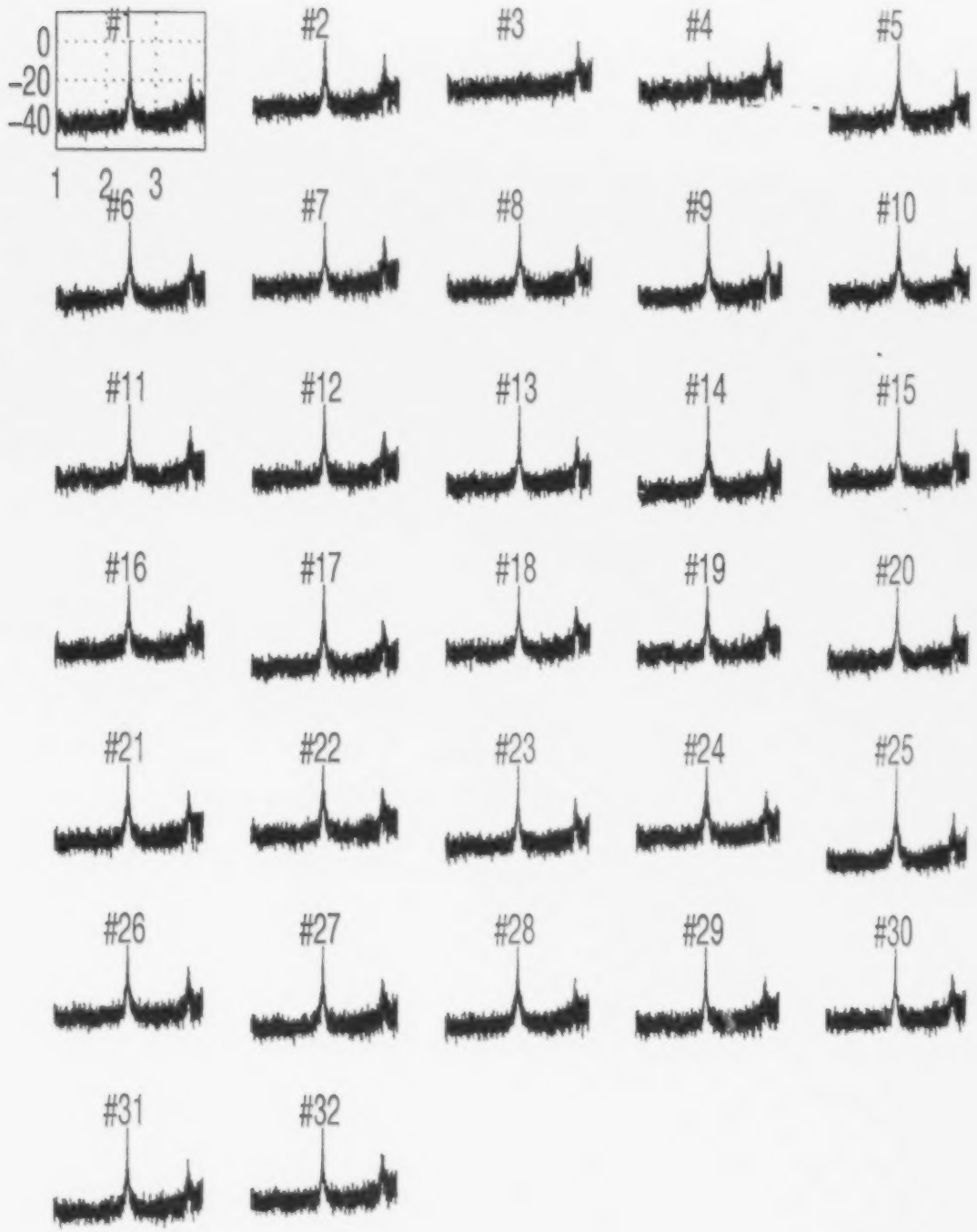
0
-20
-40
1
2
3
#1
#2
#3
#4
#5
#6
#7
#8
#9
#10
#11
#12
#13
#14
#15
#16
#17
#18
#19
#20
#21
#22
#23
#24
#25
#26
#27
#28
#29
#30
#31
#32

(f) vcs_c

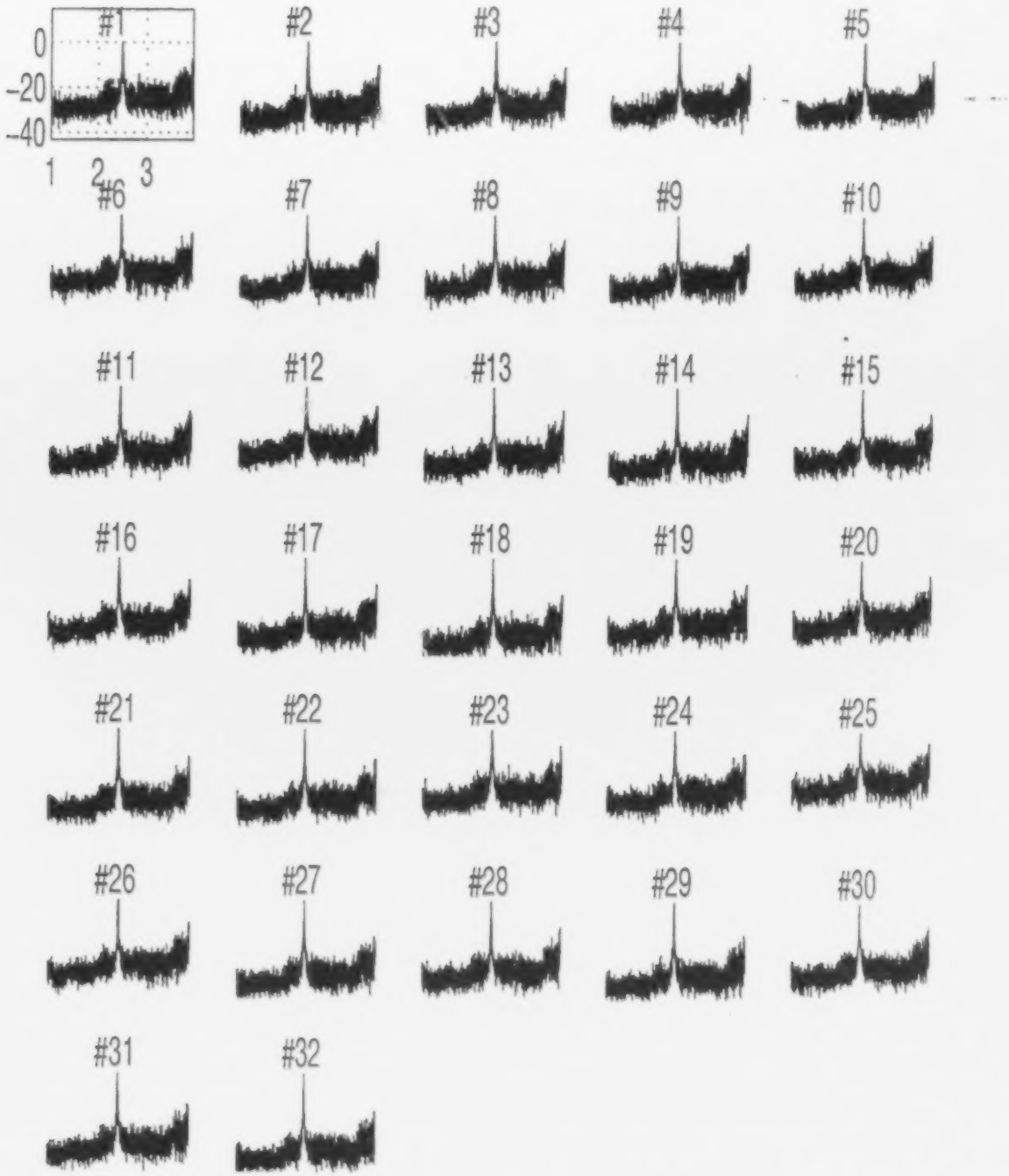
#1
0
-20
-40
1 2 3
#2
#3
#4
#5
#6
#7
#8
#9
#10
#11
#12
#13
#14
#15
#16
#17
#18
#19
#20
#21
#22
#23
#24
#25
#26
#27
#28
#29
#30
#31
#32

(g) vcs_d

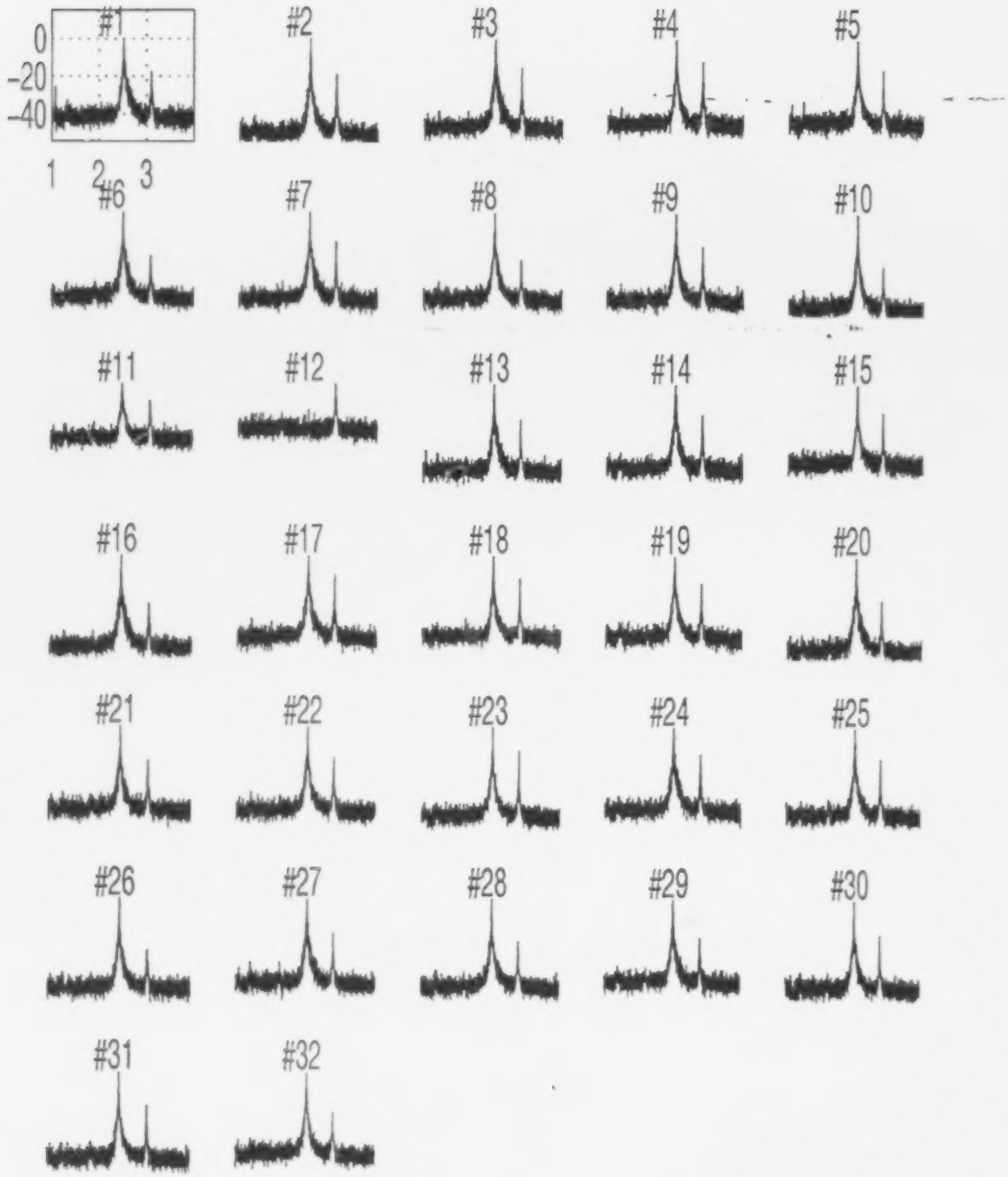
#1
0
-20
-40
1 2 3
#2
#3
#4
#5
#6
#7
#8
#9
#10
#11
#12
#13
#14
#15
#16
#17
#18
#19
#20
#21
#22
#23
#24
#25
#26
#27
#28
#29
#30
#31
#32

Table 1.1: Data Files

Filename	Simplified Name	Transmitter Location	Corrupted Data Set	# of Valid Data Set
cfh_a[1-4]	cfh_a	Halifax	Nil	32
iar_a[1-4]	iar_a	Italy	Nil	32
vai_a[1-4]	vai_a	Vancouver	Nil	32
vcs_a[1-3]	vcs_a	Halifax	#10, #11	22
vcs_b[1-4]	vcs_b	Halifax	#3	31
vcs_c[1-4]	vcs_c	Halifax	Nil	32
vcs_d[1-4]	vcs_d	Halifax	#12	31
			Total	212

1.5 Notation and Glossary

a, $\boldsymbol{a}$, $\boldsymbol{A}$	A value, a vector and a matrix respectively
$a_{m,n}$	The mnth element of $\boldsymbol{A}$
$\boldsymbol{A}^T$, $\boldsymbol{A}^\dagger$	The transpose and the conjugate transpose of $\boldsymbol{A}$ respectively
a^*	The conjugate of a
$\| \boldsymbol{A} \|_F$	The Frobenius norm of $\boldsymbol{A}$
$\mathrm{tr}(\boldsymbol{A})$	The trace of a square matrix $\boldsymbol{A}$: the sum of all diagonal elements of $\boldsymbol{A}$
$\lceil a \rceil$	The ceiling function of a: the smallest integer larger than or equal to a
$a_1 : a_2 : a_3$	A series of integers from a_1 to a_3 in step of a_2. If a_2 is omitted, the step size is by default equal to 1.
K	The number of signals, which is equal to one unless otherwise stated.
M	The number of antennas, which is equal to twelve unless otherwise stated.
θ_s	The suggested nominal azimuth angle of arrival, which is obtained by measuring

	the physical locations of the transmitter and the receiver.
θ	The azimuth angle of arrival of a point signal
ϕ	The elevation angle of arrival of a point signal
$\bar{\theta}$ / $\bar{\phi}$	The nominal azimuth / elevation angle of arrival of a dispersed signal
α_θ / α_ϕ	The half extension width of the azimuth / elevation angle of a dispersed signal. The signal power density is larger than zero within the boundary specified by these two parameters.
m_0	The effective signal dimension of a dispersed signal. It is also denoted as esd.
M_0	The total effective signal dimension, which is equal to the sum of all m_0. It is also denoted as tesd.
$\boldsymbol{R}$	Correlation matrix
$\boldsymbol{P}_S$ ($\boldsymbol{P}_N$)	Signal (Noise) subspace projector
λ/v	Eigenvalue / Eigenvector
$\boldsymbol{V}_S$ ($\boldsymbol{V}_N$)	Signal (Noise) eigenvector matrix
$\tilde{}$	A function value with parameters $\bar{\theta}$, $\bar{\phi}$, α_θ, α_ϕ and/or m_0
$\hat{}$	An estimated value computed from the observed data
Std. Dev.	The standard deviation of $\hat{\bar{\theta}}$. It measures the consistency of the estimates, and is one of the estimation performance indicators.
RMSE	The Root Mean Square Error of $\hat{\bar{\theta}}$ with respect to the suggested nominal azimuth angle θ_s. However, θ_s itself may not be true due to the random signal scattering in the ionosphere. Nevertheless, RMSE is another estimation performance indicator.

Chapter 2

Signal Model and DF Methods

2.1 Signal Model for Point Source

As the ionospheric scattering takes place far from the Vortex antenna array, the signal waves incident upon the array can be regarded as plane waves. The definitions of the azimuth angle θ and the elevation angle ϕ are illustrated in Fig.2.1. The azimuth angle θ is measured clockwise from the y-axis. The elevation angle ϕ is measured with respect to the x-y plane. Obviously, $\phi \geq 0$.

The coordinates of the mth antenna is denoted as (x_m, y_m). The time-delay, with respect to the origin, of the signal wavefront coming from a DOA of (θ, ϕ) is given by

$$\tau_m(\theta, \phi) = -\frac{1}{c}(x_m \sin\theta + y_m \cos\theta)\cos\phi \tag{2.1}$$

where c is the propagation velocity of the wavefronts. In the case of radio waves, $c = 3 \times 10^8$ m/s.

The corresponding shift in electrical angle is

$$\begin{aligned} \tau_{e,m}(\theta, \phi) &\triangleq -\omega_0 \, \tau_m(\theta, o) \\ &= \frac{\omega_0}{c}(x_m \sin\theta + y_m \cos\theta)\cos\phi \end{aligned}$$

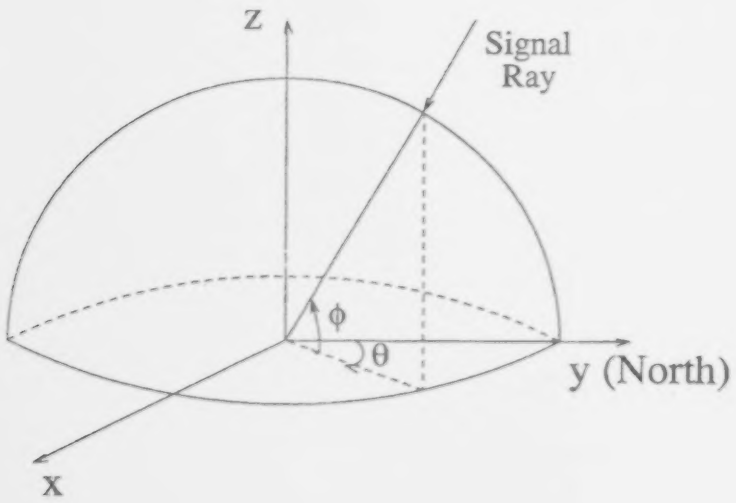

Figure 2.1: Definitions of θ and ϕ

$$= \frac{2\pi}{\lambda_0}(x_m \sin\theta + y_m \cos\theta)\cos\phi$$

where ω_0 is the carrier frequency and λ_0 is the signal wavelength.

If the coordinates (x_m, y_m) are expressed in units of λ_0, then

$$\tau_{e,m}(\theta,\phi) = 2\pi(x_m \sin\theta + y_m \cos\theta)\cos\phi \tag{2.2}$$

Thus, the mth element of the *steering vector* (array manifold) $\boldsymbol{d}$ is

$$d_m(\theta,\phi) = e^{j2\pi(x_m \sin\theta + y_m \cos\theta)\cos\phi} \tag{2.3}$$

From here onwards, the coordinates (x_m, y_m) are expressed in units of λ_0. In other words, even though employing the same physical Vortex array, the array geometries for signals of different wavelengths are different.

2.2 General Signal Model for Distributed Source

Given a narrow-band dispersed signal $s(t) = a(\theta, \phi, t)\, e^{j\omega_0 t}$, where $a(\theta, \phi, t)$ is the random complex envelope of a signal ray coming from (θ, ϕ), and ω_0 is the carrier frequency. The signal received at the mth antenna is

$$\begin{aligned} s_m(t) &\triangleq s(t - \tau_m) \\ &= \int_\Omega a(\theta, \phi, t)\, e^{j\omega_0 t}\, e^{j2\pi(x_m \sin\theta + y_m \cos\theta)\cos\phi}\, d\Omega \end{aligned} \tag{2.4}$$

where Ω is the solid angle subtended by the dispersed signal.

The correlation of the received signal between the mth and the nth antennas is

$$\begin{aligned} r_{mn} &\triangleq \mathrm{E}[s_m(t) s_n^*(t)] \\ &= \int_{\Omega_i}\int_{\Omega_j} \mathrm{E}[a(\theta_i, \phi_i, t) a^*(\theta_j, \phi_j, t)] \\ &\qquad e^{j2\pi(x_m \sin\theta_i + y_m \cos\theta_i)\cos\phi_i}\, e^{-j2\pi(x_n \sin\theta_j + y_n \cos\theta_j)\cos\phi_j}\, d\Omega_i\, d\Omega_j \end{aligned} \tag{2.5}$$

Assume the signal rays (of the same dispersed signal) coming from different directions are uncorrelated,

$$\begin{aligned} \mathrm{E}[a(\theta_i, \phi_i, t) a^*(\theta_j, \phi_j, t)] &= \mathrm{E}[|a(\theta_i, \phi_i, t)|^2]\, \delta_{ij} \\ &\triangleq p(\theta, \phi)\, \delta_{ij} \end{aligned} \tag{2.6}$$

where $p(\theta, \phi)$ is called the power density distribution function of the dispersed signal. This function is normalized so that

$$\int_\Omega p(\theta, \phi)\, d\Omega = 1 \tag{2.7}$$

Then, Eq.(2.5) can be simplified as

$$\begin{aligned} r_{mn} &= \int_\Omega p(\theta, \phi)\, e^{j2\pi[(x_m - x_n)\sin\theta + (y_m - y_n)\cos\theta]\cos\phi}\, d\Omega \\ &= \int_0^{\frac{\pi}{2}} \int_{-\pi}^{\pi} p(\theta, \phi)\, e^{j2\pi[(x_m - x_n)\sin\theta + (y_m - y_n)\cos\theta]\cos\phi}\, \cos\phi\, d\theta\, d\phi \end{aligned} \tag{2.8}$$

The last line is obtained using the relationship $d\Omega = \cos\phi \; d\theta \; d\phi$. Eq.(2.8) is called the *general signal model equation* since it does not depend on any particular power density distribution function nor any specific array geometry.

According to Eq.(2.8), the signal correlation matrix is determined by two factors: the power density distribution function $p(\theta, \phi)$ of the dispersed signal and the array geometry in units of λ_0. As the array geometry is known, by assuming a certain power density distribution type (say, uniform), $p(\theta, \phi)$ and thus r_{mn} can in general be characterized by 4 parameters: $\bar{\theta}, \bar{\phi}, \alpha_\theta$ and α_ϕ. The first two parameters denote the nominal angles of arrival and the last two parameters specify the dispersive region. The measurements made available by DREO indicate that both α_θ and α_ϕ are larger than 0.

Our target is to estimate the nominal azimuth angle of arrival $\bar{\theta}$ from the estimated correlation matrix $\hat{\boldsymbol{R}}$ of the observed data, given a particular antenna array geometry.

Example: $p(\theta, \phi)$ is uniformly distributed within a rectangular region and 0 otherwise. That is,

$$p(\theta,\phi) = \begin{cases} A_1 & |\theta - \bar{\theta}| \le \alpha_\theta \text{ and } |\phi - \bar{\phi}| \le \alpha_\phi \\ 0 & \text{elsewhere} \end{cases} \tag{2.9}$$

From Eq.(2.8), we have

$$r_{mn} = \int_{\bar{\phi}-\alpha_\phi}^{\bar{\phi}+\alpha_\phi} \int_{\bar{\theta}-\alpha_\theta}^{\bar{\theta}+\alpha_\theta} A_1 \; e^{j2\pi[(x_m - x_n)\sin\theta + (y_m - y_n)\cos\theta]\cos\phi} \; \cos\phi \; d\theta \; d\phi \tag{2.10}$$

It is difficult (if not impossible) to get an explicit form for the above integral, even using the simplest uniform distribution! In Section 3.1, we will approximate the integral by using some assumptions.

2.3 MUSIC

MUSIC stands for *MUltiple SIgnals Classification*. It was developed by R.O.Schmidt in 1979 [1].

Suppose we have K independent point signals with additive white Gaussian noise which is uncorrelated with the signals. The DOA of the kth signal is denoted as (θ_k, ϕ_k). The true covariance (or the covariance we expect if it is derived from an infinite number of data samples) will be given by

$$\boldsymbol{R} = \boldsymbol{D}\boldsymbol{P}\boldsymbol{D}^\dagger + \rho_\nu^2 \boldsymbol{I} \tag{2.11}$$

where $\boldsymbol{D}$ has K columns of steering vectors $\boldsymbol{d}(\theta_k, \phi_k)$ (from Eq.(2.3)),

$\boldsymbol{P}$ is a diagonal matrix with its elements equal to the signal powers, and

ρ_ν^2 is the noise power.

Denote λ_m and $\boldsymbol{v}_m$ $(m = 1, \ldots, M)$ as the eigenvalues and the corresponding eigenvectors of $\boldsymbol{R}$, with λ_m being sorted in descending order. By the definition of an eigenvalue and an eigenvector, we have

$$\begin{aligned}
\boldsymbol{R}\boldsymbol{v}_n &= \lambda_n \boldsymbol{v}_n \\
&= \rho_\nu^2 \boldsymbol{v}_n && \text{for } n = K+1, \ldots, M \\
\boldsymbol{D}\boldsymbol{P}\boldsymbol{D}^\dagger \boldsymbol{v}_n &= \boldsymbol{0} && \text{from Eq.(2.11)} \\
\boldsymbol{D}^\dagger \boldsymbol{v}_n &= \boldsymbol{0} && n = K+1, \ldots, M.
\end{aligned} \tag{2.12}$$

The last equation follows from the fact that $\boldsymbol{D}^\dagger\boldsymbol{D}$ and $\boldsymbol{P}$ are full rank matrices.

Eq.(2.12) indicates that each of the K steering vectors $\boldsymbol{d}(\theta_k, \phi_k)$ are orthogonal to all noise eigenvectors $\{\boldsymbol{v}_n\}_{n=K+1}^{M}$ of the matrix $\boldsymbol{R}$. The principle of the MUSIC algorithm is to determine the DOAs of the signals by searching for the steering vectors $\boldsymbol{d}(\theta_k, \phi_k)$, $k = 1, \ldots, K$, that are orthogonal to the noise subspace.

We define a noise subspace projector

$$\begin{aligned}
\boldsymbol{P}_N &\triangleq \boldsymbol{V}_N \left(\boldsymbol{V}_N{}^\dagger \boldsymbol{V}_N\right)^{-1} \boldsymbol{V}_N{}^\dagger \\
&= \boldsymbol{V}_N \boldsymbol{V}_N{}^\dagger && \text{as } \boldsymbol{v}_i{}^\dagger \boldsymbol{v}_j = \delta_{ij}
\end{aligned} \tag{2.13}$$

If $\boldsymbol{P}_N$ pre-multiplies any vector $\boldsymbol{x}$, the product will lie in the noise subspace spanned by the column vectors of $\boldsymbol{V}_N$. Thus if $\boldsymbol{P}_N$ pre-multiplies any vector in the signal subspace, the product will be $\boldsymbol{0}$.

As $\boldsymbol{d}(\theta,\phi)$ is in the signal subspace *if and only if* $(\theta,\phi)=(\theta_k,\phi_k)$, $k=1,\ldots,K$, thus

$$\| P_N\, \boldsymbol{d}(\theta,\phi) \| \begin{cases} = & 0 & \text{if } (\theta,\phi)=(\theta_k,\phi_k), \quad k=1,\ldots,K \\ \gg & 0 & \text{otherwise} \end{cases}$$

With a finite N, $\hat{\boldsymbol{R}}(N) \neq \boldsymbol{R}$. Accordingly, we do not know the true $\boldsymbol{P}_N$, but only the estimated $\hat{\boldsymbol{P}}_N$, thus we have

$$\| \hat{P}_N\, \boldsymbol{d}(\theta,\phi) \| \begin{cases} \approx & 0 & \text{if } (\theta,\phi)=(\theta_k,\phi_k), \quad k=1,\ldots,K \\ \gg & 0 & \text{otherwise} \end{cases} \tag{2.14}$$

We define the MUSIC cost function as

$$\begin{aligned} f_{MUSIC}(\theta,\phi) &\triangleq \|\hat{P}_N\, \boldsymbol{d}(\theta,\phi)\|^{-2} \\ &= [\text{tr}\ \{\boldsymbol{d}(\theta,\phi)\, \boldsymbol{d}^{\dagger}(\theta,\phi)\, \hat{P}_N\}\ ]^{-1} \end{aligned} \tag{2.15}$$

From the above discussion, we expect $f_{MUSIC}(\theta,\phi)$ to have sharp peaks at (θ_k,ϕ_k), $k=1,\ldots,K$. By plotting $f_{MUSIC}(\theta,\phi)$ against various θ and ϕ, we can estimate $\{\hat{\theta}\}$ as the x-ordinates of the K peaks.

2.4 Effective Signal Dimension

2.4.1 Effective Signal Dimension and Notation

Before describing other DF methods, we need to develop a concept of *effective signal dimension (esd)* for dispersed signal.

Let us denote $\boldsymbol{R}_k$ as the true covariance of the kth signal. In the point source case, the dimension of $\boldsymbol{R}_k$ is 1. Thus it can be completely represented by 1 eigenvector (i.e. the steering vector). In general, if there are K independent point sources, they can be represented by K eigenvectors. In practice, if the number of sensors M is larger than K, we can partition the

eigenvectors of the estimated covariance $\hat{R}$ and form two matrices: the one consists of the K eigenvectors corresponding to the K largest eigenvalues is called the signal eigenvector matrix; and the other one composes of the remaining $(M-K)$ eigenvectors is called the noise eigenvector matrix. This concept is used implicitly in the last section.

However, in the distributed source case, the true covariance $\boldsymbol{R}_k$ is already full rank: its dimension is equal to M. In strict sense, we need to use all the M eigenvectors to describe one dispersed signal. However, we know that $\alpha_{\theta,k}$ and $\alpha_{\phi,k}$ are not too large in practice. Under such circumstances, the eigenvalues of $\boldsymbol{R}_k$ diminish quickly. Thus, by tolerating a small amount of energy leakage, the signal dimension can be reduced to a smaller number m_{0k}, where $m_{0k} < M$. This number is called the effective signal dimension (esd) for $\boldsymbol{R}_k$. In this report, esd and m_0 are the same, and are used interchangeably. According to [3], the value of m_0 that produces the best estimate varies with different estimation methods. In all cases, it is much smaller than M for ranges of $\alpha_{\theta,k}$ and $\alpha_{\phi,k}$ of practical interest.

We define the total effective signal dimension (tesd) as

$$M_0 \triangleq \sum_{k=1}^{K} m_{0k} \tag{2.16}$$

If M is larger than M_0, then as in the point source case, we can classify the M eigenvectors into M_0 signal eigenvectors and $(M-M_0)$ noise eigenvectors[1]. They form the signal eigenvector matrix $\boldsymbol{V}_S$ and the noise eigenvector matrix $\boldsymbol{V}_N$ respectively. From these matrices, we can define the signal subspace projector $\boldsymbol{P}_S$ and the noise subspace projector $\boldsymbol{P}_N$. If the eigenvectors are sorted such that the corresponding eigenvalues are in descending order, then

$$\boldsymbol{V}_S \doteq [\boldsymbol{v}_1 \cdots \boldsymbol{v}_{M_0}] \tag{2.17}$$

$$\boldsymbol{V}_N \doteq [\boldsymbol{v}_{M_0+1} \cdots \boldsymbol{v}_M] \tag{2.18}$$

$$\boldsymbol{P}_S \doteq \boldsymbol{V}_S \boldsymbol{V}_S^\dagger \tag{2.19}$$

$$\boldsymbol{P}_N \doteq \boldsymbol{V}_N \boldsymbol{V}_N^\dagger \tag{2.20}$$

Finally, let us explain the notations $\hat{R}$ and $\bar{R}$. The former is the correlation matrix estimated

[1]Here, we tacitly assume that none of the eigenvalues of those noise eigenvectors is larger than that of signal eigenvectors. This is true for equal power sources

in practice from a finite number of snapshots of the observed signals. That is,

$$\hat{\boldsymbol{R}} = \frac{1}{N}\sum_{n=1}^{N} \boldsymbol{x}(n)\,\boldsymbol{x}(n)^{\dagger} \tag{2.21}$$

The latter is a model-derived correlation matrix depending on four parameters $(\bar{\theta}, \bar{\phi}, \alpha_\theta, \alpha_\phi)$ after assuming certain power density distribution type. That is, the r_{mn} in Eq.(2.5), Eq.(2.8) and Eq. 2.10) will be denoted as $\bar{r}_{mn}$ from here onwards.

From both $\hat{\boldsymbol{R}}$ and $\bar{\boldsymbol{R}}$, we have the corresponding $\boldsymbol{V}_S, \boldsymbol{V}_N, \boldsymbol{P}_S$ and $\boldsymbol{P}_N$.[2] To avoid confusion, $\hat{[\cdot]}$ means that it is derived from $\hat{\boldsymbol{R}}$; $\bar{[\cdot]}$ means that it is derived from $\bar{\boldsymbol{R}}$.

2.4.2 Approach to Estimate $\hat{M}_0$

As will be seen later, all the four dispersive methods require an estimate of $\hat{M}_0$ or $\hat{m}_0$. By assuming one dispersive signal, $\hat{M}_0 = \hat{m}_0$ according to Eq.(2.16). The following outlines the procedure to estimate them. More will be discussed in Section 5.2.

Step 1 Apply singular value decomposition on $\hat{\boldsymbol{R}}$ and get the estimated eigenvalues $\{\hat{\lambda}_i\}_{i=1}^{M}$. Sort the eigenvalues in descending order.

Step 2 In order to get rid of the noise effect, the noise power ρ_ν^2 is subtracted from $\{\hat{\lambda}_i\}$. It is a common practice to estimate the noise power by taking the average of several smallest eigenvalues. We use the average of the smallest 6 (i.e. $\frac{M}{2}$) eigenvalues as ρ_ν^2.

$$\begin{aligned} \hat{\lambda}_i &= \hat{\lambda}_i - \tfrac{1}{6}\textstyle\sum_{j=7}^{12}\hat{\lambda}_j \qquad \text{for } i = 1,\ldots,6 \\ \hat{\lambda}_i &= 0 \qquad\qquad\qquad\qquad\quad \text{for } i = 7,\ldots,12 \end{aligned}$$

The integer 6 is called the compensation (cp) factor as it compensates the noise effect. It is arbitrarily set to 6 here. Different cp factors will be tested in Section 5.2.

Step 3 Normalize the eigenvalues such that the sum equals 1.

$$\hat{\lambda}_i = \frac{\hat{\lambda}_i}{\sum_{j=1}^{12}\hat{\lambda}_j} \qquad i = 1,\ldots,12$$

[2] Similar to Eq.(2.17) to Eq.(2.20), $\bar{V}_{S,k}$ of $\bar{R}_k$ consists of m_0 (another parameter) signal eigenvectors as its columns, $\bar{V}_{N,k}$ consists of the remaining $(M - m_0)$ noise eigenvectors, $\bar{P}_{S,k}$ and $\bar{P}_{N,k}$ are defined accordingly.

Step 4 Estimate $\hat{M}_0$ as the smallest integer such that the sum of the $\hat{M}_0$ largest eigenvalues is greater than or equal to a certain threshold γ.

$$\begin{cases} \sum_{i=1}^{\hat{M}_0} \hat{\lambda}_i & \geq \gamma \\ \sum_{i=1}^{\hat{M}_0 - 1} \hat{\lambda}_i & < \gamma \end{cases}$$

The term γ is named as the coverage (cv) factor as it controls the signal power coverage. We set γ to 0.95 by allowing 5% energy leakage. We will try other cv factors in Section 5.2.

2.5 Dispersive Methods

2.5.1 DISPAREs

DISPARE stands for *DIstributed Signal PARametric Estimation*. It was developed by Meng et. al. in 1993 [2]. Here is a brief derivation of the methods.

Suppose the true parameter values of the kth dispersed signal are $(\bar{\theta}_k, \bar{\phi}_k, \alpha_{\theta,k}, \alpha_{\phi,k})$. Let us examine the weighted inner product of the eigenvectors of $\bar{R}_k(\bar{\theta}_k, \bar{\phi}_k, \alpha_{\theta,k}, \alpha_{\phi,k})$ and the noise eigenvectors of $\hat{R}$,

$$\epsilon_{k,ij} = \bar{\lambda}_{k,i}^{\frac{1}{2}} \, \bar{v}_{k,i}^{\dagger} \, \hat{v}_j \qquad \begin{array}{l} \text{for } i = 1 \ldots M; \\ \qquad j = M_0 + 1 \ldots M. \end{array} \tag{2.22}$$

For $i \leq m_{0k}$, $\bar{v}_{k,i}$ is a signal eigenvector of the kth source, thus the inner product $(\bar{v}_{k,i}, \hat{v}_j)$ is close to 0 and $\epsilon_{k,ij}$ should be small for all j. For $i > m_{0k}$, $\bar{v}_{k,i}$ is *effectively* a noise eigenvector, thus $\bar{\lambda}_{k,i}$ should be small[3], again giving a small $\epsilon_{k,ij}$ for all j. Therefore, we expect that at the true values $(\bar{\theta}_k, \bar{\phi}_k, \alpha_{\theta,k}, \alpha_{\phi,k})$ $\forall k$, $\epsilon_{k,ij}$ is small for all i, j.

The DISPARE I algorithm is to search a quadruple $(\hat{\bar{\theta}}_k, \hat{\bar{\phi}}_k, \hat{\alpha}_{\theta,k}, \hat{\alpha}_{\phi,k})$ such that the sum of

[3]This is the eigenvalue of the kth parametric covariance, and is independent of the estimated data covariance or the noise injected.

the square of all $\epsilon_{k,ij}$ is minimized.

$$\begin{aligned}(\hat{\bar{\theta}}_k, \hat{\bar{\phi}}_k, \hat{\alpha}_{\theta,k}, \hat{\alpha}_{\phi,k}) &\triangleq \arg \min_{\bar{\theta},\bar{\phi},\alpha_\theta,\alpha_\phi} \sum_{i,j} |\, \epsilon_{k,ij} \,|^2 \qquad \text{for } \epsilon_{k,ij} \text{ defined in Eq.(2.22)} \quad (2.23)\\ &= \arg \min_{\bar{\theta},\bar{\phi},\alpha_\theta,\alpha_\phi} \text{tr}\,\{\tilde{\boldsymbol{R}}_k\, \hat{\boldsymbol{V}}_N\, \hat{\boldsymbol{V}}_N^\dagger\}\\ &= \arg \min_{\bar{\theta},\bar{\phi},\alpha_\theta,\alpha_\phi} \text{tr}\,\{\tilde{\boldsymbol{R}}_k\, \hat{\boldsymbol{P}}_N\}\\ &= \arg \min_{\bar{\theta},\bar{\phi},\alpha_\theta,\alpha_\phi} f_{DISP1} \qquad (2.24)\end{aligned}$$

where

$$f_{DISP1} \triangleq \text{tr}\,\{\tilde{\boldsymbol{R}}_k\, \hat{\boldsymbol{P}}_N\} \qquad (2.25)$$

The cost functions of all the subsequent algorithms can be expressed in terms of $\epsilon_{k,ij}$, but with different weightings on the inner product and different selections of the eigenvectors.

By changing the weighting from $\bar{\lambda}_{k,i}^{\frac{1}{2}}$ to $\tilde{\lambda}_{k,i}$ in Eq.(2.22), we have

$$\begin{aligned}\epsilon_{k,ij} &= \tilde{\lambda}_{k,i}\, \tilde{v}_{k,i}^\dagger\, \hat{v}_j \qquad \text{for } \; i = 1 \ldots M;\\ &\qquad\qquad\quad\; j = M_0 + 1 \ldots M.\end{aligned} \qquad (2.26)$$

Using a similar argument as before, $\epsilon_{k,ij}$ should be small at the true values $(\bar{\theta}_k, \bar{\phi}_k, \alpha_{\theta,k}, \alpha_{\phi,k})$ $\forall k$. DISPARE II tries to find

$$\begin{aligned}(\hat{\bar{\theta}}_k, \hat{\bar{\phi}}_k, \hat{\alpha}_{\theta,k}, \hat{\alpha}_{\phi,k}) &\triangleq \arg \min_{\bar{\theta},\bar{\phi},\alpha_\theta,\alpha_\phi} \sum_{i,j} |\, \epsilon_{k,ij} \,|^2 \qquad \text{for } \epsilon_{k,ij} \text{ defined in Eq.(2.26)}\\ &= \arg \min_{\bar{\theta},\bar{\phi},\alpha_\theta,\alpha_\phi} \text{tr}\,\{\tilde{\boldsymbol{R}}_k\, \tilde{\boldsymbol{R}}_k\, \hat{\boldsymbol{P}}_N\}\\ &= \arg \min_{\bar{\theta},\bar{\phi},\alpha_\theta,\alpha_\phi} \|\, \tilde{\boldsymbol{R}}_k\, \hat{\boldsymbol{V}}_N \,\|_F^2\\ &= \arg \min_{\bar{\theta},\bar{\phi},\alpha_\theta,\alpha_\phi} f_{DISP2} \qquad (2.27)\end{aligned}$$

where

$$f_{DISP2} \triangleq \|\, \tilde{\boldsymbol{R}}_k\, \hat{\boldsymbol{V}}_N \,\|_F^2 \qquad (2.28)$$

Note that in the above derivation, we assume that $\tilde{\boldsymbol{R}}_k$ depends on $(\bar{\theta}_k, \bar{\phi}_k, \alpha_{\theta,k}, \alpha_{\phi,k})$ only. This is over-simplified as $\tilde{\boldsymbol{R}}_k$ is actually dependent of the normalized power density distribution $p(\theta, \phi)$. In other words, we have to assume a certain distribution type before applying DISPAREs. Of course, a wrong distribution assumption will introduce some error. It is stated in [2] that, if

we assume a uniform distribution, this error will be small regardless of the actual distribution. As such, we always assume a uniform distribution to estimate the DOA, unless otherwise stated.

2.5.2 DISCs

The DISC methods were developed by To et. al. in 1996 [3].

As stated in Section 2.3, the rationale for the MUSIC algorithm is: *The entire range spanned by the eigenvectors of* $\boldsymbol{R}$ *can be partitioned into a signal subspace and a noise subspace. The steering vectors at the true DOAs span the signal subspace, thus are orthogonal to every eigenvector in the noise subspace.* As such, the DOAs can be found according to Eq.(2.15), which is rewritten below.

$$(\hat{\theta}, \hat{\phi}) \;=\; \arg \min_{\theta,\phi} \; \mathrm{tr}\,\{\boldsymbol{d}(\theta,\phi)\, \boldsymbol{d}^{\dagger}(\theta,\phi)\, \hat{\boldsymbol{P}}_N\} \tag{2.29}$$

Comparing this with the cost functions of DISPAREs, $[d(\theta,\phi)\; \boldsymbol{d}^{\dagger}(\theta,\phi)]$ is replaced by $\bar{\boldsymbol{R}}_k$ in DISPARE I or $\bar{\boldsymbol{R}}_k \bar{\boldsymbol{R}}_k$ in DISPARE II. However, since $\bar{\boldsymbol{R}}_k$ (or $\bar{R}_k \bar{R}_k$) is full rank, it can never be exactly orthogonal to $\hat{\boldsymbol{P}}_N$. The only exception is when $\alpha_{\theta,k} = \alpha_{\phi,k} = 0$, which means point source and DISPAREs reduce to MUSIC.

Thus, a *natural* extension of MUSIC for distributed source was suggested as

$$\begin{aligned}(\hat{\bar{\theta}}_k, \hat{\bar{\phi}}_k, \hat{\alpha}_{\theta,k}, \hat{\alpha}_{\phi,k}) \;&=\; \arg \min_{\bar{\theta},\bar{\phi},\alpha_\theta,\alpha_\phi} \; \mathrm{tr}\,\{\bar{\boldsymbol{P}}_{S,k}\, \hat{\boldsymbol{P}}_N\} \\ &=\; \arg \min_{\bar{\theta},\bar{\phi},\alpha_\theta,\alpha_\phi} \; f_{MUDI}\end{aligned} \tag{2.30}$$

where

$$f_{MUDI} \;\triangleq\; \mathrm{tr}\,\{\bar{\boldsymbol{P}}_{S,k}\, \hat{\boldsymbol{P}}_N\} \tag{2.31}$$

The method is called MUSIC DISC, which stands for "*MUSIC for DIstributed SourCes*". In terms of inner products, the above equation can be expressed as

$$(\hat{\bar{\theta}}_k, \hat{\bar{\phi}}_k, \hat{\alpha}_{\theta,k}, \hat{\alpha}_{\phi,k}) \;=\; \arg \min_{\bar{\theta},\bar{\phi},\alpha_\theta,\alpha_\phi} \; \sum_{i,j} |\, \epsilon_{k,ij}\,|^2 \tag{2.32}$$

where

$$\epsilon_{k,ij} = \tilde{v}_{k,i}^{\dagger}\, \hat{v}_j \qquad \begin{array}{l} \text{for } i = 1 \ldots m_{0k}; \\ \quad\; j = M_0 + 1 \ldots M. \end{array} \tag{2.33}$$

In this method, the parametric noise eigenvectors $\tilde{v}_{k,i}$ for $i = (m_{0k}+1), \ldots, M$ are *not* considered and there is *no* weighting added to the inner product.

The point source Beamforming equation is given by

$$(\hat{\theta}, \hat{\phi}) = \arg \max_{\theta,\phi} \text{ tr } \{d(\theta,\phi)\, d^{\dagger}(\theta,\phi)\, \hat{R}\} \tag{2.34}$$

This cost function is the same as that of deterministic Maximum Likelihood Estimation (MLE) in the single point source case. By following a similar argument as above, a natural extension of point source Beamforming for distributed source is

$$\begin{aligned} (\hat{\bar{\theta}}_k, \hat{\bar{\phi}}_k, \hat{\alpha}_{\theta,k}, \hat{\alpha}_{\phi,k}) &= \arg \max_{\bar{\theta},\bar{\phi},\alpha_\theta,\alpha_\phi} \text{ tr } \{\tilde{P}_{S,k}\, \hat{R}\} \\ &= \arg \max_{\bar{\theta},\bar{\phi},\alpha_\theta,\alpha_\phi} f_{BFDI} \end{aligned} \tag{2.35}$$

where

$$f_{BFDI} \triangleq \text{ tr } \{\tilde{P}_{S,k}\, \hat{R}\} \tag{2.36}$$

This method is named BF DISC, which means "*BeamForming for DIstributed SourCes*". In terms of the inner product,

$$(\hat{\bar{\theta}}_k, \hat{\bar{\phi}}_k, \hat{\alpha}_{\theta,k}, \hat{\alpha}_{\phi,k}) = \arg \max_{\bar{\theta},\bar{\phi},\alpha_\theta,\alpha_\phi} \sum_{i,j} |\, \epsilon_{k,ij}\, |^2 \tag{2.37}$$

where

$$\epsilon_{k,ij} = \hat{\lambda}_j^{\frac{1}{2}}\, \tilde{v}_{k,i}^{\dagger}\, \hat{v}_j \qquad \begin{array}{l} \text{for } i = 1 \ldots m_{0k}; \\ \quad\; j = 1 \ldots M. \end{array} \tag{2.38}$$

In this method, we use all the eigenvectors of the estimated covariance $\hat{R}$ and the weighting $\hat{\lambda}_j^{\frac{1}{2}}$ is derived from $\hat{R}$ rather than $\tilde{R}_k$. Intuitively speaking, such a cost function lets $\tilde{R}_k$ shift such that its dominant eigenvectors align with (some of) the first M_0 eigenvectors of $\hat{R}$. Obviously, for $\tilde{R}_k$ at the true values $(\bar{\theta}_k, \bar{\phi}_k, \alpha_{\theta,k}, \alpha_{\phi,k})$, such alignment would become the best.

Chapter 3

Approximated Models and Direction Finding Approaches

3.1 Approximated Models for Uniform Distribution

In Section 2.2, we derived the general signal model equation Eq.(2.8). Then, by assuming a uniform power density distribution with a rectangular region, we obtained Eq.(2.10), an integral which is hard to solve. In this section, we approximate and solve the integral in three different ways.

3.1.1 Model 1a: Dispersive Azimuth / Non-Dispersive Elevation

As only azimuth angles are concerned, we neglect the elevation dispersive effect in this model. By *assuming no dispersion on the elevation angle range* (i.e. $\alpha_\phi = 0$), Eq.(2.8) becomes

$$\tilde{r}_{mn}|_{\alpha_\phi=0} = \int_{-\pi}^{\pi} p(\theta,\bar{\phi}) \cos\bar{\phi}\ e^{j2\pi[(x_m-x_n)\sin\theta+(y_m-y_n)\cos\theta]\cos\bar{\phi}}\ d\theta \tag{3.1}$$

We denote $p(\theta)$ as the power density distribution function of θ at $\phi = \bar{\phi}$. The total energy received by the antenna system will remain the same, thus

$$\begin{aligned}
\int_{-\pi}^{\pi} p(\theta)\, d\theta &= \int_{\Omega} p(\theta,\phi)\, d\Omega \\
&= \int_{0}^{\frac{\pi}{2}} \int_{-\pi}^{\pi} p(\theta, o) \cos o \; d\theta \; d\phi \\
&= \int_{-\pi}^{\pi} p(\theta,\bar{\phi}) \cos\bar{\phi}\; d\theta \\
p(\theta) &= p(\theta,\bar{\phi}) \cos\bar{\phi}
\end{aligned} \tag{3.2}$$

From Eq.(3.1) and Eq.(3.2),

$$\tilde{r}_{mn}|_{\alpha_\phi=0} = \int_{-\pi}^{\pi} p(\theta)\; e^{j2\pi[(x_m-x_n)\sin\theta+(y_m-y_n)\cos\theta]\cos\bar{\phi}}\; d\theta \tag{3.3}$$

By substituting a particular $p(\theta)$ into the above equation, we can compute $\tilde{R}$. Let us go back to the previous example of uniform distribution. That is,

$$p(\theta) = \begin{cases} \frac{1}{2\alpha_\theta} & |\theta-\bar{\theta}| \le \alpha_\theta \\ 0 & \text{elsewhere} \end{cases} \tag{3.4}$$

Substituting $p(\theta)$ into Eq.(3.3), we get

$$\tilde{r}_{mn}|_{\alpha_\phi=0} = \frac{1}{2\alpha_\theta}\int_{\bar{\theta}-\alpha_\theta}^{\bar{\theta}+\alpha_\theta} e^{j2\pi[(x_m-x_n)\sin\theta+(y_m-y_n)\cos\theta]\cos\bar{\phi}}\; d\theta \tag{3.5}$$

Let

$$\begin{cases} \cos\varphi = \frac{x_m-x_n}{\sqrt{(x_m-x_n)^2+(y_m-y_n)^2}} \\ \sin\varphi = \frac{y_m-y_n}{\sqrt{(x_m-x_n)^2+(y_m-y_n)^2}} \end{cases} \tag{3.6}$$

then,

$$\begin{aligned}
\tilde{r}_{mn}|_{\alpha_\phi=0} &= \frac{1}{2\alpha_\theta}\int_{\bar{\theta}-\alpha_\theta}^{\bar{\theta}+\alpha_\theta} e^{j2\pi\sqrt{(x_m-x_n)^2+(y_m-y_n)^2}(\sin\theta\cos\varphi+\cos\theta\sin\varphi)\cos\bar{\phi}}\; d\theta \\
&= \frac{1}{2\alpha_\theta}\int_{\bar{\theta}-\alpha_\theta}^{\bar{\theta}+\alpha_\theta} e^{j2\pi\cos\bar{\phi}\sqrt{(x_m-x_n)^2+(y_m-y_n)^2}\sin(\theta+\varphi)}\; d\theta
\end{aligned} \tag{3.7}$$

Let $z = 2\pi\cos\bar{\phi}\sqrt{(x_m-x_n)^2+(y_m-y_n)^2}$, then

$$\begin{aligned}
\tilde{r}_{mn}|_{\alpha_\phi=0} &= \frac{1}{2\alpha_\theta}\int_{\bar{\theta}-\alpha_\theta}^{\bar{\theta}+\alpha_\theta} e^{jz\sin(\theta+\varphi)}\; d\theta \\
&\approx \frac{1}{2j\alpha_\theta z\cos(\bar{\theta}+\varphi)}\int_{\bar{\theta}-\alpha_\theta}^{\bar{\theta}+\alpha_\theta} e^{jz\sin(\theta+\varphi)}\; d[jz\sin(\theta+\varphi)]
\end{aligned} \tag{3.8}$$

To get the last line, we assume that $\cos(\bar{\theta}+\varphi) \approx \cos(\bar{\theta}+\varphi+\alpha_\theta) \approx \cos(\bar{\theta}+\varphi-\alpha_\theta)$. This is valid if α_θ is small.

We look at the integral and denote it as I,

$$\begin{aligned} I &= \int_{\bar{\theta}-\alpha_\theta}^{\bar{\theta}+\alpha_\theta} e^{jz\sin(\theta+\varphi)}\, d[jz\sin(\theta+\varphi)] \\ &= e^{jz\sin(\bar{\theta}+\varphi+\alpha_\theta)} - e^{jz\sin(\bar{\theta}+\varphi-\alpha_\theta)} \\ &= e^{jz[\sin(\bar{\theta}+\varphi)\cos\alpha_\theta+\cos(\bar{\theta}+\varphi)\sin\alpha_\theta]} - e^{jz[\sin(\bar{\theta}+\varphi)\cos\alpha_\theta-\cos(\bar{\theta}+\varphi)\sin\alpha_\theta]} \\ &= e^{jz\sin(\bar{\theta}+\varphi)\cos\alpha_\theta}\left\{e^{jz\cos(\bar{\theta}+\varphi)\sin\alpha_\theta} - e^{-jz\cos(\bar{\theta}+\varphi)\sin\alpha_\theta}\right\} \\ &= e^{jz\sin(\bar{\theta}+\varphi)\cos\alpha_\theta}\,\{2j\sin[z\cos(\bar{\theta}+\varphi)\sin\alpha_\theta]\} \\ &\approx e^{jz\sin(\bar{\theta}+\varphi)}\,\{2j\sin[\alpha_\theta z\cos(\bar{\theta}+\varphi)]\} \end{aligned} \tag{3.9}$$

Again, the last line is valid if α_θ is small.

Substituting Eq.(3.9) into Eq.(3.8), we get

$$\bar{r}_{mn}|_{\alpha_\phi=0} = e^{jz\sin(\bar{\theta}+\varphi)}\,\frac{\sin[\alpha_\theta z\cos(\bar{\theta}+\varphi)]}{\alpha_\theta z\cos(\bar{\theta}+\varphi)} \tag{3.10}$$

Substituting back z and φ, we get $\bar{r}_{mn}$ with

$$\text{Angular Part} = e^{j2\pi\cos\bar{\phi}[(x_m-x_n)\sin\bar{\theta}+(y_m-y_n)\cos\bar{\theta}]} \tag{3.11}$$

$$\text{Modulus Part} = \text{sinc}\{2\alpha_\theta\,(\cos\bar{\phi})\,[(x_m-x_n)\cos\bar{\theta}-(y_m-y_n)\sin\bar{\theta}]\} \tag{3.12}$$

Example: $p(\theta)$ is an impulse function, i.e. $\alpha_\theta = 0$

From Eq.(3.12), for $\alpha_\theta \to 0$, the modulus part tends to 1. Thus,

$$\bar{r}_{mn}|_{\alpha_\theta=0,\alpha_\phi=0} = e^{j2\pi\cos\bar{\phi}[(x_m-x_n)\sin\bar{\theta}+(y_m-y_n)\cos\bar{\theta}]} \tag{3.13}$$

This is exactly the $\bar{r}_{mn}$ of a point signal, as can be seen from Eq.(2.3) and the relation $\bar{r}_{mn} = d_m d_n^*$, where d_i is the ith element of the steering vector d.

3.1.2 Model 1b: Dispersive Azimuth / Multiple Elevation Layers

From the first principle of integration, an integral can be approximated by a summation. Thus, from Eq.(2.8),

$$\begin{aligned}\tilde{r}_{mn} &= \int_{\bar{\phi}-\alpha_\phi}^{\bar{\phi}+\alpha_\phi}\int_{\bar{\theta}-\alpha_\theta}^{\bar{\theta}+\alpha_\theta} p(\theta,\phi)e^{j2\pi[(x_m-x_n)\sin\theta+(y_m-y_n)\cos\theta]\cos\phi}\cos\phi\ d\theta\ d\phi \\ &\approx \sum_{i=1}^{n}\left[\int_{\bar{\theta}-\alpha_\theta}^{\bar{\theta}+\alpha_\theta} p(\theta,\phi_i)e^{j2\pi[(x_m-x_n)\sin\theta+(y_m-y_n)\cos\theta]\cos\phi_i}\cos\phi_i\ d\theta\right]\Delta\phi \qquad (3.14)\end{aligned}$$

Here, we assume $p(\theta,\phi) > 0$ within a rectangular region bounded by $(\bar{\theta}-\alpha_\theta \le \theta \le \bar{\theta}+\alpha_\theta, \bar{\phi}-\alpha_\phi \le \phi \le \bar{\phi}+\alpha_\phi)$. The elements of $\{\phi_i\}$ are evenly displaced: $\phi_1 = \bar{\phi}-\alpha_\phi$, $\phi_n = \bar{\phi}+\alpha_\phi$, $\Delta\phi = \phi_{i+1}-\phi_i$.

We look at the integral of Eq.(3.14) and assume a uniform distribution,

$$\begin{aligned}&\int_{\bar{\theta}-\alpha_\theta}^{\bar{\theta}+\alpha_\theta} p(\theta,\phi_i)\ e^{j2\pi[(x_m-x_n)\sin\theta+(y_m-y_n)\cos\theta]\cos\phi_i}\ \cos\phi_i\ d\theta \\ =\ &\int_{\bar{\theta}-\alpha_\theta}^{\bar{\theta}+\alpha_\theta} A_1\ e^{j2\pi[(x_m-x_n)\sin\theta+(y_m-y_n)\cos\theta]\cos\phi_i}\ \cos\phi_i\ d\theta \\ =\ &A_2\ \mathrm{Ang}(\bar{\theta},\phi_i)\ \mathrm{Mod}(\bar{\theta},\phi_i)\ \cos\phi_i \qquad (3.15)\end{aligned}$$

where 'Ang' and 'Mod' are the angular and the modular parts stated in Eq.(3.11) and Eq.(3.12) respectively, and $(\cos\bar{\phi})$ in these equations are replaced by $(\cos\phi_i)$ here. The terms A_1, A_2 are constants.

Substitute Eq.(3.15) back into Eq.(3.14), we have,

$$\begin{aligned}\tilde{r}_{mn} &= A_2\ \Delta\phi \sum_{i=1}^{n}\left[\ \mathrm{Ang}(\bar{\theta},\phi_i)\ \mathrm{Mod}(\bar{\theta},\phi_i)\ \cos\phi_i\right] \\ &= A_3 \sum_{i=1}^{n}\left[\ \mathrm{Ang}(\bar{\theta},\phi_i)\ \mathrm{Mod}(\bar{\theta},\phi_i)\ \cos\phi_i\right] \qquad (3.16)\end{aligned}$$

where A_3 is another constant.

We say that this is a semi-dispersive elevation model as the expression in Eq.(3.14) is an approximation of Eq.(2.10). Such approximation becomes exact when $n \to \infty$ and $\Delta\phi \to 0$. In the actual implementation, we need not calculate A_3 explicitly. We compute $\tilde{R}$ by neglecting A_3, and then normalize $\tilde{R}$ such that its diagonal elements equal to 1.

3.1.3 Model 2: Multiple Points Approximation

The models discussed in the last two subsections are not exact due to the approximations made in deriving Eq.(3.8) and Eq.(3.9) besides their respective non-dispersive and semi-dispersive elevation assumptions. Thus, Eq.(3.10) and Eq.(3.16) are acceptable only if α_θ is small. However, as the spread of an ionospheric scattering signal is usually quite large, such an approximation may not be valid. Here, we suggest approximating the parametric covariance $\bar{R}$ of a dispersed source by using the covariances of a large number of point sources, which are uniformly and closely spaced in the rectangular region where $p(\theta, \phi) > 0$.

From Eq.(3.14), and assuming a uniform distribution,

$$\begin{aligned}
\bar{r}_{mn} &\approx \sum_{i=1}^{n1} \left[\int_{\bar{\theta}-\alpha_\theta}^{\bar{\theta}+\alpha_\theta} A_1 \, e^{j2\pi[(x_m-x_n)\sin\theta+(y_m-y_n)\cos\theta]\cos\phi_i} \cos\phi_i \, d\theta \right] \triangle\phi \\
&\approx \sum_{i=1}^{n1} \sum_{j=1}^{n2} A_1 \, e^{j2\pi[(x_m-x_n)\sin\theta_j+(y_m-y_n)\cos\theta_j]\cos\phi_i} \cos\phi_i \, \triangle\theta \, \triangle\phi \\
&= A_4 \sum_{i=1}^{n1} \sum_{j=1}^{n2} \left[e^{j2\pi[(x_m-x_n)\sin\theta_j+(y_m-y_n)\cos\theta_j]\cos\phi_i} \cos\phi_i \right] \qquad (3.17)
\end{aligned}$$

As in the previous model, the elements of $\{\theta_j\}$ are evenly displaced: $\theta_1 = \bar{\theta} - \alpha_\theta$, $\theta_{n2} = \bar{\theta} + \alpha_\theta$, $\triangle\theta = \theta_{i+1} - \theta_i$. The term A_4 is a constant.

Compared with Eq.(3.13), the quantity in the bracket in Eq.(3.17) is just the covariance of a point source at (θ_j, ϕ_i) multiplied by $(\cos\phi_i)$. The term $(\cos\phi_i)$ is a balancing factor as the solid angle $d\Omega$ subtended at a low altitude (i.e. small ϕ) is larger than one at a high altitude (large ϕ).

By using a very small $\triangle\phi$ and $\triangle\theta$ (say, $\triangle\phi = \triangle\theta = 0.1^0$), we can compute an *ideal* parametric covariance $\bar{R}$ of a dispersed source at certain $(\bar{\theta}, \bar{\phi}, \alpha_\theta, \alpha_\phi)$. As a test of the fitness of the above models, we use the array geometry of cfh_a data and set $\bar{\theta} = 50^0, \bar{\phi} = 0^0, \alpha_\phi = 0^0$. We first compute the ideal covariance $\bar{R}_1(\alpha_\theta)$ at different α_θ. Then, we use Model 1a of Eq.(3.10) and compute the covariance $\bar{R}_2(\alpha_\theta)$ at different α_θ. The frobenius norms of the difference of these two covariances are plotted (solid line) versus α_θ in Fig.3.1. As expected, the norm value increases as α_θ increases, which means $\bar{R}_2$ becomes less accurate.

For comparison, we also compute the covariances $\tilde{R}_3(\alpha_\theta)$ and $\tilde{R}_4(\alpha_\theta)$ by Model 2 with $\Delta\theta$ setting at 1^0 and 2^0 respectively. The $\| \tilde{R}_1 - \tilde{R}_3 \|_F$ and $\| \tilde{R}_1 - \tilde{R}_4 \|_F$ are plotted in dashed line and dash-dot line in Fig.3.1. As α_θ increases, $\tilde{R}_3$ and $\tilde{R}_4$ are based on a larger number of points, thus become more accurate (closer to $\tilde{R}_1$). In Subsection 3.4.1, we will test the effectiveness of these 3 approximated signal models.

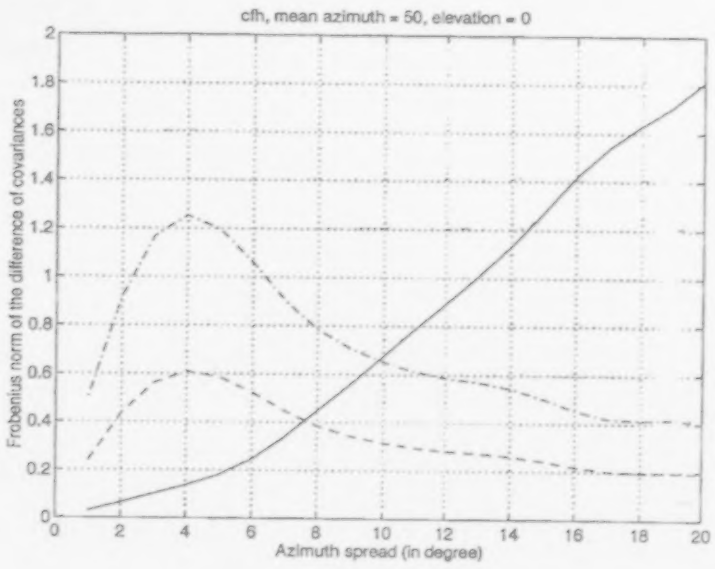

Figure 3.1: Frobenius Norm of Difference of Covariances

If the assumed power density distribution is *not* uniform or the region in which $p(\theta, \phi) > 0$ is *not* rectangular, then Eq.(3.10) and Eq.(3.16) are no longer applicable and we have to integrate Eq.(2.8) again for that particular distribution or boundary region. On the other hand, in the multiple points approximation model, we only need to weight the covariance at each point by following the required power density distribution to get $\tilde{R}$. Thus, Model 2 offers the greatest flexibility in implementing different distribution types.

3.2 Approaches for Estimating $\hat{\bar{\theta}}$

One of the implementation complexities of the dispersive methods is that 4 parameters $\bar{\theta}, \bar{\phi}, \alpha_\theta, \alpha_\phi$ are involved in the criterion functions. It would be computationally prohibitive to perform a 4-dimensional exhaustive search. As our target is to estimate the nominal azimuth angle $\bar{\theta}$ only, we try to avoid searching exhaustively the other parameters. This section outlines three such approaches.

3.2.1 Assume $\hat{\bar{\phi}} = \hat{\alpha}_\phi$

In order to bypass the estimation of $\hat{\bar{\phi}}$, we need another assumption. In Fig.3.2, we plot $\hat{\phi}$ versus $\hat{\theta}$, which were estimated using MUSIC. The cfh_a, iar_a and vai_a estimates are marked as 'o', while the vcs_[a-d] estimates are marked as '+'. As shown, most estimates are at low elevation angles. Although the MUSIC estimates are not accurate, they can be taken as a reference. Thus it is reasonable to assume the signal dispersion in the ϕ-range starts at 0^0. As $\hat{\bar{\phi}}$ is defined as the center of the ϕ-range dispersion, thus

$$\hat{\bar{\phi}} - \hat{\alpha}_\phi = 0^0 \tag{3.18}$$

In other words, the dispersion in the ϕ-range starts at 0^0 and ends at $2\alpha_\phi$. In particular, if α_ϕ is 0^0, $\bar{\phi}$ will also be 0^0.

3.2.2 Approach 1: 2-D Search on $\bar{\theta}$ and α_θ, Pre-determined $\hat{\alpha}_\phi$

The procedure for Approach 1 is listed below.

Step 1 Pre-determine $\hat{\alpha}_\phi$. Estimate $\hat{\bar{\phi}}$ from Eq.(3.18).

Step 2 From $\hat{\boldsymbol{R}}$, estimate $\hat{M}_0$ (according to the method outlined in Subsection 2.4.2), then compute $\hat{\boldsymbol{V}}_N$ and $\hat{\boldsymbol{P}}_N$.

Step 3 Plot the cost function values at various $\bar{\theta}$ and α_θ:
For DISPARE I, plot $-10\log_{10} f_{DISP1}$, with f_{DISP1} specified in Eq.(2.25).

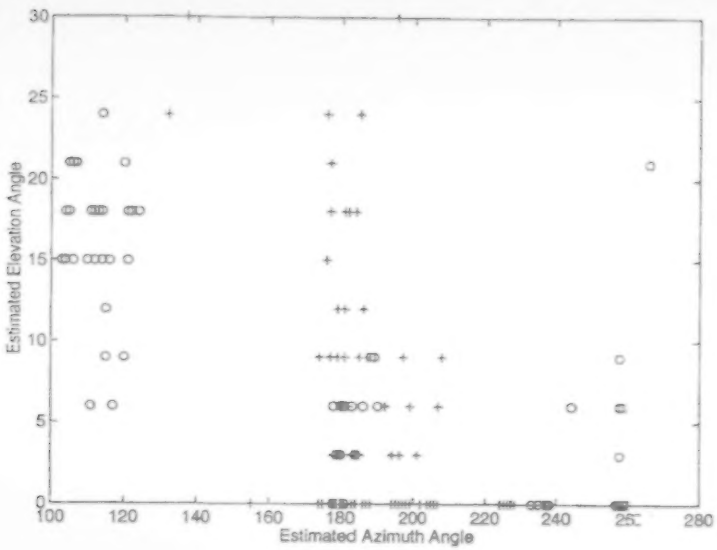

Figure 3.2: $\hat{\theta}$ and $\hat{\phi}$ from MUSIC

For DISPARE II, plot $-10\log_{10} f_{DISP2}$, with f_{DISP2} specified in Eq.(2.28).

For MUSIC DISC, plot $-10\log_{10} f_{MUDI}$, with f_{MUDI} specified in Eq.(2.31).

For BF DISC, plot $10\log_{10} f_{BFDI}$, with f_{BFDI} specified in Eq.(2.36).

Step 4 Pick out the global peak, and estimate $\hat{\theta}$.[1]

3.2.3 Approach 2: 2-D Search on θ and α_θ, $\hat{\alpha}_\phi = \frac{1}{2}\hat{\alpha}_\theta$

In Approach 1, there is no guarantee that the pre-determined $\hat{\alpha}_\phi$ will be near to the true value. If not, the estimation performance may be adversely affected. On the other hand, it is logical to assume that if a signal is dispersed largely [or little] in the azimuth range, it should also disperse largely [little] in the elevation range. In other words, $\hat{\alpha}_\phi$ should be proportional to $\hat{\alpha}_\theta$. In this approach, we assume that

$$\hat{\alpha}_\phi = \frac{1}{2}\hat{\alpha}_\theta \tag{3.19}$$

[1] As there is only 1 signal, we pick out the global peak. If there are K signals, then we need to pick out the K highest peaks.

rather than pre-determining $\hat{\alpha}_\phi$. The factor $\frac{1}{2}$ is quite arbitrary and could be fine-tuned. The rest of the procedure is the same as Approach 1: we perform a 2-D search on $\bar{\theta}$ and α_θ, and pick out the peak to estimate $\hat{\bar{\theta}}$.

3.2.4 Approach 3: 1-D Search on $\bar{\theta}$

Previous approaches search along α_θ, which is wasteful of computation power as $\hat{\alpha}_\theta$ is not our primary interest. Here, we suggest estimating $\hat{\alpha}_\theta$ separately rather than searching exhaustively.

In this approach, we estimate $\hat{\alpha}_\theta$ from $\{\hat{\lambda}\}$, the eigenvalues of the estimated covariance $\hat{\boldsymbol{R}}$. It is shown in [3] that for a linearly and uniformly spaced antenna array, the eigenvalues of a parametric covariance $\bar{\boldsymbol{R}}$ will depend on the spread *alone* and not on the DOA. For an irregular array like the one in Vortex system, we want to show that the eigenvalues $\{\bar{\lambda}\}$ will *heavily* depend on α_θ and slightly depend on $\bar{\theta}$. By assuming single dispersed signal, $\{\bar{\lambda}\} \approx \{\hat{\lambda}\}$. Thus, it is justified to use $\{\hat{\lambda}\}$ to estimate $\hat{\alpha}_\theta$.

With $\bar{\phi} = \alpha_\phi = 0^0$ and using the array geometry for cfh_a data, we compute the ideal $\bar{\boldsymbol{R}}$ (by using multiple points simulation with $\triangle\theta = 0.1^0$) at various $\bar{\theta}/\alpha_\theta$ combination. Then we plot the first three eigenvalues ($\bar{\lambda}_1$, $\bar{\lambda}_2$, $\bar{\lambda}_3$) of $\bar{\boldsymbol{R}}$ versus $\bar{\theta}$ and α_θ in Fig.3.3. The corresponding contours are shown side by side. The figure shows that $\{\bar{\lambda}\}$ is mainly depending on α_θ if α_i is small. It also shows that

$$\bar{\lambda}_i(\theta) \;=\; \bar{\lambda}_i(\theta + 180^0) \tag{3.20}$$

at any particular α_θ. Alhough $\{\bar{\lambda}\}$ is also highly depending on $\bar{\theta}$ for large α_θ, we may minimize such dependency by taking the average of $\{\bar{\lambda}\}$ at various values of $\bar{\theta}$.

The procedures of Approach 3 are listed below.

Step 1 By assuming $\hat{\alpha}_\phi = \frac{1}{2}\hat{\alpha}_\theta$, we pre-store a file containing the eigenvalues of $\bar{\boldsymbol{R}}$ at $\alpha_\theta = 1^0 : 30^0$. The method to find the eigenvalues is:

for $\alpha_\theta = 1^0 : 30^0$

for $\bar{\theta} = 0^0 : 30^0 : 150^0$

Figure 3.3: Eigenvalues at various $\bar{\theta}$ and α_θ

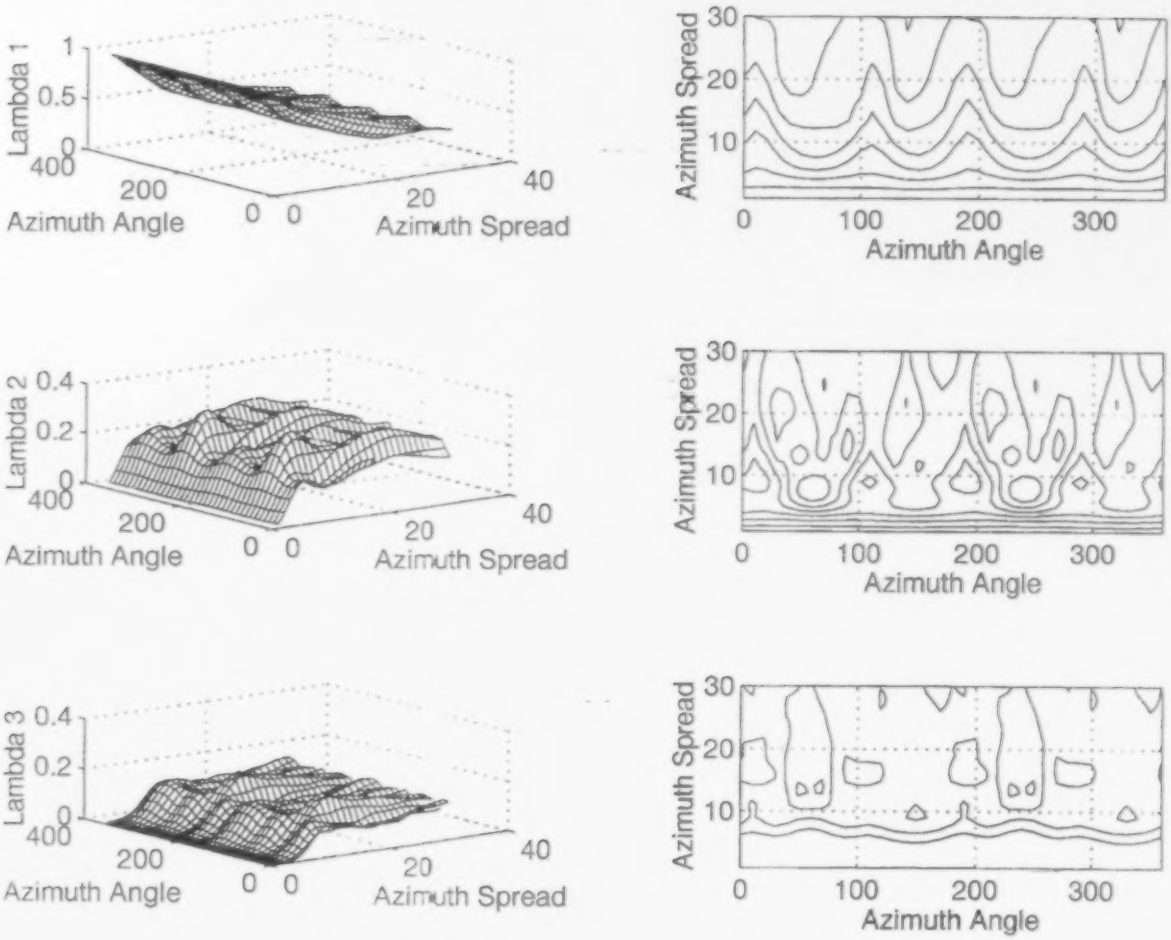

compute the ideal $\tilde{\boldsymbol{R}}$ by using $\triangle\theta = 0.1^0$, then compute $\{\bar{\lambda}\}$

end

find the average $\{\bar{\lambda}\}$ at that particular α_θ

end

The file is stored up to $\alpha_\theta = 30^0$ as we believe that the dispersiveness is unlikely to exceed this value.

Step 2 From $\hat{\boldsymbol{R}}$, compute $\{\hat{\lambda}\}$ and estimate $\hat{M}_0$.

Step 3 Compare $\{\hat{\lambda}\}$ with the $\{\bar{\lambda}\}$s from the pre-stored file. Pick out the nearest $\{\bar{\lambda}\}$ and get the corresponding α_θ as $\hat{\alpha}_\theta$. From $\hat{\alpha}_\theta$, calculate $\hat{\alpha}_\phi$ by Eq.(3.19) and $\hat{\bar{\phi}}$ by Eq.(3.18).

Step 4 From $\hat{\boldsymbol{R}}$, estimate $\hat{M}_0$ and then compute $\hat{V}_N$ and $\hat{P}_N$.

Step 5 By using $\hat{\alpha}_\phi$, $\hat{\alpha}_\theta$ and $\hat{\bar{\phi}}$, plot the function values of the dispersive methods against $\bar{\theta}$ (i.e. a 1-D search).

Step 6 Pick out the peak and estimate $\hat{\bar{\theta}}$.

3.3 Plots of Cost Function Values

Experiment 3.1: Plotting Cost Function Values

Objective: To plot the cost function values for various methods.

Scenario: We use all 64K samples of the '1' files (i.e. cfh_a1, iar_a1 etc.) to compute $\hat{\boldsymbol{R}}$ and estimate $\hat{\bar{\theta}}$. For MUSIC, we perform a 2-D search on ϕ and θ. For the dispersive methods, we employ Model 1a ($\bar{\phi} = \alpha_\phi = 0^0$) and Approach 1 (i.e. a 2-D search on α_θ and $\bar{\theta}$). The search ranges (ϕ and θ for MUSIC, α_θ and α_ϕ for the dispersive methods) are listed in Table 3.1.

Results: The estimates of $\hat{\phi}$ and $\hat{\theta}$ for MUSIC, and $\hat{\alpha}_\theta$ and $\hat{\bar{\theta}}$ for the dispersive methods are listed in Table 3.1. The first column shows the data file name and the data size in computing each $\hat{\boldsymbol{R}}$. The θ_s are the suggested nominal azimuth angles. The plots are shown in Fig.3.4 to Fig.3.8. Each figure contains 7 subfigures, and each subfigure is based on all 64K samples of one data file. All figures are normalized such that the

peak has a value of 0 dB.

Findings:

(a) $\hat{\phi}$ from MUSIC are small in most cases, thus justifying Eq.(3.18).

(b) From Fig.3.5, DISPARE I give local peaks at an $\alpha_\theta > 0^0$. However, the global peaks are at $\alpha_\theta = 0^0$ in most cases, and they are *false* peaks. This kind of result was also obtained from computer simulations in [2] and [3].

(c) Comparing Fig.3.5 and Fig.3.6, the corresponding profiles at $\alpha_\theta = 0^0$ are exactly the same. In fact, both DISPARE I and DISPARE II reduce to MUSIC (with $K = M_0$, $\phi = 0^0$) when $\alpha_\theta = \alpha_\phi = 0^0$.

(d) In some figures, there are trends that the cost function value increases with α_θ, resulting in an over-estimated α_θ.

(e) In general, the function values of BFDI are less dependent on α_θ. Thus, even if $\hat{\alpha}_\theta$ is not accurate, its adverse effect in estimating $\hat{\tilde{\theta}}$ would not be much. This may explain why BFDI gives better $\hat{\tilde{\theta}}$ estimates in general.

Remarks:

(a) The estimates of $\hat{\tilde{\theta}}$ are a little bit different from those shown in the April progress report. In the previous report, Model 1a was employed for $\alpha_\theta < 8^0$ and Model 2 was employed otherwise. Here, we use Model 1a regardless of α_θ.

(b) For iar_a1/64K, all methods give $\hat{\theta}/\hat{\tilde{\theta}} \geq 107^0$, which is much larger than θ_s (98.4^0). A similar situation occurs for vcs_c1. It is highly likely that the suggested azimuth angles θ_s are not the correct ones due to the random ionospheric scattering process. Thus, θ_s should be treated as a reference only.

Table 3.1: Settings and Results of Experiment 3.1

		MUSIC	DISP1	DISP2	MUDI	BFDI
(a)	ϕ / α_θ range	$0^0 : 30^0$	$0^0 : 30^0$	$0^0 : 30^0$	$0^0 : 30^0$	$0^0 : 30^0$
cfh_a1/64K	θ / $\bar{\theta}$ range	$100^0 : 250^0$	$100^0 : 250^0$	$100^0 : 250^0$	$100^0 : 250^0$	$100^0 : 250^0$
$\theta_s = 181.9^0$	$\hat{\phi}$ / $\hat{\alpha}_\theta$	0^0	0^0	15^0	19^0	22^0
	$\hat{\theta}$ / $\hat{\bar{\theta}}$	179^0	189^0	179^0	181^0	184^0
(b)	ϕ / α_θ range	$0^0 : 30^0$	$0^0 : 30^0$	$0^0 : 30^0$	$0^0 : 30^0$	$0^0 : 30^0$
iar_a1/64K	θ / $\bar{\theta}$ range	$0^0 : 150^0$	$0^0 : 150^0$	$0^0 : 150^0$	$0^0 : 150^0$	$0^0 : 150^0$
$\theta_s = 98.4^0$	$\hat{\phi}$ / $\hat{\alpha}_\theta$	14^0	0^0	22^0	30^0	26^0
	$\hat{\theta}$ / $\hat{\bar{\theta}}$	115^0	112^0	121^0	107^0	108^0
(c)	ϕ / α_θ range	$0^0 : 30^0$	$0^0 : 30^0$	$0^0 : 30^0$	$0^0 : 30^0$	$0^0 : 30^0$
vai_a1/64K	θ / $\bar{\theta}$ range	$150^0 : 300^0$	$150^0 : 300^0$	$150^0 : 300^0$	$150^0 : 300^0$	$150^0 : 300^0$
$\theta_s = 249.1^0$	$\hat{\phi}$ / $\hat{\alpha}_\theta$	0^0	0^0	16^0	18^0	18^0
	$\hat{\theta}$ / $\hat{\bar{\theta}}$	258^0	234^0	247^0	246^0	247^0
(d)	ϕ / α_θ range	$0^0 : 30^0$	$0^0 : 30^0$	$0^0 : 30^0$	$0^0 : 30^0$	$0^0 : 30^0$
vcs_a1/64K	θ / $\bar{\theta}$ range	$50^0 : 300^0$	$50^0 : 300^0$	$50^0 : 300^0$	$50^0 : 300^0$	$50^0 : 300^0$
$\theta_s = 181.5^0$	$\hat{\phi}$ / $\hat{\alpha}_\theta$	0^0	0^0	18^0	30^0	30^0
	$\hat{\theta}$ / $\hat{\bar{\theta}}$	226^0	164^0	163^0	158^0	168^0
(e)	ϕ / α_θ range	$0^0 : 30^0$	$0^0 : 30^0$	$0^0 : 30^0$	$0^0 : 30^0$	$0^0 : 30^0$
vcs_b1/64K	θ / $\bar{\theta}$ range	$100^0 : 250^0$	$100^0 : 250^0$	$100^0 : 250^0$	$100^0 : 250^0$	$100^0 : 250^0$
$\theta_s = 181.5^0$	$\hat{\phi}$ / $\hat{\alpha}_\theta$	0^0	0^0	5^0	20^0	24^0
	$\hat{\theta}$ / $\hat{\bar{\theta}}$	183^0	184^0	183^0	179^0	186^0
(f)	ϕ / α_θ range	$0^0 : 30^0$	$0^0 : 30^0$	$0^0 : 30^0$	$0^0 : 30^0$	$0^0 : 30^0$
vcs_c1/64K	θ / $\bar{\theta}$ range	$100^0 : 250^0$	$100^0 : 250^0$	$100^0 : 250^0$	$100^0 : 250^0$	$100^0 : 250^0$
$\theta_s = 181.5^0$	$\hat{\phi}$ / $\hat{\alpha}_\theta$	0^0	0^0	14^0	24^0	24^0
	$\hat{\theta}$ / $\hat{\bar{\theta}}$	197^0	192^0	194^0	192^0	187^0
(g)	ϕ / α_θ range	$0^0 : 30^0$	$0^0 : 30^0$	$0^0 : 30^0$	$0^0 : 30^0$	$0^0 : 30^0$
vcs_d1/64K	θ / $\bar{\theta}$ range	$100^0 : 250^0$	$100^0 : 250^0$	$100^0 : 250^0$	$100^0 : 250^0$	$100^0 : 250^0$
$\theta_s = 181.5^0$	$\hat{\phi}$ / $\hat{\alpha}_\theta$	4^0	0^0	18^0	21^0	19^0
	$\hat{\theta}$ / $\hat{\bar{\theta}}$	180^0	193^0	192^0	187^0	177^0

Figure 3.4: Plots of MUSIC Cost Function Values

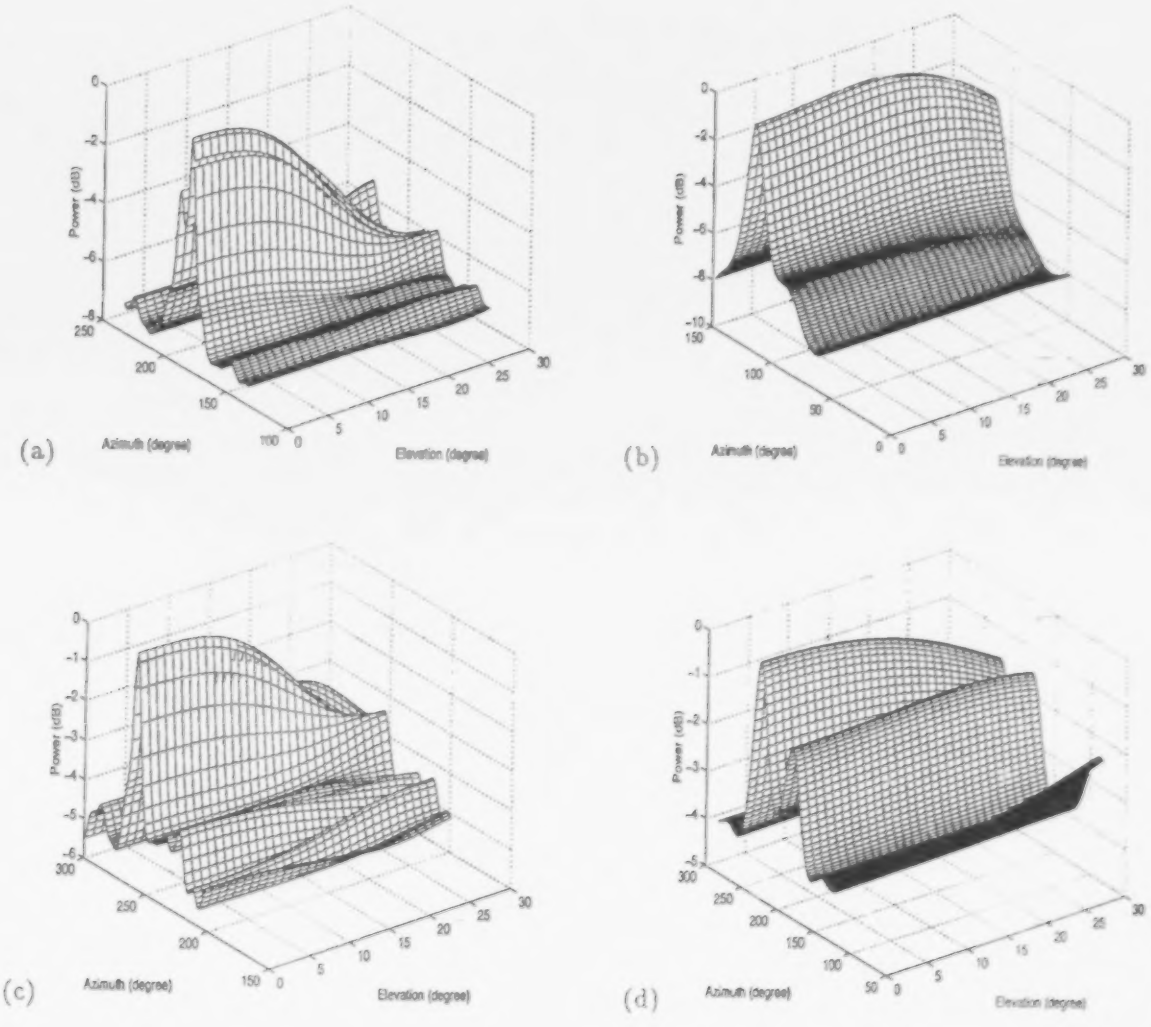

Figure 3.4: Plots of MUSIC Cost Function Values (Cont'd)

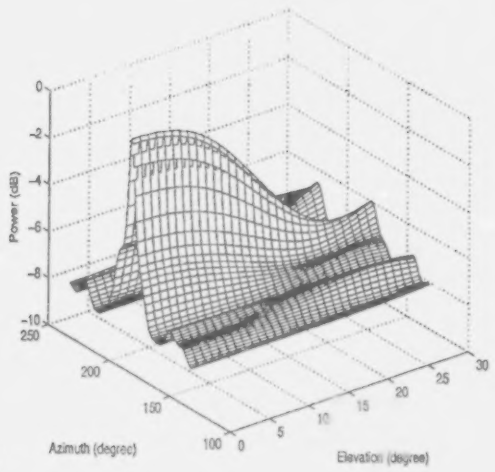

(e)

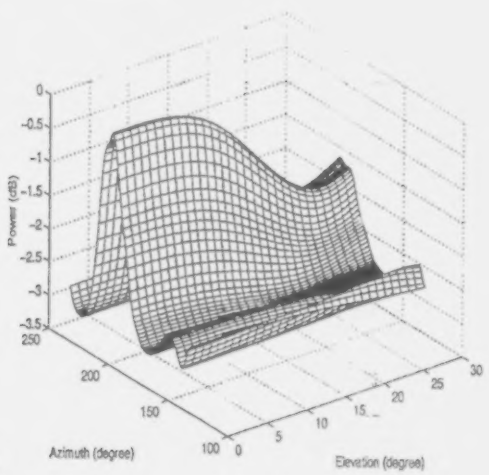

(f)

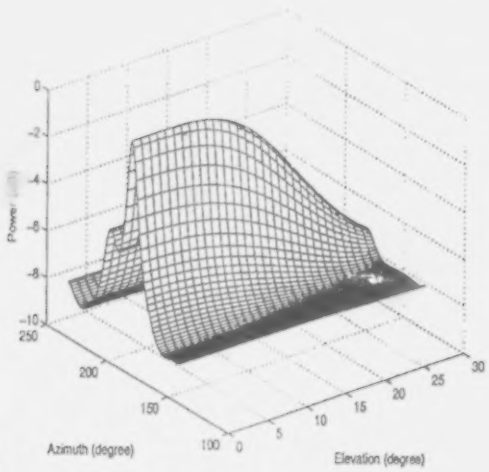

(g)

Figure 3.5: Plots of DISPARE I Cost Function Values

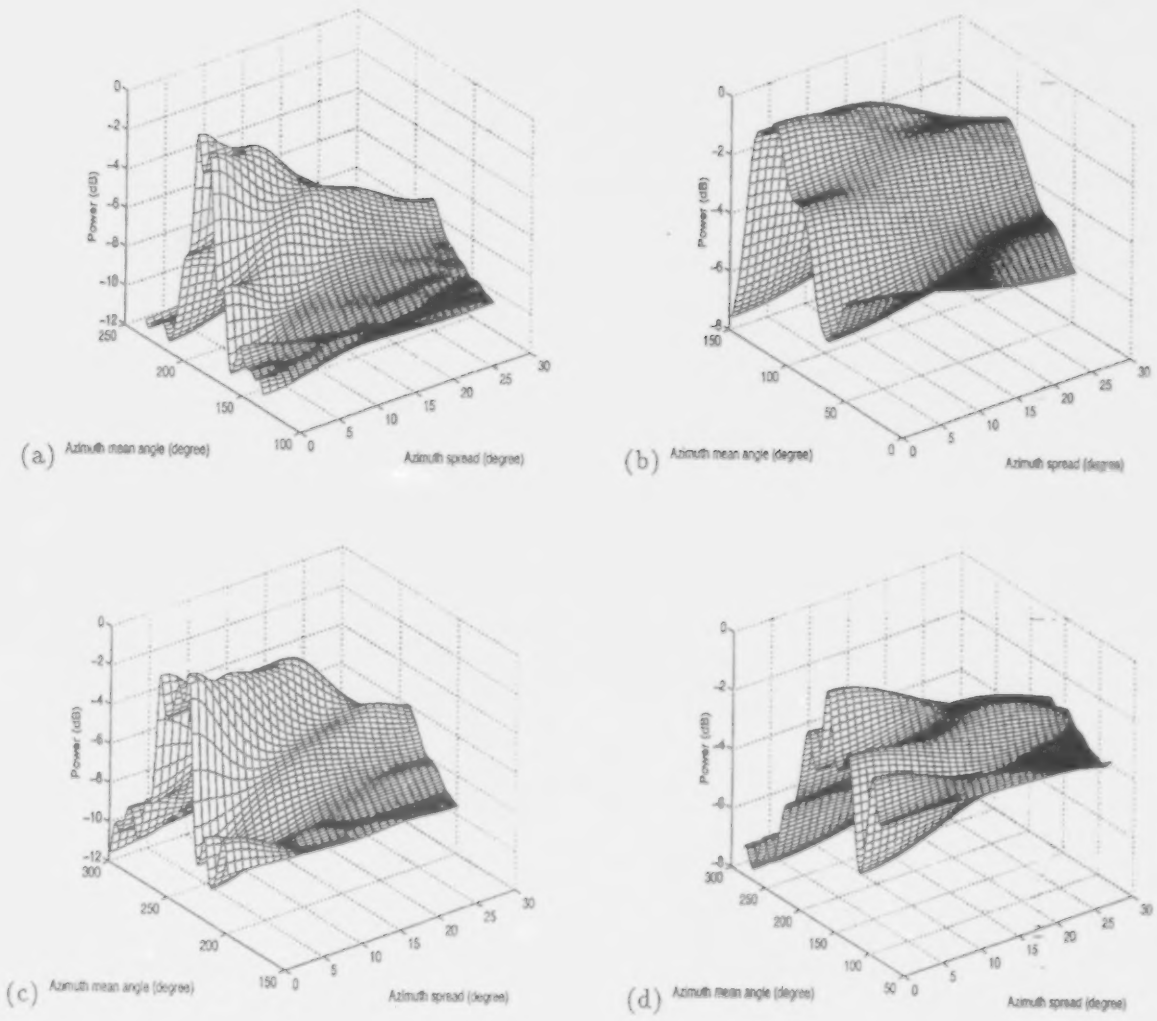

Figure 3.5: Plots of DISPARE I Cost Function Values (Cont'd)

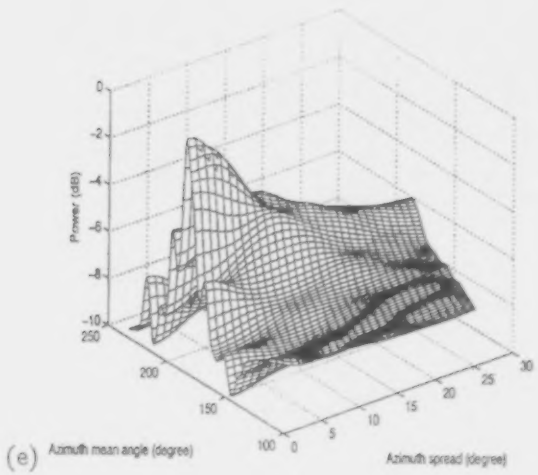

(e)

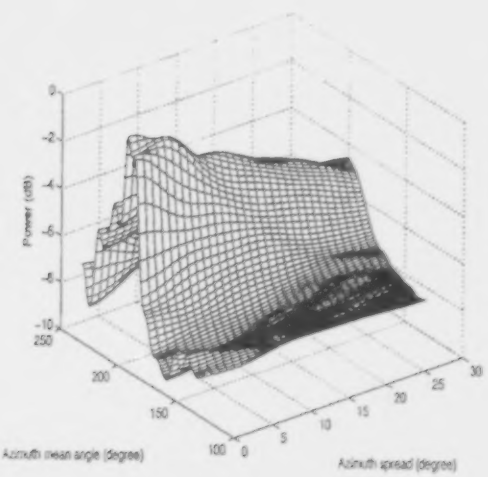

(f)

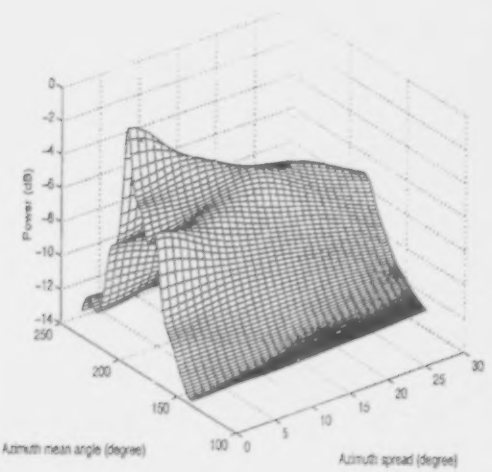

(g)

Figure 3.6: Plots of DISPARE II Cost Function Values

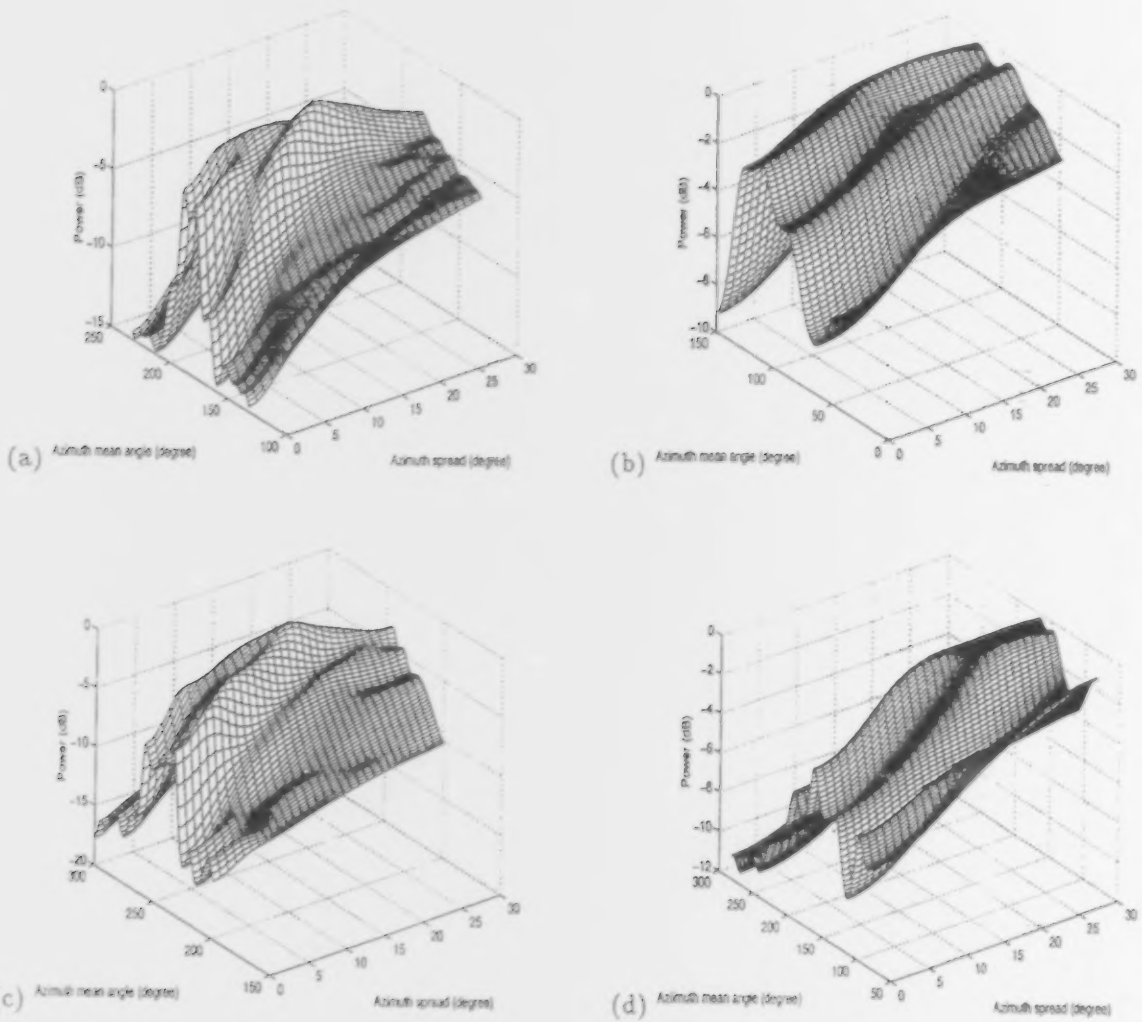

Figure 3.6: Plots of DISPARE II Cost Function Values (Cont'd)

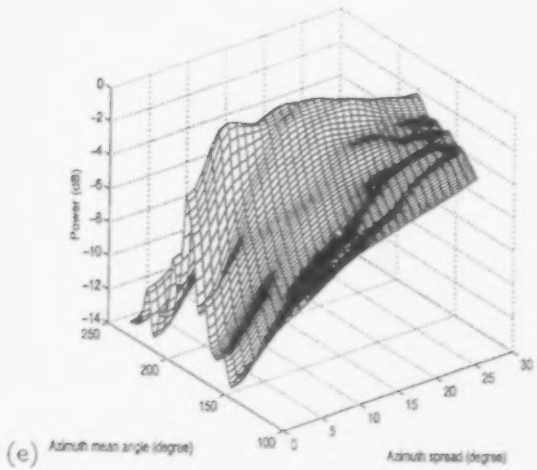

(e)

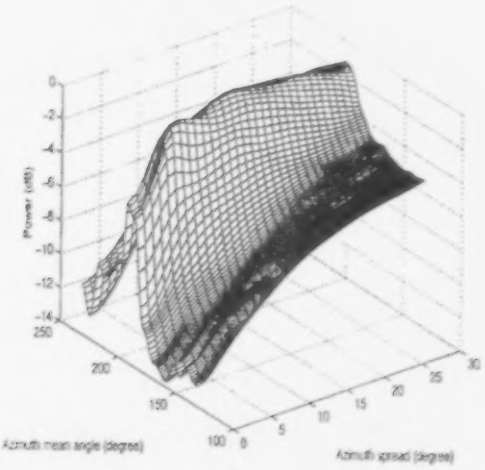

(f)

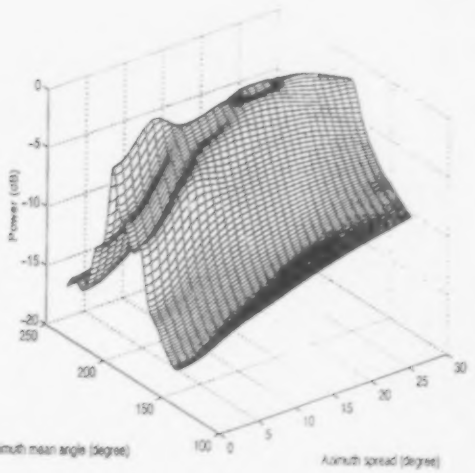

(g)

Figure 3.7: Plots of MUSIC DISC Cost Function Values

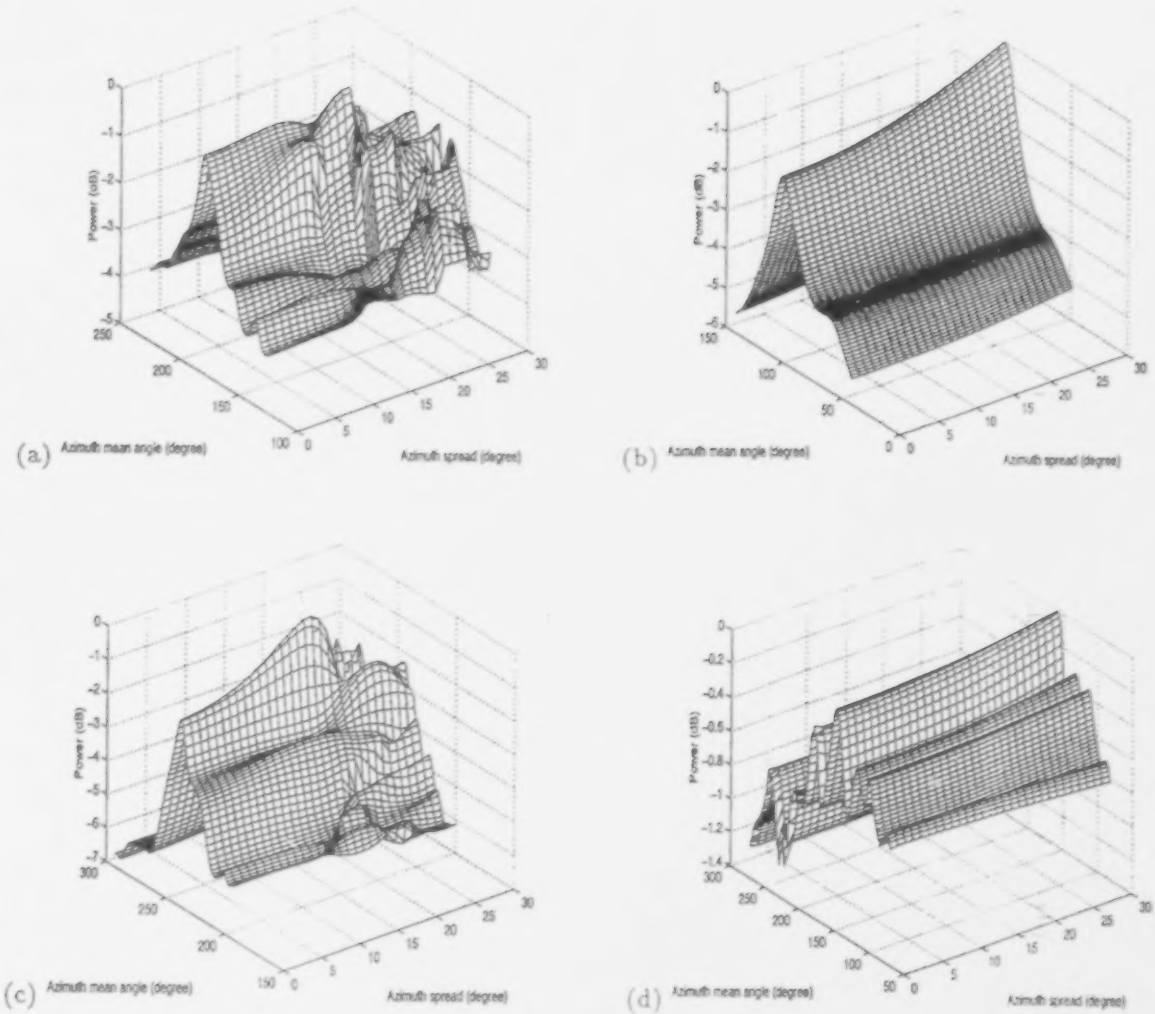

Figure 3.7: Plots of MUSIC DISC Cost Function Values (Cont'd)

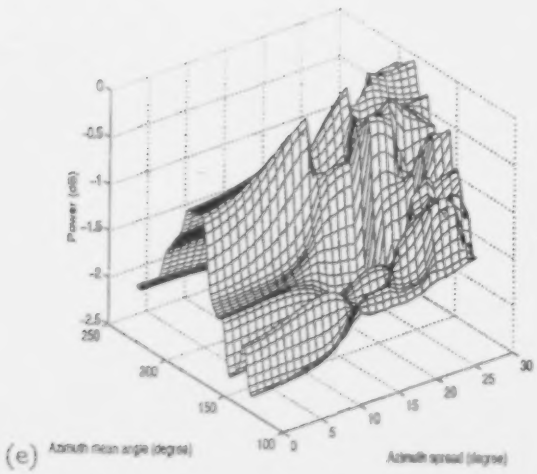

(e)

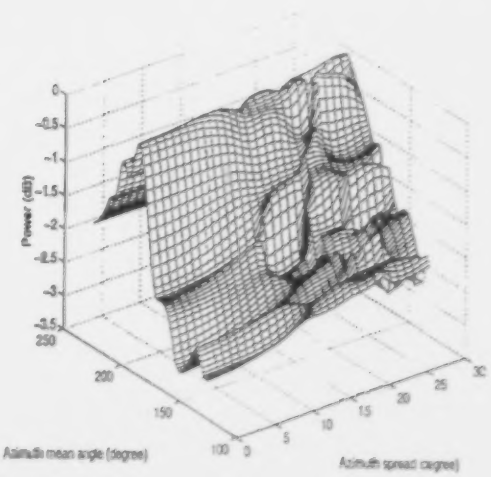

(f)

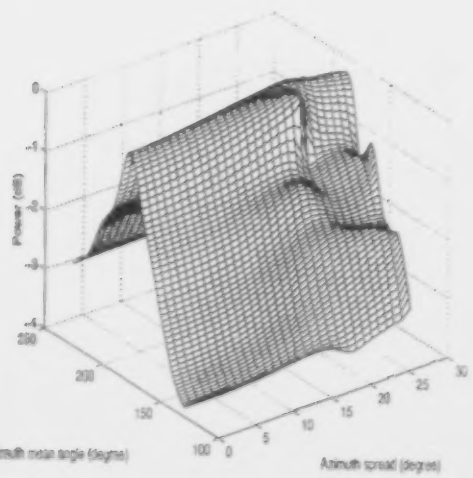

(g)

Figure 3.8: Plots of BF DISC Cost Function Values

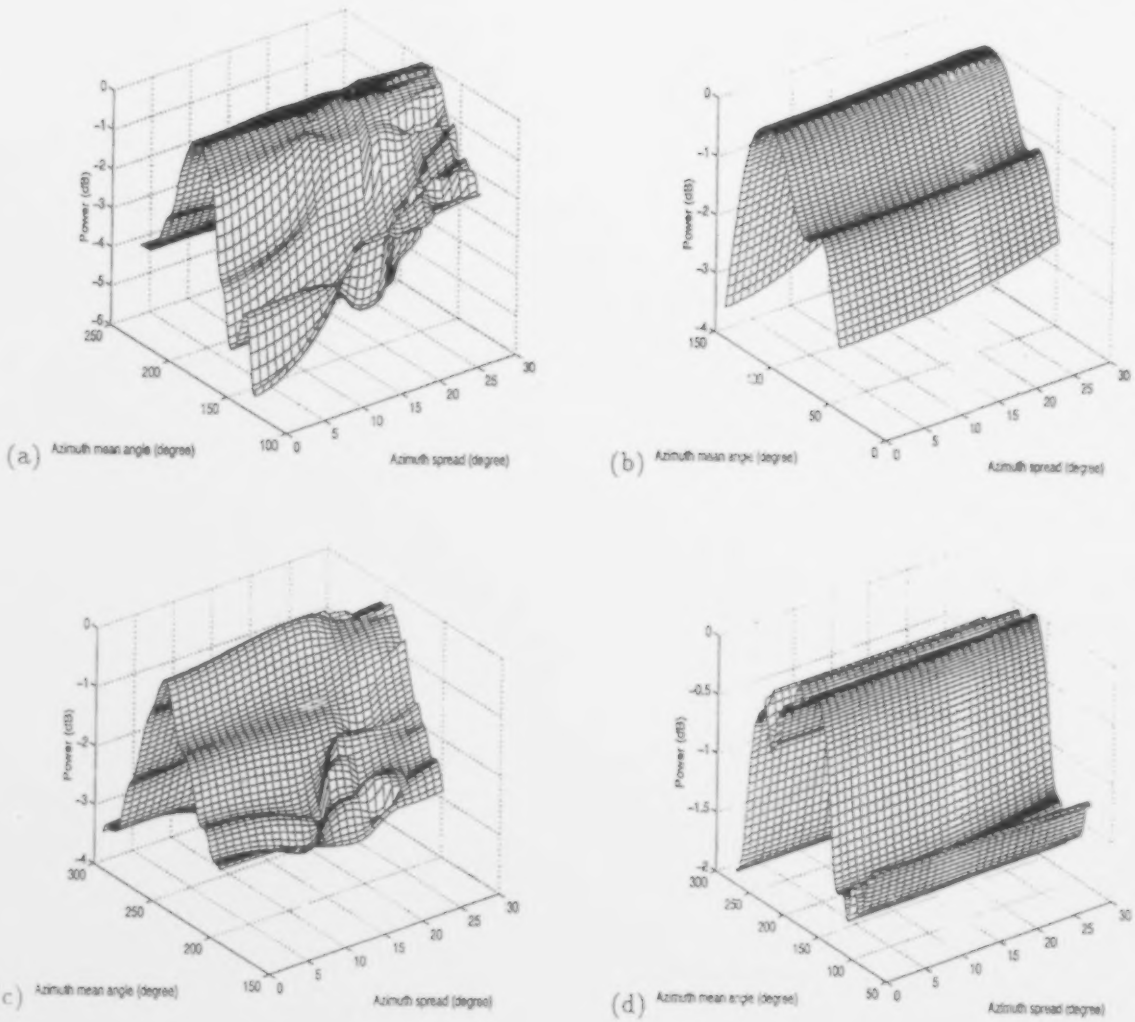

Figure 3.8: Plots of BF DISC Cost Function Values (Cont'd)

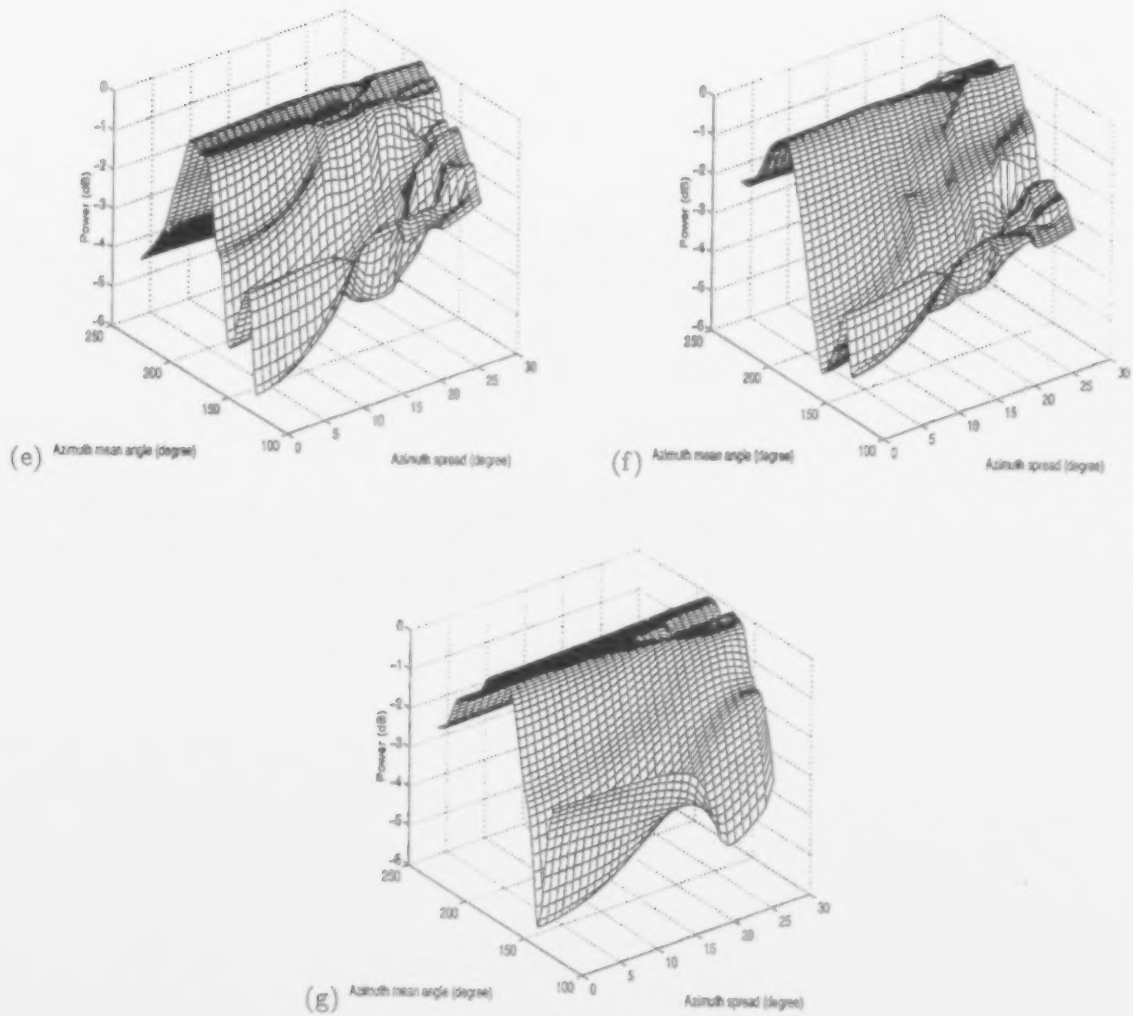

(e) (f) (g)

3.4 Testing of Models and Approaches

3.4.1 Testing of the Approximated Signal Models

In Section 3.1, we developed 3 approximated models to calculate $\bar{\boldsymbol{R}}$ by assuming a uniform distribution density function and a rectangular boundary. This subsection tests these 3 models. In this report, we perform many tests and compare the performances. The term "performance" refers to the consistency and the accuracy of the estimates $\hat{\bar{\theta}}$. Consistency is measured by the Standard Deviation (Std. Dev.) among the estimates, while accuracy is measured by the Root Mean Square Error (RMSE) with respect to the suggested nominal azimuth angle θ_s.

For a fair comparison, we only adopt Approach 1 in this subsection. That is, $\hat{\alpha}_\phi$ is a pre-determined value while $\hat{\bar{\theta}}$ and $\hat{\alpha}_\theta$ are found by an exhaustive 2-D search.

Experiment 3.2: Model 1a, Approach 1

Objective: To test Model 1a, Approach 1.

Scenario:
(a) We set $\hat{\alpha}_\phi = 0^0$ for Model 1a (i.e. neglecting elevation dispersiveness). Thus, $\hat{\bar{\phi}} = 0^0$ from Eq.(3.18).
(b) We assume 1 dispersed signal, thus $\hat{m}_0 = \hat{M}_0$ from Eq.(2.16). $\hat{M}_0$ is estimated by the approach outlined in Subsection 2.4.2.
(c) We perform a 2-dimensional search of $\bar{\theta}$ and α_θ. The search range of $\bar{\theta}$ is $\pm 50^0$ of the suggested nominal azimuth angle[2] with steps of 1^0. The search range of α_θ is from 0^0 to 28^0 with steps of 4^0.
(d) The MUSIC results act as a benchmark. Its estimates are found from a 2-dimensional search of θ and ϕ. The search range of θ is again $\pm 50^0$ of θ_s with steps of 1^0. The search range of ϕ is from 0^0 to 30^0 with steps of 3^0.

Results:
(a) The results are shown in Table 3.2.
(b) In the first two rows of each section, we list $E[\hat{\phi}]$ and $E[\hat{\theta}]$ for MUSIC, and $E[\hat{\alpha}_\theta]$

[2] The only reason not to search the whole range $0^0 : 360^0$ is to save the testing time. It is highly unlikely that the $\hat{\theta}$ differs from θ_s by more than 50^0.

and $E[\hat{\bar{\theta}}]$ for the dispersive methods.

(c) The terms "Bias", "Std. Dev." (standard deviation) and "RMSE" (root mean square error) are defined below. The Bias is not shown in the Table but can be calculated easily. The smallest value (the best one) of Std. Dev. and RMSE in each row is bold-faced.

$$\text{Bias} \triangleq E[\hat{\bar{\theta}}] - \theta_s \tag{3.21}$$

$$\text{Std. Dev.} \triangleq \sqrt{E[(\hat{\bar{\theta}} - E[\hat{\bar{\theta}}])^2]} \tag{3.22}$$

$$\text{RMSE} \triangleq \sqrt{E[(\hat{\bar{\theta}} - \theta_s)^2]} \tag{3.23}$$

$$\text{MSE} = (\text{Bias})^2 + (\text{Std. Dev.})^2 \tag{3.24}$$

Findings: (a) The estimates $\hat{\alpha}_\theta$ found by DISPARE I are nearly always equal to 0.

(b) MUSIC failed to give any reasonable estimate for vcs_a. The standard deviation was so large that the estimated $\hat{\theta}$ were actually randomly distributed across the 101^0 search range.

Experiment 3.3: Model 1b, Approach 1

Objective: To test Model 1b, Approach 1.

Scenario: (a) We use several ϕ-layers to approximate elevation dispersiveness. The ϕ-layers are pre-determined at $0^0, 2^0, 4^0, \ldots$, up to 14^0.

(b) We perform a 2-dimensional search on $\bar{\theta}$ and α_θ. The search ranges are the same as Experiment 3.2.

Results: The results are listed in Table 3.3.

Findings: The estimation performance is similar to that in Experiment 3.1. However, the computation load is nearly twice as much before (see Subsection 3.4.3).

Experiment 3.4: Model 2, Approach 1

Objective: To test Model 2, Approach 1.

Scenario: (a) We use multiple points to simulate both the azimuth and the elevation dispersiveness. As in Experiment 3.3, the ϕ-layers are at $0^0, 2^0, 4^0, \ldots$, up to 14^0. In

each ϕ-layer, the azimuth distance between adjacent points is 1^0.

(b) We perform a 2-dimensional search on $\bar{\theta}$ and α_θ. The search ranges are the same as Experiment 3.2.

Results: The results are shown in Table 3.4.

Findings: The estimation performance using Model 2 is marginally better than the previous 2 models.

To conclude, we would adopt Model 2 among the three models. The major advantage is its flexibility: we can simulate different distribution types of various regions simply by multiplying different weightings on the covariances of the points inside the region. Besides, Model 2 yields marginally better estimates than the other two models. Its only disadvantage is a larger computation load than Model 1a (Subsection 3.4.3). However, the load can be much reduced by using Approach 3, as will be shown in the next two sub-sections.

Table 3.2: Model 1a, Approach 1

		MUSIC	DISP1	DISP2	MUDI	BFDI
cfh_a/8K $E[\hat{M}_0] = 3.7$	$E[\hat{\phi}]$ / $E[\hat{\alpha}_\theta]$	2.2^0	0.0^0	12.0^0	18.2^0	22.8^0
	$E[\hat{\theta}]$ / $E[\hat{\bar{\theta}}]$	181.0^0	183.6^0	181.4^0	181.9^0	182.7^0
	Std. Dev.	3.2^0	4.8^0	2.8^0	4.6^0	2.7^0
	RMSE	3.4^0	5.1^0	2.8^0	4.6^0	2.8^0
iar_a/8K $E[\hat{M}_0] = 3.6$	$E[\hat{\phi}]$ / $E[\hat{\alpha}_\theta]$	16.3^0	0.0^0	25.6^0	27.6^0	24.8^0
	$E[\hat{\theta}]$ / $E[\hat{\bar{\theta}}]$	112.4^0	105.1^0	116.1^0	107.9^0	108.2^0
	Std. Dev.	5.8^0	10.4^0	14.2^0	8.7^0	6.1^0
	RMSE	15.1^0	12.4^0	22.7^0	12.9^0	11.6^0
vai_a/8K $E[\hat{M}_0] = 4.4$	$E[\hat{\phi}]$ / $E[\hat{\alpha}_\theta]$	1.6^0	0.0^0	14.8^0	19.2^0	18.0^0
	$E[\hat{\theta}]$ / $E[\hat{\bar{\theta}}]$	254.3^0	249.2^0	248.7^0	246.2^0	246.2^0
	Std. Dev.	8.4^0	9.3^0	3.5^0	1.9^0	1.5^0
	RMSE	9.9^0	9.3^0	3.5^0	3.5^0	3.2^0
vcs_a/8K $E[\hat{M}_0] = 4.0$	$E[\hat{\phi}]$ / $E[\hat{\alpha}_\theta]$	8.9^0	0.2^0	20.0^0	28.0^0	26.9^0
	$E[\hat{\theta}]$ / $E[\hat{\bar{\theta}}]$	197.6^0	166.5^0	163.2^0	166.2^0	176.3^0
	Std. Dev.	31.2^0	14.4^0	9.0^0	18.5^0	13.5^0
	RMSE	35.1^0	20.7^0	20.4^0	24.0^0	14.5^0
vcs_b/8K $E[\hat{M}_0] = 3.2$	$E[\hat{\phi}]$ / $E[\hat{\alpha}_\theta]$	0.8^0	0.0^0	9.3^0	23.6^0	24.6^0
	$E[\hat{\theta}]$ / $E[\hat{\bar{\theta}}]$	183.9^0	183.8^0	184.8^0	186.8^0	184.7^0
	Std. Dev.	5.2^0	2.6^0	7.2^0	8.0^0	3.6^0
	RMSE	5.7^0	3.5^0	7.9^0	9.5^0	4.8^0
vcs_c/8K $E[\hat{M}_0] = 4.0$	$E[\hat{\phi}]$ / $E[\hat{\alpha}_\theta]$	1.1^0	0.0^0	14.2^0	23.6^0	20.0^0
	$E[\hat{\theta}]$ / $E[\hat{\bar{\theta}}]$	196.3^0	190.2^0	194.9^0	197.8^0	189.6^0
	Std. Dev.	6.5^0	3.4^0	4.4^0	5.2^0	4.3^0
	RMSE	16.2^0	9.3^0	14.1^0	17.1^0	9.2^0
vcs_d/8K $E[\hat{M}_0] = 3.3$	$E[\hat{\phi}]$ / $E[\hat{\alpha}_\theta]$	5.6^0	0.0^0	15.7^0	21.0^0	19.9^0
	$E[\hat{\theta}]$ / $E[\hat{\bar{\theta}}]$	181.1^0	183.1^0	183.6^0	186.6^0	181.1^0
	Std. Dev.	4.4^0	6.5^0	5.1^0	12.4^0	8.4^0
	RMSE	4.4^0	6.7^0	5.5^0	13.4^0	8.4^0
Overall Result	Std. Dev.	13.0^0	8.3^0	7.6^0	9.9^0	6.9^0
	RMSE	16.4^0	11.0^0	13.3^0	13.8^0	8.8^0

Table 3.3: Model 1b, Approach 1

		MUSIC	DISP1	DISP2	MUDI	BFDI
cfh_a/8K $E[\hat{M}_0] = 3.7$	$E[\hat{\phi}]$ / $E[\hat{\alpha}_\theta]$	2.2^0	0.0^0	10.4^0	18.4^0	23.0^0
	$E[\hat{\theta}]$ / $E[\hat{\bar{\theta}}]$	181.0^0	183.5^0	183.0^0	182.3^0	183.3^0
	Std. Dev.	3.2^0	4.9^0	$\mathbf{2.7^0}$	4.8^0	3.4^0
	RMSE	3.4^0	5.1^0	$\mathbf{2.9^0}$	4.8^0	3.7^0
iar_a/8K $E[\hat{M}_0] = 3.6$	$E[\hat{\phi}]$ / $E[\hat{\alpha}_\theta]$	16.3^0	0.0^0	26.4^0	23.5^0	22.8^0
	$E[\hat{\theta}]$ / $E[\hat{\bar{\theta}}]$	112.4^0	103.4^0	115.4^0	109.1^0	108.7^0
	Std. Dev.	5.8^0	10.1^0	13.5^0	$\mathbf{2.2^0}$	4.6^0
	RMSE	15.1^0	11.3^0	21.7^0	$\mathbf{11.0^0}$	11.3^0
vai_a/8K $E[\hat{M}_0] = 4.4$	$E[\hat{\phi}]$ / $E[\hat{\alpha}_\theta]$	1.6^0	0.5^0	18.1^0	21.1^0	18.6^0
	$E[\hat{\theta}]$ / $E[\hat{\bar{\theta}}]$	254.3^0	249.8^0	247.2^0	246.3^0	245.9^0
	Std. Dev.	8.4^0	8.4^0	1.4^0	2.8^0	$\mathbf{1.3^0}$
	RMSE	9.9^0	8.4^0	$\mathbf{2.4^0}$	4.0^0	3.5^0
vcs_a/8K $E[\hat{M}_0] = 4.0$	$E[\hat{\phi}]$ / $E[\hat{\alpha}_\theta]$	8.9^0	0.0^0	20.5^0	26.4^0	17.3^0
	$E[\hat{\theta}]$ / $E[\hat{\bar{\theta}}]$	197.6^0	166.9^0	164.5^0	166.8^0	172.6^0
	Std. Dev.	31.2^0	14.4^0	$\mathbf{9.7^0}$	18.5^0	14.3^0
	RMSE	35.1^0	20.5^0	19.6^0	23.6^0	$\mathbf{16.9^0}$
vcs_b/8K $E[\hat{M}_0] = 3.2$	$E[\hat{\phi}]$ / $E[\hat{\alpha}_\theta]$	0.8^0	0.0^0	12.4^0	23.7^0	23.2^0
	$E[\hat{\theta}]$ / $E[\hat{\bar{\theta}}]$	183.9^0	183.6^0	185.7^0	185.9^0	186.3^0
	Std. Dev.	5.2^0	$\mathbf{2.9^0}$	7.0^0	4.2^0	4.6^0
	RMSE	5.7^0	$\mathbf{3.5^0}$	8.1^0	6.1^0	6.7^0
vcs_c/8K $E[\hat{M}_0] = 4.0$	$E[\hat{\phi}]$ / $E[\hat{\alpha}_\theta]$	1.1^0	0.0^0	20.4^0	23.4^0	19.4^0
	$E[\hat{\theta}]$ / $E[\hat{\bar{\theta}}]$	196.3^0	191.2^0	198.2^0	197.9^0	190.8^0
	Std. Dev.	6.5^0	$\mathbf{3.7^0}$	4.6^0	5.7^0	5.6^0
	RMSE	16.2^0	$\mathbf{10.4^0}$	17.4^0	17.4^0	10.9^0
vcs_d/8K $E[\hat{M}_0] = 3.3$	$E[\hat{\phi}]$ / $E[\hat{\alpha}_\theta]$	5.6^0	0.0^0	17.9^0	19.1^0	19.9^0
	$E[\hat{\theta}]$ / $E[\hat{\bar{\theta}}]$	181.1^0	185.5^0	183.9^0	184.7^0	182.9^0
	Std. Dev.	4.4^0	7.6^0	$\mathbf{4.3^0}$	10.7^0	8.3^0
	RMSE	$\mathbf{4.4^0}$	8.5^0	5.0^0	11.2^0	8.4^0
Overall Result	Std. Dev.	13.0^0	8.3^0	7.3^0	8.8^0	$\mathbf{7.2^0}$
	RMSE	16.4^0	10.9^0	13.4^0	13.0^0	9.8^0

Table 3.4: Model 2, Approach 1

		MUSIC	DISP1	DISP2	MUDI	BFDI
cfh_a/8K $E[\hat{M}_:] = 3.7$	$E[\hat{\phi}]$ / $E[\hat{\alpha}_\theta]$	2.2^0	0.0^0	8.8^0	19.5^0	24.2^0
	$E[\hat{\theta}]$ / $E[\hat{\tilde{\theta}}]$	181.0^0	183.5^0	183.2^0	179.5^0	183.4^0
	Std. Dev.	$\mathbf{3.2^0}$	4.9^0	3.3^0	7.7^0	7.6^0
	RMSE	$\mathbf{3.4^0}$	5.1^0	3.5^0	8.1^0	7.8^0
iar_a/8K $E[\hat{M}_:] = 3.6$	$E[\hat{\phi}]$ / $E[\hat{\alpha}_\theta]$	16.3^0	0.0^0	27.6^0	28.0^0	26.9^0
	$E[\hat{\theta}]$ / $E[\hat{\tilde{\theta}}]$	112.4^0	103.4^0	112.4^0	107.9^0	108.5^0
	Std. Dev.	5.8^0	10.1^0	9.7^0	$\mathbf{3.2^0}$	4.2^0
	RMSE	15.1^0	11.3^0	17.1^0	$\mathbf{10.1^0}$	10.9^0
vai_a/8K $E[\hat{M}_:] = 4.4$	$E[\hat{\phi}]$ / $E[\hat{\alpha}_\theta]$	1.6^0	0.0^0	18.0^0	21.5^0	21.4^0
	$E[\hat{\theta}]$ / $E[\hat{\tilde{\theta}}]$	254.3^0	250.2^0	248.4^0	248.0^0	247.5^0
	Std. Dev.	8.4^0	8.4^0	$\mathbf{2.8^0}$	3.5^0	3.0^0
	RMSE	9.9^0	8.5^0	$\mathbf{2.9^0}$	3.6^0	3.4^0
vcs_a/8K $E[\hat{M}_:] = 4.0$	$E[\hat{\phi}]$ / $E[\hat{\alpha}_\theta]$	8.9^0	0.2^0	23.6^0	28.0^0	27.6^0
	$E[\hat{\theta}]$ / $E[\hat{\tilde{\theta}}]$	197.6^0	166.9^0	166.0^0	161.9^0	165.2^0
	Std. Dev.	31.2^0	14.4^0	$\mathbf{9.2^0}$	11.5^0	10.7^0
	RMSE	35.1^0	20.5^0	$\mathbf{18.0^0}$	22.8^0	19.5^0
vcs_b/8K $E[\hat{M}_:] = 3.2$	$E[\hat{\phi}]$ / $E[\hat{\alpha}_\theta]$	0.8^0	0.0^0	10.8^0	22.2^0	21.4^0
	$E[\hat{\theta}]$ / $E[\hat{\tilde{\theta}}]$	183.9^0	183.6^0	183.4^0	184.2^0	189.3^0
	Std. Dev.	5.2^0	$\mathbf{2.9^0}$	5.1^0	9.1^0	5.6^0
	RMSE	5.7^0	$\mathbf{3.5^0}$	5.4^0	9.5^0	9.6^0
vcs_c/8K $E[\hat{M}_:] = 4.0$	$E[\hat{\phi}]$ / $E[\hat{\alpha}_\theta]$	1.1^0	0.0^0	22.5^0	20.9^0	9.4^0
	$E[\hat{\theta}]$ / $E[\hat{\tilde{\theta}}]$	196.3^0	191.2^0	204.3^0	199.3^0	197.3^0
	Std. Dev.	6.5^0	3.7^0	6.3^0	4.6^0	$\mathbf{3.3^0}$
	RMSE	16.2^0	$\mathbf{10.4^0}$	23.6^0	18.4^0	16.1^0
vcs_d/8K $E[\hat{M}_:] = 3.3$	$E[\hat{\phi}]$ / $E[\hat{\alpha}_\theta]$	5.6^0	0.0^0	16.6^0	21.7^0	19.2^0
	$E[\hat{\theta}]$ / $E[\hat{\tilde{\theta}}]$	181.1^0	185.5^0	183.5^0	187.1^0	186.4^0
	Std. Dev.	4.4^0	7.6^0	3.9^0	8.3^0	7.7^0
	RMSE	$\mathbf{4.4^0}$	8.5^0	4.4^0	10.1^0	9.2^0
Overall Result	Std. Dev.	13.0^0	8.3^0	6.3^0	7.4^0	6.6^0
	RMSE	16.4^0	$\mathbf{11.0^0}$	13.3^0	13.2^0	12.0^0

3.4.2 Testing of Approaches

In Section 3.2, we suggested 3 approaches to estimate $\hat{\bar{\theta}}$. This subsection tests these approaches. As we have already done the Approach 1, we only test the other two approaches here.

Experiment 3.5: Approach 2, Model 2

Objective: To test Approach 2, Model 2.

Scenario:
(a) We use Model 2 to simulate a dispersed signal with a uniform distribution bounded by a rectangle. The distance between adjacent elevation points is 2^0, and between adjacent azimuth points is 1^0.
(b) We set $\hat{\bar{\phi}} = \hat{\alpha}_\phi$ and $\hat{\alpha}_\phi = \frac{1}{2}\hat{\alpha}_\theta$.
(c) We perform a 2-dimensional search on $\bar{\theta}$ and α_θ. The search ranges are the same as Experiment 3.2.

Results: The results are shown in Table 3.5.

Findings: We got similar performance as Experiment 3.4.

Experiment 3.6: Approach 3, Model 2

Objective: To test Approach 3, Model 2.

Scenario:
(a) Like Experiment 3.5, we set $\hat{\bar{\phi}} = \hat{\alpha}_\phi$ and $\hat{\alpha}_\phi = \frac{1}{2}\hat{\alpha}_\theta$.
(b) We estimate $\hat{\alpha}_\theta$ from $\{\hat{\lambda}\}$. The $\hat{\alpha}_\theta$ are limited to a maximum of 30^0.
(c) We perform a 1-dimensional search on $\bar{\theta}$. The search range is $\pm$ 50^0 of the suggested nominal azimuth angle θ_s with steps of 1^0.

Results: The results are shown in Table 3.6.

Findings:
(a) Approach 3 gives much better estimates than the other two. One probable reason is: the dispersive methods are not good in estimating $\hat{\alpha}_\theta$ (a typical example is DISPARE I which nearly always estimates $\hat{\alpha}_\theta = 0^0$). Comparatively, we could obtain a more accurate $\hat{\alpha}_\theta$ from $\{\hat{\lambda}\}$, and thus a more accurate $\hat{\bar{\theta}}$.
(b) The computation load is also much reduced since only a 1-dimensional search is involved (see next subsection).

Table 3.5: Approach 2, Model 2

		MUSIC	DISP1	DISP2	MUDI	BFDI
cfh_a/8K $E[\hat{M}_0] = 3.7$	$E[\hat{\phi}]$ / $E[\hat{\alpha}_\theta]$	2.2^0	0.0^0	9.0^0	12.2^0	19.5^0
	$E[\hat{\theta}]$ / $E[\hat{\bar{\theta}}]$	181.0^0	183.6^0	183.5^0	184.0^0	188.6^0
	Std. Dev.	3.2^0	4.8^0	2.0^0	6.8^0	3.7^0
	RMSE	3.4^0	5.1^0	2.6^0	7.1^0	7.7^0
icr_a/8K $E[\hat{M}_0] = 3.6$	$E[\hat{\phi}]$ / $E[\hat{\alpha}_\theta]$	16.3^0	0.5^0	27.5^0	27.9^0	26.4^0
	$E[\hat{\theta}]$ / $E[\hat{\bar{\theta}}]$	112.4^0	105.1^0	109.6^0	107.6^0	106.3^0
	Std. Dev.	5.8^0	10.4^0	8.6^0	2.5^0	7.9^0
	RMSE	15.1^0	12.4^0	14.1^0	9.5^0	11.2^0
vai_a/8K $E[\hat{M}_0] = 4.4$	$E[\hat{\phi}]$ / $E[\hat{\alpha}_\theta]$	1.6^0	0.0^0	15.1^0	18.9^0	14.0^0
	$E[\hat{\theta}]$ / $E[\hat{\bar{\theta}}]$	254.3^0	249.2^0	248.5^0	248.1^0	246.8^0
	Std. Dev.	8.4^0	9.3^0	4.5^0	2.1^0	1.5^0
	RMSE	9.9^0	9.3^0	4.6^0	2.3^0	2.8^0
vcs_a/8K $E[\hat{M}_0] = 4.0$	$E[\hat{\phi}]$ / $E[\hat{\alpha}_\theta]$	8.9^0	0.4^0	24.9^0	27.6^0	27.8^0
	$E[\hat{\theta}]$ / $E[\hat{\bar{\theta}}]$	197.6^0	166.5^0	169.4^0	163.0^0	166.4^0
	Std. Dev.	31.2^0	14.4^0	9.8^0	12.8^0	7.9^0
	RMSE	35.1^0	20.7^0	15.6^0	22.5^0	17.1^0
vcs_b/8K $E[\hat{M}_0] = 3.2$	$E[\hat{\phi}]$ / $E[\hat{\alpha}_\theta]$	0.8^0	0.0^0	6.5^0	18.3^0	17.0^0
	$E[\hat{\theta}]$ / $E[\hat{\bar{\theta}}]$	183.9^0	183.8^0	184.7^0	187.3^0	190.1^0
	Std. Dev.	5.2^0	2.6^0	3.8^0	8.1^0	9.2^0
	RMSE	5.7^0	3.5^0	5.0^0	10.0^0	12.6^0
vcs_c/8K $E[\hat{M}_0] = 4.0$	$E[\hat{\phi}]$ / $E[\hat{\alpha}_\theta]$	1.1^0	0.0^0	8.2^0	17.0^0	16.8^0
	$E[\hat{\theta}]$ / $E[\hat{\bar{\theta}}]$	196.3^0	190.2^0	194.4^0	196.2^0	196.9^0
	Std. Dev.	6.5^0	3.4^0	7.2^0	4.6^0	4.0^0
	RMSE	16.2^0	9.3^0	14.8^0	15.4^0	15.9^0
vcs_d/8K $E[\hat{M}_0] = 3.3$	$E[\hat{\phi}]$ / $E[\hat{\alpha}_\theta]$	5.6^0	0.0^0	13.5^0	24.5^0	16.9^0
	$E[\hat{\theta}]$ / $E[\hat{\bar{\theta}}]$	181.1^0	183.1^0	184.2^0	190.0^0	186.9^0
	Std. Dev.	4.4^0	6.5^0	4.7^0	7.6^0	7.7^0
	RMSE	4.4^0	6.7^0	5.4^0	11.4^0	9.4^0
Overall Result	Std. Dev.	13.0^0	8.3^0	6.4^0	7.2^0	6.5^0
	RMSE	16.4^0	11.0^0	10.3^0	12.6^0	11.9^0

Table 3.6: Approach 3, Model 2

		MUSIC	DISP1	DISP2	MUDI	BFDI
cfh_a/8K $E[\hat{M}_0] = 3.7$	$E[\hat{\phi}]$ / $E[\hat{\alpha}_\theta]$	2.2^0	8.4^0	8.4^0	8.4^0	8.4^0
	$E[\hat{\theta}]$ / $E[\hat{\tilde{\theta}}]$	181.0^0	184.1^0	183.0^0	186.1^0	185.2^0
	Std. Dev.	3.2^0	1.8^0	2.0^0	1.9^0	2.9^0
	RMSE	3.4^0	2.8^0	2.3^0	4.6^0	4.4^0
iar_a/8K $E[\hat{M}_0] = 3.6$	$E[\hat{\phi}]$ / $E[\hat{\alpha}_\theta]$	16.3^0	20.4^0	20.4^0	20.4^0	20.4^0
	$E[\hat{\theta}]$ / $E[\hat{\tilde{\theta}}]$	112.4^0	110.7^0	112.3^0	108.3^0	108.4^0
	Std. Dev.	5.8^0	5.3^0	10.5^0	2.5^0	4.9^0
	RMSE	15.1^0	13.4^0	17.4^0	10.3^0	11.1^0
vai_a/8K $E[\hat{M}_0] = 4.4$	$E[\hat{\phi}]$ / $E[\hat{\alpha}_\theta]$	1.6^0	12.0^0	12.0^0	12.0^0	12.0^0
	$E[\hat{\theta}]$ / $E[\hat{\tilde{\theta}}]$	254.3^0	247.3^0	249.6^0	246.2^0	246.6^0
	Std. Dev.	8.4^0	3.5^0	4.2^0	1.9^0	1.2^0
	RMSE	9.9^0	3.9^0	4.2^0	3.4^0	2.8^0
vcs_a/8K $E[\hat{M}_0] = 4.0$	$E[\hat{\phi}]$ / $E[\hat{\alpha}_\theta]$	8.9^0	28.2^0	28.2^0	28.2^0	28.2^0
	$E[\hat{\theta}]$ / $E[\hat{\tilde{\theta}}]$	197.6^0	169.6^0	169.0^0	161.8^0	167.1^0
	Std. Dev.	31.2^0	10.2^0	10.3^0	12.4^0	8.3^0
	RMSE	35.1^0	15.7^0	16.3^0	23.3^0	16.7^0
vcs_b/8K $E[\hat{M}_0] = 3.2$	$E[\hat{\phi}]$ / $E[\hat{\alpha}_\theta]$	0.8^0	7.5^0	7.5^0	7.5^0	7.5^0
	$E[\hat{\theta}]$ / $E[\hat{\tilde{\theta}}]$	183.9^0	184.8^0	184.3^0	183.9^0	187.7^0
	Std. Dev.	5.2^0	3.4^0	3.3^0	8.0^0	5.1^0
	RMSE	5.7^0	4.7^0	4.4^0	8.4^0	8.1^0
vcs_c/8K $E[\hat{M}_0] = 4.0$	$E[\hat{\phi}]$ / $E[\hat{\alpha}_\theta]$	1.1^0	13.9^0	13.9^0	13.9^0	13.9^0
	$E[\hat{\theta}]$ / $E[\hat{\tilde{\theta}}]$	196.3^0	196.3^0	197.2^0	197.3^0	196.9^0
	Std. Dev.	6.5^0	3.2^0	4.6^0	2.9^0	2.0^0
	RMSE	16.2^0	15.2^0	16.4^0	16.1^0	15.6^0
vcs_d/8K $E[\hat{M}_0] = 3.3$	$E[\hat{\phi}]$ / $E[\hat{\alpha}_\theta]$	5.6^0	7.7^0	7.7^0	7.7^0	7.7^0
	$E[\hat{\theta}]$ / $E[\hat{\tilde{\theta}}]$	181.1^0	182.4^0	181.3^0	184.7^0	179.5^0
	Std. Dev.	4.4^0	4.9^0	5.7^0	8.8^0	4.3^0
	RMSE	4.4^0	5.0^0	5.7^0	9.4^0	4.7^0
Overall Result	Std. Dev.	13.0^0	5.3^0	6.6^0	6.7^0	4.7^0
	RMSE	16.4^0	10.2^0	11.4^0	12.5^0	10.4^0

3.4.3 Computation Load

Here, we compare the computation load of different models and approaches. The load is expressed in terms of the cpu time required by a Sparc 20 station running MATLAB codes. The time measurements started when $\hat{R}$ was available. The results are listed in Table 3.7. Except for MUSIC, the time shows the total execution time for all the 4 dispersive methods.

The cpu time quoted for MUSIC is much reduced when compared to that shown in the April report. It is because the inner for-loops are replaced by matrix manipulations. In all programs, we try to avoid looping wherever possible.

For Approach 3, the cpu time varies and is highly dependent on the estimated value $\hat{\alpha}_\theta$. Larger $\hat{\alpha}_\theta$ means computing more point covariances, and thus a longer cpu time.

Table 3.7: cpu Time Required

Approach and Model	cpu Time in Second
MUSIC	0.8s
Approach 1, Model 1a	18s
Approach 1, Model 1b	37s
Approach 1, Model 2	32s
Approach 2, Model 2	33s
Approach 3, Model 2	3s to 6s

To conclude the findings, in considering the implementation flexibility, the estimation performance achieved and the required computation load, we choose Model 2 to compute $\bar{R}$ and Approach 3 to estimate $\hat{\theta}$.

Chapter 4

Distribution Types and Combinations

4.1 Distribution Types

In Section 2.2, we learnt that if the power density function $p(\theta, \phi)$ is known, the true covariance $\tilde{R}$ can be computed. By assuming a certain distribution type, $p(\theta, \phi)$ and thus $\tilde{R}$ becomes a parametric function depending on $(\bar{\theta}, \bar{\phi}, \alpha_\theta, \alpha_\phi)$. In this section, we suggest the following distribution types.

- Distribution Type 1: a uniform distribution with a rectangular region,
- Distribution Type 2: a uniform distribution with a square region,
- Distribution Type 3: a uniform distribution with a semi-circular region,
- Distribution Type 4: a uniform distribution with a circular region,
- Distribution Type 5: a Gaussian distribution with a semi-circular region, and
- Distribution Type 6: a Gaussian distribution with a circular region.

The meaning of "region" is the area in which $p(\theta, \phi) > 0$. It can be viewed that $\alpha_\theta = \alpha_\phi$ for all types, and that the *centres* of the regions are at $(\theta = \bar{\theta}, \phi = 0^0)$ for Distribution Types 1, 3, and 5, and at $(\theta = \bar{\theta}, \phi = \alpha_\phi)$ for Distribution Types 2, 4, and 6. In all cases, the signal dispersion

in the ϕ-range starts at 0^0, as stated in Subsection 3.2.1.

All these distributions are realized by adding weightings on the covariances of different points in the Multiple Points Approximation Model (Subsection 3.1.3). Suppose the azimuth nominal angle is $\bar{\theta}_i$ and the azimuth dispersion is $\alpha_{\theta,i}$, then the weighting w_i at ($x_i \in \theta$-range, $y_i \in \phi$-range) are shown below. It is understood that $y_i \geq 0$.

Distribution Type 1: Uniform distribution with rectangular region[1]

$$w_i = \begin{cases} 1 & \text{if } |x_i - \bar{\theta}_i| < \alpha_{\theta,i} \text{ and } y_i < \alpha_{\theta,i} \\ 0 & \text{otherwise} \end{cases} \tag{4.1}$$

Distribution Type 2: Uniform distribution with square region

$$w_i = \begin{cases} 1 & \text{if } |x_i - \bar{\theta}_i| < \alpha_{\theta,i} \text{ and } |y_i - \alpha_{\theta,i}| < \alpha_{\theta,i} \\ 0 & \text{otherwise} \end{cases} \tag{4.2}$$

Distribution Type 3: Uniform distribution with semi-circular region

$$w_i = \begin{cases} 1 & \text{if } (x_i - \bar{\theta}_i)^2 + y_i^2 \leq \alpha_{\theta,i}^2 \\ 0 & \text{otherwise} \end{cases} \tag{4.3}$$

Distribution Type 4: Uniform distribution with circular region

$$w_i = \begin{cases} 1 & \text{if } (x_i - \bar{\theta}_i)^2 + (y_i - \alpha_{\theta,i})^2 \leq \alpha_{\theta,i}^2 \\ 0 & \text{otherwise} \end{cases} \tag{4.4}$$

Distribution Type 5: Gaussian distribution with semi-circular region

$$w_i = \begin{cases} e^{-\frac{d_1^2}{2d_2^2}} & \text{if } |d_1| \leq \alpha_{\theta,i} \\ 0 & \text{otherwise} \end{cases} \tag{4.5}$$

[1]Note that this is exactly the distribution type that we discussed in Chapter 3, but with a different notation. In the model presented in Chapter 3, the ϕ-range dispersion is from 0^0 to $2\alpha_\phi$ and $\bar{\phi} = \alpha_\phi = \frac{1}{2}\alpha_\theta$. Here, the ϕ-range dispersion is from 0^0 to α_ϕ and $\alpha_\phi = \alpha_\theta$. We use another notation here to get a unified view for the six distribution types.

where $d_1^2 = (x_i - \bar{\theta}_i)^2 + y_i^2$ and $d_2 = \frac{1}{3}\alpha_{\theta,i}$.

Distribution Type 6: Gaussian distribution with circular region

$$w_i = \begin{cases} e^{-\frac{d_1^2}{2d_2^2}} & \text{if } |d_1| \leq \alpha_{\theta,i} \\ 0 & \text{otherwise} \end{cases} \tag{4.6}$$

where $d_1^2 = (x_i - \bar{\theta}_i)^2 + (y_i - \alpha_{\theta,i})^2$ and $d_2 = \frac{1}{3}\alpha_{\theta,i}$.

Note that for Gaussian distributions in Types 5 and 6, d_2 is approximately the standard deviation of the distribution and we only consider a range of $\pm 3d_2$ from the region centre.

Fig.4.1 shows the weighting functions for different distribution types with $\bar{\theta}_i = 0$, $\alpha_{\theta,i} = \alpha_{\phi,i} = 10^0$. For Types 3 to 6, the circular and semi-circular boundaries are *not* smooth. The boundaries would become smooth only if the points of which their covariances would be computed are closely spaced.

Figure 4.1: Weighting Functions for Different Distribution Types

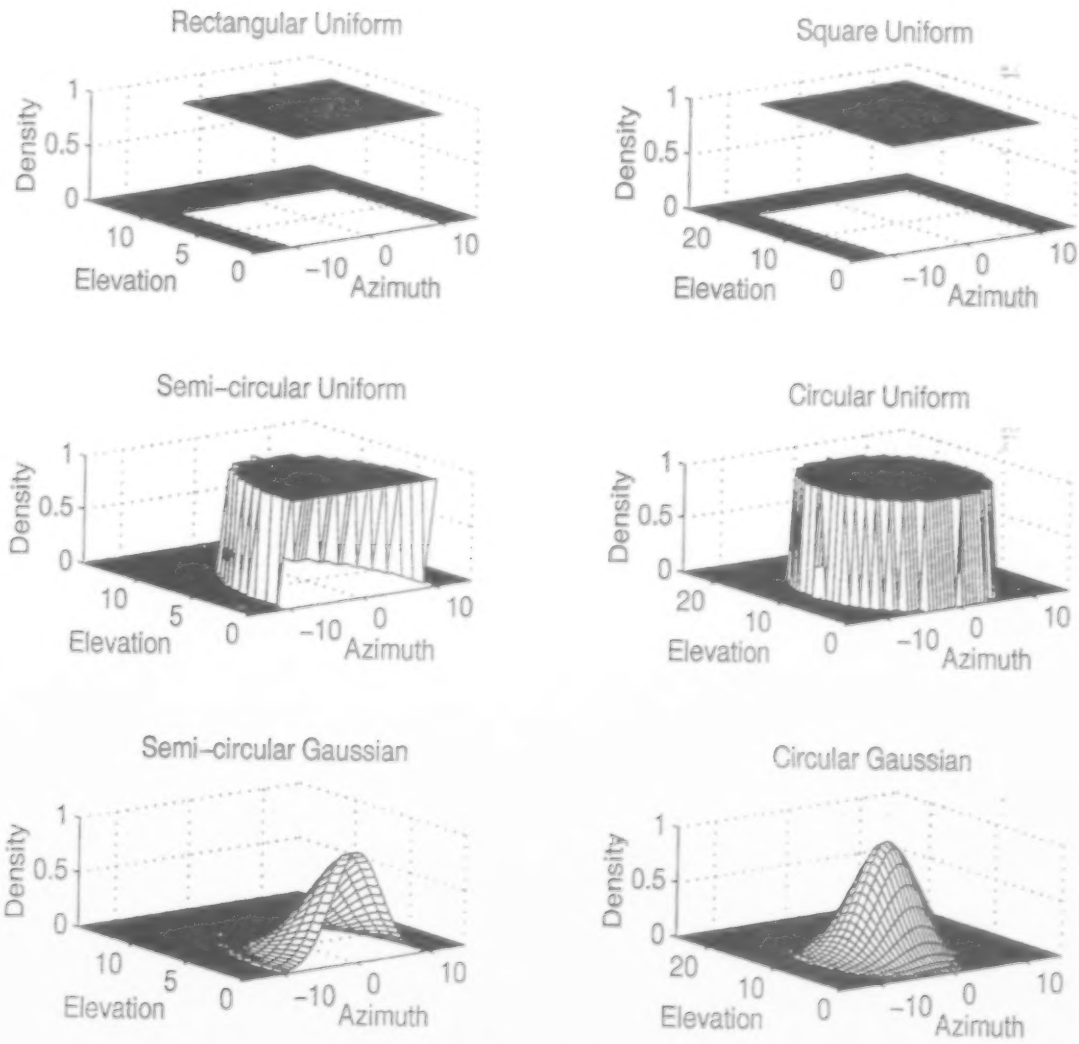

4.2 Testing of Distribution Types

Experiment 4.1: Different Distribution Types

Objective: To test the dispersive methods by using different distribution types.

Scenario:
(a) We use Approach 3: $\hat{\alpha}_\theta$ is estimated from $\{\hat{\lambda}\}$, $\hat{\bar{\theta}}$ is found from a 1-dimensional search on $\bar{\theta}$-range. The search range is $\theta_s \pm 50^0$ with steps of 1^0.
(b) MUSIC results are used for benchmark purposes.
(c) The number of signals K is assumed equal to 1.
(d) The six distribution types described in the last section are used.

Results:
(a) The results are listed in Tables 4.1 to 4.6.
(b) $\mathrm{E}[\hat{M}_0]$ and $\mathrm{E}[\hat{\alpha}_\theta]$ are the means of $\hat{M}_0$ and $\hat{\alpha}_\theta$, which had to be estimated for the dispersive methods.

Findings:
(a) Table 4.1 is actually a copy of Table 3.6, as both use the same distribution type.
(b) The estimation performance is not very sensitive to the distribution types. Types 1 and 2 give marginally better performances than the others.

Remarks:
(a) As stated in Step 1 of Subsection 3.2.4, we have to pre-calculate the eigenvalues of $\tilde{\boldsymbol{R}}$ at various α_θ before applying Approach 3. As these eigenvalues are dependent of the distribution type, we have to pre-store 6 sets of eigenvalue matrices before performing this experiment.
(b) By considering the computation requirement, Types 1 and 2 have obvious advantage over the others. From here onwards, Distribution Type 2 only is used.

Table 4.1: Distribution Type 1

		MUSIC	DISP1	DISP2	MUDI	BFDI
	$E[\hat{\theta}]$ / $E[\hat{\tilde{\theta}}]$	181.0^0	184.1^0	183.0^0	186.1^0	185.2^0
cfh_a/8K	Bias	-0.9^0	2.2^0	1.1^0	4.2^0	3.3^0
$E[\hat{M}_0] = 3.7$	Std. Dev.	3.2^0	1.8^0	2.0^0	1.9^0	2.9^0
$E[\hat{\alpha}_\theta] = 8.4^0$	RMSE	3.4^0	2.8^0	2.3^0	4.6^0	4.4^0
	$E[\hat{\theta}]$ / $E[\hat{\tilde{\theta}}]$	112.4^0	110.7^0	112.3^0	108.3^0	108.4^0
iar_a/8K	Bias	14.0^0	12.3^0	13.9^0	9.9^0	10.0^0
$E[\hat{M}_0] = 3.6$	Std. Dev.	5.8^0	5.3^0	10.5^0	2.5^0	4.9^0
$E[\hat{\alpha}_\theta] = 20.4^0$	RMSE	15.1^0	13.4^0	17.4^0	10.3^0	11.1^0
	$E[\hat{\theta}]$ / $E[\hat{\tilde{\theta}}]$	254.3^0	247.3^0	249.6^0	246.2^0	246.6^0
vai_a/8K	Bias	5.2^0	-1.8^0	0.5^0	-2.8^0	-2.5^0
$E[\hat{M}_0] = 4.4$	Std. Dev.	8.4^0	3.5^0	4.2^0	1.9^0	1.2^0
$E[\hat{\alpha}_\theta] = 12.0^0$	RMSE	9.9^0	3.9^0	4.2^0	3.4^0	2.8^0
	$E[\hat{\theta}]$ / $E[\hat{\tilde{\theta}}]$	197.6^0	169.6^0	169.0^0	161.8^0	167.1^0
vcs_a/8K	Bias	16.1^0	-11.9^0	-12.5^0	-19.7^0	-14.4^0
$E[\hat{M}_0] = 4.0$	Std. Dev.	31.2^0	10.2^0	10.3^0	12.4^0	8.3^0
$E[\hat{\alpha}_\theta] = 28.2^0$	RMSE	35.1^0	15.7^0	16.3^0	23.3^0	16.7^0
	$E[\hat{\theta}]$ / $E[\hat{\tilde{\theta}}]$	183.9^0	184.8^0	184.3^0	183.9^0	187.7^0
vcs_b/8K	Bias	2.4^0	3.3^0	2.8^0	2.4^0	6.2^0
$E[\hat{M}_0] = 3.2$	Std. Dev.	5.2^0	3.4^0	3.3^0	8.0^0	5.1^0
$E[\hat{\alpha}_\theta] = 7.5^0$	RMSE	5.7^0	4.7^0	4.4^0	8.4^0	8.1^0
	$E[\hat{\theta}]$ / $E[\hat{\tilde{\theta}}]$	196.3^0	196.3^0	197.2^0	197.3^0	196.9^0
vcs_c/8K	Bias	14.8^0	14.8^0	15.8^0	15.8^0	15.4^0
$E[\hat{M}_0] = 4.0$	Std. Dev.	6.5^0	3.2^0	4.6^0	2.9^0	2.0^0
$E[\hat{\alpha}_\theta] = 13.9^0$	RMSE	16.2^0	15.2^0	16.4^0	16.1^0	15.6^0
	$E[\hat{\theta}]$ / $E[\hat{\tilde{\theta}}]$	181.1^0	182.4^0	181.3^0	184.7^0	179.5^0
vcs_d/8K	Bias	-0.4^0	0.9^0	-0.2^0	3.2^0	-2.0^0
$E[\hat{M}_0] = 3.3$	Std. Dev.	4.4^0	4.9^0	5.7^0	8.8^0	4.3^0
$E[\hat{\alpha}_\theta] = 7.7^0$	RMSE	4.4^0	5.0^0	5.7^0	9.4^0	4.7^0
Overall	Std. Dev.	13.0^0	5.3^0	6.6^0	6.7^0	4.7^0
Result	RMSE	16.4^0	10.2^0	11.4^0	12.5^0	10.4^0

Table 4.2: Distribution Type 2

		MUSIC	DISP1	DISP2	MUDI	BFDI
	$E[\hat{\theta}]$ / $E[\hat{\tilde{\theta}}]$	181.0^0	183.8^0	183.3^0	184.2^0	185.2^0
cfh_a/8K	Bias	-0.9^0	1.9^0	1.4^0	2.3^0	3.3^0
$E[\hat{M}_0] = 3.7$	Std. Dev.	3.2^0	1.8^0	1.8^0	1.5^0	3.0^0
$E[\hat{\alpha}_\theta] = 7.9^0$	RMSE	3.4^0	2.6^0	2.3^0	2.7^0	4.5^0
	$E[\hat{\theta}]$ / $E[\hat{\tilde{\theta}}]$	112.4^0	109.1^0	108.8^0	107.3^0	109.3^0
iar_a/8K	Bias	14.0^0	10.7^0	10.4^0	8.9^0	10.9^0
$E[\hat{M}_0] = 3.6$	Std. Dev.	5.8^0	5.4^0	8.2^0	4.0^0	4.7^0
$E[\hat{\alpha}_\theta] = 18.8^0$	RMSE	15.1^0	12.0^0	13.2^0	9.8^0	11.9^0
	$E[\hat{\theta}]$ / $E[\hat{\tilde{\theta}}]$	254.3^0	247.2^0	248.0^0	246.4^0	247.3^0
vai_a/8K	Bias	5.2^0	-1.8^0	-1.1^0	-2.7^0	-1.8^0
$E[\hat{M}_0] = 4.4$	Std. Dev.	8.4^0	5.1^0	5.3^0	2.4^0	2.1^0
$E[\hat{\alpha}_\theta] = 10.8^0$	RMSE	9.9^0	5.4^0	5.4^0	3.6^0	2.8^0
	$E[\hat{\theta}]$ / $E[\hat{\tilde{\theta}}]$	197.6^0	170.2^0	172.0^0	163.6^0	167.6^0
vcs_a/8K	Bias	16.1^0	-11.3^0	-9.5^0	-17.9^0	-13.9^0
$E[\hat{M}_0] = 4.0$	Std. Dev.	31.2^0	11.7^0	11.7^0	9.8^0	8.0^0
$E[\hat{\alpha}_\theta] = 25.4^0$	RMSE	35.1^0	16.3^0	15.1^0	20.4^0	16.1^0
	$E[\hat{\theta}]$ / $E[\hat{\tilde{\theta}}]$	183.9^0	184.7^0	184.4^0	185.1^0	186.2^0
vcs_b/8K	Bias	2.4^0	3.2^0	2.9^0	3.6^0	4.7^0
$E[\hat{M}_0] = 3.2$	Std. Dev.	5.2^0	3.0^0	3.1^0	6.7^0	5.8^0
$E[\hat{\alpha}_\theta] = 7.0^0$	RMSE	5.7^0	4.4^0	4.3^0	7.6^0	7.5^0
	$E[\hat{\theta}]$ / $E[\hat{\tilde{\theta}}]$	196.3^0	196.2^0	199.3^0	195.0^0	196.7^0
vcs_c/8K	Bias	14.8^0	14.8^0	17.8^0	13.5^0	15.2^0
$E[\hat{M}_0] = 4.0$	Std. Dev.	6.5^0	3.5^0	6.9^0	2.3^0	2.1^0
$E[\hat{\alpha}_\theta] = 12.3^0$	RMSE	16.2^0	15.2^0	19.1^0	13.7^0	15.4^0
	$E[\hat{\theta}]$ / $E[\hat{\tilde{\theta}}]$	181.1^0	181.8^0	182.0^0	184.6^0	178.6^0
vcs_d/8K	Bias	-0.4^0	0.3^0	0.5^0	3.1^0	-2.9^0
$E[\hat{M}_0] = 3.3$	Std. Dev.	4.4^0	5.1^0	6.9^0	8.0^0	4.2^0
$E[\hat{\alpha}_\theta] = 7.5^0$	RMSE	4.4^0	5.1^0	6.9^0	8.6^0	5.1^0
Overall	Std. Dev.	13.0^0	5.9^0	7.0^0	5.8^0	4.7^0
Result	RMSE	16.4^0	10.2^0	11.1^0	11.0^0	10.3^0

Table 4.3: Distribution Type 3

		MUSIC	DISP1	DISP2	MUDI	BFDI
cfh_a/8K $E[\hat{M}_0] = 3.7$ $E[\hat{\alpha}_\theta] = 9.6^0$	$E[\hat{\theta}]$ / $E[\hat{\tilde{\theta}}]$	181.0^0	184.0^0	182.9^0	186.0^0	185.3^0
	Bias	-0.9^0	2.1^0	1.0^0	4.1^0	3.4^0
	Std. Dev.	3.2^0	1.8^0	2.0^0	2.0^0	3.3^0
	RMSE	3.4^0	2.7^0	2.3^0	4.6^0	4.7^0
iar_a/8K $E[\hat{M}_0] = 3.6$ $E[\hat{\alpha}_\theta] = 23.1^0$	$E[\hat{\theta}]$ / $E[\hat{\tilde{\theta}}]$	112.4^0	110.8^0	112.5^0	108.4^0	107.2^0
	Bias	14.0^0	12.4^0	14.1^0	10.0^0	8.8^0
	Std. Dev.	5.8^0	5.0^0	11.5^0	2.5^0	5.9^0
	RMSE	15.1^0	13.4^0	18.2^0	10.3^0	10.6^0
vai_a/8K $E[\hat{M}_0] = 4.4$ $E[\hat{\alpha}_\theta] = 14.0^0$	$E[\hat{\theta}]$ / $E[\hat{\tilde{\theta}}]$	254.3^0	247.2^0	249.8^0	246.4^0	246.8^0
	Bias	5.2^0	-1.9^0	0.7^0	-2.7^0	-2.3^0
	Std. Dev.	8.4^0	3.4^0	4.0^0	2.0^0	1.1^0
	RMSE	9.9^0	3.9^0	4.1^0	3.3^0	2.5^0
vcs_a/8K $E[\hat{M}_0] = 4.0$ $E[\hat{\alpha}_\theta] = 28.9^0$	$E[\hat{\theta}]$ / $E[\hat{\tilde{\theta}}]$	197.6^0	172.4^0	169.7^0	162.9^0	166.7^0
	Bias	16.1^0	-9.1^0	-11.8^0	-18.6^0	-14.8^0
	Std. Dev.	31.2^0	11.3^0	10.1^0	14.1^0	11.4^0
	RMSE	35.1^0	14.6^0	15.5^0	23.4^0	18.7^0
vcs_b/8K $E[\hat{M}_0] = 3.2$ $E[\hat{\alpha}_\theta] = 8.8^0$	$E[\hat{\theta}]$ / $E[\hat{\tilde{\theta}}]$	183.9^0	184.5^0	184.2^0	184.2^0	187.6^0
	Bias	2.4^0	3.0^0	2.7^0	2.7^0	6.1^0
	Std. Dev.	5.2^0	3.2^0	3.2^0	7.6^0	5.2^0
	RMSE	5.7^0	4.4^0	4.2^0	8.0^0	8.1^0
vcs_c/8K $E[\hat{M}_0] = 4.0$ $E[\hat{\alpha}_\theta] = 16.4^0$	$E[\hat{\theta}]$ / $E[\hat{\tilde{\theta}}]$	196.3^0	196.5^0	197.4^0	197.3^0	197.0^0
	Bias	14.8^0	15.0^0	15.9^0	15.8^0	15.5^0
	Std. Dev.	6.5^0	3.1^0	4.9^0	3.0^0	1.8^0
	RMSE	16.2^0	15.3^0	16.7^0	16.1^0	15.6^0
vcs_d/8K $E[\hat{M}_0] = 3.3$ $E[\hat{\alpha}_\theta] = 9.0^0$	$E[\hat{\theta}]$ / $E[\hat{\tilde{\theta}}]$	181.1^0	182.0^0	181.4^0	184.9^0	179.5^0
	Bias	-0.4^0	0.5^0	-0.1^0	3.4^0	-2.0^0
	Std. Dev.	4.4^0	4.7^0	5.5^0	8.9^0	4.5^0
	RMSE	4.4^0	4.8^0	5.5^0	9.6^0	4.9^0
Overall Result	Std. Dev.	13.0^0	5.5^0	6.7^0	7.2^0	5.7^0
	RMSE	16.4^0	9.9^0	11.5^0	12.5^0	10.9^0

Table 4.4: Distribution Type 4

		MUSIC	DISP1	DISP2	MUDI	BFDI
cfh_a/8K	$E[\hat{\theta}]$ / $E[\hat{\bar{\theta}}]$	181.0^0	183.8^0	183.2^0	184.4^0	185.1^0
$E[\hat{M}_0] = 3.7$	Bias	-0.9^0	1.9^0	1.3^0	2.5^0	3.2^0
$E[\hat{\alpha}_\theta] = 9.1^0$	Std. Dev.	3.2^0	1.8^0	1.8^0	1.7^0	2.7^0
	RMSE	3.4^0	2.6^0	2.2^0	3.0^0	4.2^0
iar_a/8K	$E[\hat{\theta}]$ / $E[\hat{\bar{\theta}}]$	112.4^0	108.2^0	107.3^0	107.7^0	109.5^0
$E[\hat{M}_0] = 3.6$	Bias	14.0^0	9.8^0	8.9^0	9.3^0	11.1^0
$E[\hat{\alpha}_\theta] = 21.0^0$	Std. Dev.	5.8^0	5.8^0	8.1^0	5.3^0	4.2^0
	RMSE	15.1^0	11.4^0	12.0^0	10.7^0	11.8^0
vai_a/8K	$E[\hat{\theta}]$ / $E[\hat{\bar{\theta}}]$	254.3^0	247.7^0	248.5^0	246.3^0	247.1^0
$E[\hat{M}_0] = 4.4$	Bias	5.2^0	-1.4^0	-0.6^0	-2.8^0	-2.0^0
$E[\hat{\alpha}_\theta] = 12.3^0$	Std. Dev.	8.4^0	5.2^0	6.5^0	3.5^0	2.4^0
	RMSE	9.9^0	5.4^0	6.5^0	4.5^0	3.1^0
vcs_a/8K	$E[\hat{\theta}]$ / $E[\hat{\bar{\theta}}]$	197.6^0	169.9^0	171.6^0	163.3^0	167.0^0
$E[\hat{M}_0] = 4.0$	Bias	16.1^0	-11.6^0	-9.9^0	-18.2^0	-14.5^0
$E[\hat{\alpha}_\theta] = 27.6^0$	Std. Dev.	31.2^0	12.0^0	12.0^0	9.7^0	7.8^0
	RMSE	35.1^0	16.7^0	15.6^0	20.6^0	16.5^0
vcs_b/8K	$E[\hat{\theta}]$ / $E[\hat{\bar{\theta}}]$	183.9^0	184.5^0	184.1^0	185.2^0	186.3^0
$E[\hat{M}_0] = 3.2$	Bias	2.4^0	3.0^0	2.6^0	3.7^0	4.8^0
$E[\hat{\alpha}_\theta] = 8.1^0$	Std. Dev.	5.2^0	2.9^0	3.7^0	6.7^0	6.0^0
	RMSE	5.7^0	4.2^0	4.5^0	7.6^0	7.7^0
vcs_c/8K	$E[\hat{\theta}]$ / $E[\hat{\bar{\theta}}]$	196.3^0	196.0^0	201.4^0	194.7^0	196.9^0
$E[\hat{M}_0] = 4.0$	Bias	14.8^0	14.5^0	19.9^0	13.2^0	15.4^0
$E[\hat{\alpha}_\theta] = 13.7^0$	Std. Dev.	6.5^0	3.4^0	8.0^0	2.0^0	2.1^0
	RMSE	16.2^0	14.9^0	21.4^0	13.3^0	15.5^0
vcs_d/8K	$E[\hat{\theta}]$ / $E[\hat{\bar{\theta}}]$	181.1^0	182.4^0	182.1^0	185.2^0	178.6^0
$E[\hat{M}_0] = 3.3$	Bias	-0.4^0	0.9^0	0.6^0	3.7^0	-2.9^0
$E[\hat{\alpha}_\theta] = 8.7^0$	Std. Dev.	4.4^0	5.4^0	7.0^0	7.9^0	4.0^0
	RMSE	4.4^0	5.5^0	7.1^0	8.7^0	5.0^0
Overall Result	Std. Dev.	13.0^0	6.1^0	7.4^0	5.9^0	4.6^0
	RMSE	16.4^0	10.1^0	11.7^0	11.2^0	10.5^0

Table 4.5: Distribution Type 5

		MUSIC	DISP1	DISP2	MUDI	BFDI
cfh_a/8K $E[\hat{M}_0] = 3.7$ $E[\hat{\alpha}_\theta] = 15.5^0$	$E[\hat{\theta}]$ / $E[\hat{\tilde{\theta}}]$	181.0^0	184.0^0	183.2^0	186.3^0	186.2^0
	Bias	-0.9^0	2.1^0	1.3^0	4.4^0	4.3^0
	Std. Dev.	3.2^0	1.9^0	2.9^0	2.5^0	3.2^0
	RMSE	3.4^0	2.8^0	3.2^0	5.1^0	5.4^0
iar_a/8K $E[\hat{M}_0] = 3.6$ $E[\hat{\alpha}_\theta] = 28.6^0$	$E[\hat{\theta}]$ / $E[\hat{\tilde{\theta}}]$	112.4^0	108.9^0	113.3^0	108.7^0	107.5^0
	Bias	14.0^0	10.5^0	14.9^0	10.3^0	9.1^0
	Std. Dev.	5.8^0	5.9^0	11.6^0	2.4^0	7.7^0
	RMSE	15.1^0	12.1^0	18.9^0	10.5^0	11.9^0
vai_a/8K $E[\hat{M}_0] = 4.4$ $E[\hat{\alpha}_\theta] = 22.6^0$	$E[\hat{\theta}]$ / $E[\hat{\tilde{\theta}}]$	254.3^0	247.9^0	249.2^0	246.2^0	246.9^0
	Bias	5.2^0	-1.2^0	0.1^0	-2.9^0	-2.2^0
	Std. Dev.	8.4^0	4.6^0	6.0^0	2.3^0	1.4^0
	RMSE	9.9^0	4.8^0	6.0^0	3.7^0	2.6^0
vcs_a/8K $E[\hat{M}_0] = 4.0$ $E[\hat{\alpha}_\theta] = 30.0^0$	$E[\hat{\theta}]$ / $E[\hat{\tilde{\theta}}]$	197.6^0	168.7^0	165.6^0	162.0^0	168.8^0
	Bias	16.1^0	-12.8^0	-15.9^0	-19.5^0	-12.7^0
	Std. Dev.	31.2^0	12.6^0	10.5^0	14.7^0	9.2^0
	RMSE	35.1^0	18.0^0	19.0^0	24.4^0	15.7^0
vcs_b/8K $E[\hat{M}_0] = 3.2$ $E[\hat{\alpha}_\theta] = 14.6^0$	$E[\hat{\theta}]$ / $E[\hat{\tilde{\theta}}]$	183.9^0	184.3^0	183.9^0	185.0^0	188.3^0
	Bias	2.4^0	2.8^0	2.4^0	3.5^0	6.8^0
	Std. Dev.	5.2^0	2.9^0	3.3^0	7.3^0	4.5^0
	RMSE	5.7^0	4.1^0	4.0^0	8.1^0	8.1^0
vcs_c/8K $E[\hat{M}_0] = 4.0$ $E[\hat{\alpha}_\theta] = 25.8^0$	$E[\hat{\theta}]$ / $E[\hat{\tilde{\theta}}]$	196.3^0	195.5^0	196.3^0	195.0^0	195.0^0
	Bias	14.8^0	14.0^0	14.8^0	13.5^0	13.5^0
	Std. Dev.	6.5^0	2.4^0	4.8^0	2.7^0	2.0^0
	RMSE	16.2^0	14.2^0	15.6^0	13.8^0	13.6^0
vcs_d/8K $E[\hat{M}_0] = 3.3$ $E[\hat{\alpha}_\theta] = 14.8^0$	$E[\hat{\theta}]$ / $E[\hat{\tilde{\theta}}]$	181.1^0	181.8^0	181.7^0	185.1^0	179.8^0
	Bias	-0.4^0	0.3^0	0.2^0	3.6^0	-1.7^0
	Std. Dev.	4.4^0	4.4^0	5.5^0	8.9^0	4.4^0
	RMSE	4.4^0	4.4^0	5.5^0	9.6^0	4.7^0
Overall Result	Std. Dev.	13.0^0	6.0^0	7.1^0	7.3^0	5.3^0
	RMSE	16.4^0	10.3^0	12.3^0	12.5^0	10.0^0

Table 4.6: Distribution Type 6

		MUSIC	DISP1	DISP2	MUDI	BFDI
	$E[\hat{\theta}]$ / $E[\hat{\bar{\theta}}]$	181.0^0	182.5^0	181.9^0	184.1^0	185.3^0
cfh_a/8K	Bias	-0.9^0	0.6^0	0.0^0	2.2^0	3.4^0
$E[\tilde{M}_0] = 3.7$	Std. Dev.	3.2^0	6.6^0	6.7^0	$\mathbf{1.7^0}$	3.1^0
$E[\hat{\alpha}_\theta] = 14.1^0$	RMSE	3.4^0	6.6^0	6.7^0	$\mathbf{2.8^0}$	4.6^0
	$E[\hat{\theta}]$ / $E[\hat{\bar{\theta}}]$	112.4^0	104.5^0	102.8^0	109.3^0	109.8^0
iar_a/8K	Bias	14.0^0	6.1^0	4.4^0	10.9^0	11.3^0
$E[\tilde{M}_0] = 3.6$	Std. Dev.	5.8^0	7.3^0	11.3^0	6.7^0	$\mathbf{4.2^0}$
$E[\hat{\alpha}_\theta] = 28.3^0$	RMSE	15.1^0	$\mathbf{9.5^0}$	12.1^0	12.9^0	12.1^0
	$E[\hat{\theta}]$ / $E[\hat{\bar{\theta}}]$	254.3^0	248.1^0	244.8^0	246.9^0	247.4^0
vai_a/8K	Bias	5.2^0	-1.0^0	-4.3^0	-2.2^0	-1.7^0
$E[\tilde{M}_0] = 4.4$	Std. Dev.	8.4^0	9.8^0	7.3^0	9.1^0	$\mathbf{4.9^0}$
$E[\hat{\alpha}_\theta] = 17.9^0$	RMSE	9.9^0	9.8^0	8.5^0	9.4^0	$\mathbf{5.2^0}$
	$E[\hat{\theta}]$ / $E[\hat{\bar{\theta}}]$	197.6^0	176.0^0	174.5^0	164.4^0	168.4^0
vcs_a/8K	Bias	16.1^0	-5.5^0	-7.0^0	-17.1^0	-13.1^0
$E[\tilde{M}_0] = 4.0$	Std. Dev.	31.2^0	14.5^0	16.5^0	9.3^0	$\mathbf{2.7^0}$
$E[\hat{\alpha}_\theta] = 30.0^0$	RMSE	35.1^0	15.5^0	17.9^0	19.5^0	$\mathbf{13.4^0}$
	$E[\hat{\theta}]$ / $E[\hat{\bar{\theta}}]$	183.9^0	183.4^0	182.6^0	185.1^0	185.4^0
vcs_b/8K	Bias	2.4^0	1.9^0	1.1^0	3.6^0	3.9^0
$E[\tilde{M}_0] = 3.2$	Std. Dev.	5.2^0	$\mathbf{2.1^0}$	3.7^0	5.0^0	6.5^0
$E[\hat{\alpha}_\theta] = 12.5^0$	RMSE	5.7^0	$\mathbf{2.8^0}$	3.9^0	6.2^0	7.6^0
	$E[\hat{\theta}]$ / $E[\hat{\bar{\theta}}]$	196.3^0	198.3^0	208.3^0	194.5^0	198.2^0
vcs_c/8K	Bias	14.8^0	16.8^0	26.8^0	13.0^0	16.7^0
$E[\tilde{M}_0] = 4.0$	Std. Dev.	6.5^0	6.2^0	8.1^0	2.7^0	$\mathbf{2.5^0}$
$E[\hat{\alpha}_\theta] = 19.6^0$	RMSE	16.2^0	17.9^0	25.0^0	$\mathbf{13.2^0}$	16.9^0
	$E[\hat{\theta}]$ / $E[\hat{\bar{\theta}}]$	181.1^0	182.2^0	181.5^0	183.7^0	180.7^0
vcs_d/8K	Bias	-0.4^0	0.7^0	0.0^0	2.2^0	-0.8^0
$E[\tilde{M}_0] = 3.3$	Std. Dev.	$\mathbf{4.4^0}$	5.3^0	8.0^0	7.5^0	5.7^0
$E[\hat{\alpha}_\theta] = 13.9^0$	RMSE	$\mathbf{4.4^0}$	5.3^0	8.0^0	7.8^0	5.7^0
Overall	Std. Dev.	13.0^0	8.2^0	9.6^0	6.6^0	$\mathbf{4.5^0}$
Result	RMSE	16.4^0	10.9^0	14.4^0	11.4^0	$\mathbf{10.3^0}$

4.3 Combination of Dispersive Methods

Generally speaking, all the four dispersive methods give more stable estimates than MUSIC. These four methods have different cost functions and different rationales behind them. Here, we try to combine the methods by adding the normalized cost function values together. An example of adding the cost function values of DISP1 and BFDI is illustrated below.

Step 1 Compute the cost function values of f_{DISP1} and f_{BFDI} at various θ. Denote the two series of function values as two vectors fv_1 and fv_2.

Step 2 Normalize the vectors by dividing them by their norms.

$$fv_1 = \frac{fv_1}{\| fv_1 \|}, \qquad fv_2 = \frac{fv_2}{\| fv_2 \|}$$

Step 3 The combined cost function values are the elements of the vector

$$cfv = fv_1 + fv_2$$

We test for the following combinations.

- Combination 1: combine DISPARE I and BF DISC,
- Combination 2: combine DISPARE I, MUSIC DISC and BF DISC
- Combination 3: combine all the 4 dispersive methods.

As an example, the cost function values of an 8K vai_a data are plotted in Fig.4.2. The suggested nominal azimuth angle θ_s is around 250^0. The false peaks produced by DISPAREs have cost function values greater than the true peak, thus producing erroneous results. However, by combining with the DISCs, the true peak dominates.

Experiment 4.2: Combined Methods

Objective: To test the combined methods.

Scenario: Same as Experiment 4.1, and using Distribution Type 2 only. MUSIC results are used as a benchmark.

Results: The results are listed in Table 4.7. The terms COMB1, COMB2 and COMB3 are the abbreviations for Combinations 1 to 3 respectively.

Findings: The estimation performance is improved, but the computation load is also increased.

Remarks: This experiment shows another path of performance improvement. However, we do not go further on this path. Instead, in the next two chapters, we adjust various parameters to see if we can employ one particular dispersive method and achieve an even better estimation performance.

Figure 4.2: Cost Function Values for Different Methods and Combinations

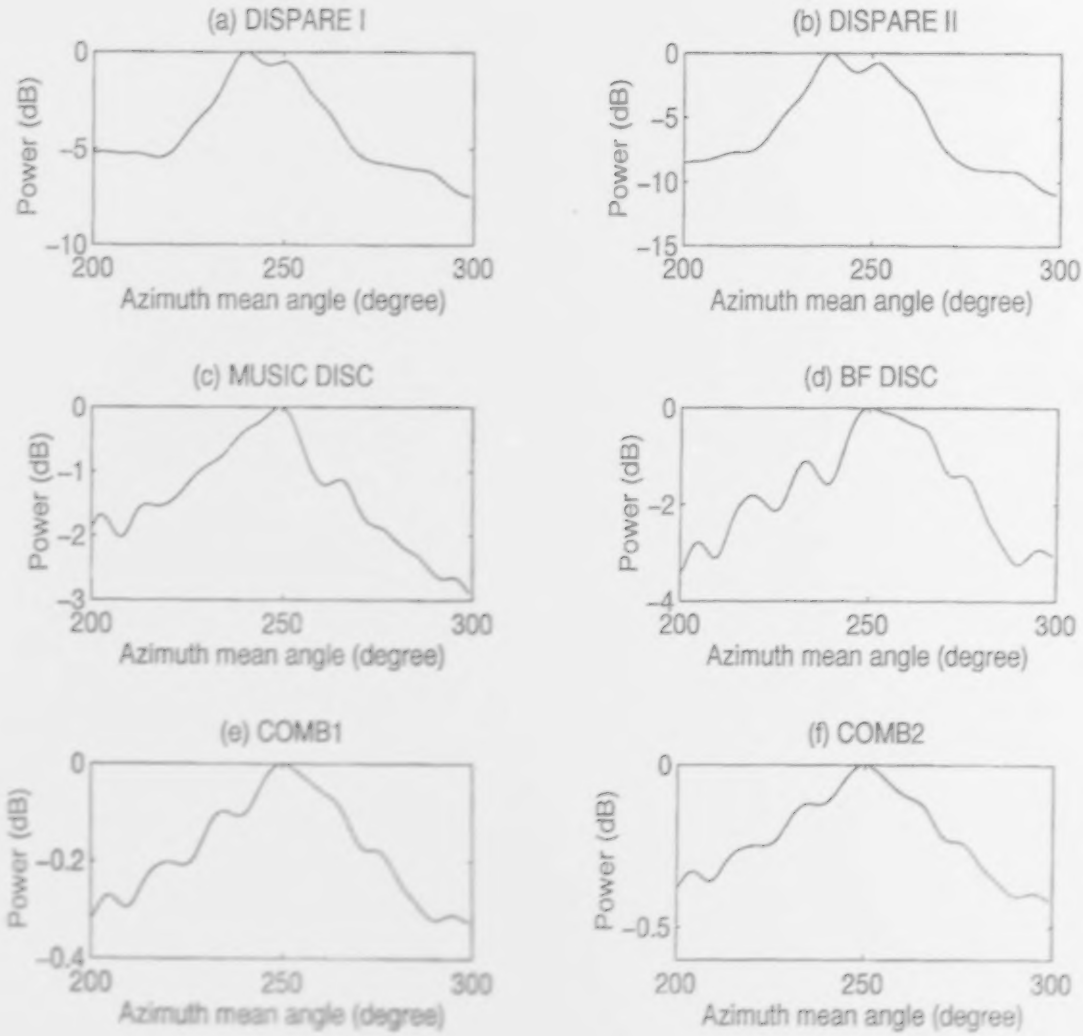

Table 4.7: Combination of Multiple Dispersive Methods

		MUSIC	COMB1	COMB2	COMB3
	$E[\hat{\theta}]$ / $E[\hat{\bar{\theta}}]$	181.0^0	184.6^0	184.3^0	184.0^0
cfh_a/8K	Bias	-0.9^0	2.7^0	2.4^0	2.1^0
$E[\hat{M}_0] = 3.7$	Std. Dev.	3.2^0	2.6^0	1.7^0	2.0^0
$E[\hat{\alpha}_\theta] = 7.9^0$	RMSE	3.4^0	3.8^0	3.0^0	2.9^0
	$E[\hat{\theta}]$ / $E[\hat{\bar{\theta}}]$	112.4^0	109.4^0	108.7^0	108.8^0
iar_a/8K	Bias	14.0^0	11.0^0	10.3^0	10.4^0
$E[\hat{M}_0] = 3.6$	Std. Dev.	5.8^0	4.2^0	4.1^0	4.0^0
$E[\hat{\alpha}_\theta] = 18.8^0$	RMSE	15.1^0	11.7^0	11.1^0	11.2^0
	$E[\hat{\theta}]$ / $E[\hat{\bar{\theta}}]$	254.3^0	247.7^0	247.0^0	247.7^0
vai_a/8K	Bias	5.2^0	-1.4^0	-2.1^0	-1.4^0
$E[\hat{M}_0] = 4.4$	Std. Dev.	8.4^0	3.2^0	2.3^0	3.5^0
$E[\hat{\alpha}_\theta] = 10.8^0$	RMSE	9.9^0	3.5^0	3.1^0	3.8^0
	$E[\hat{\theta}]$ / $E[\hat{\bar{\theta}}]$	197.6^0	168.3^0	168.9^0	169.6^0
vcs_a/8K	Bias	16.1^0	-13.2^0	-12.6^0	-11.9^0
$E[\hat{M}_0] = 4.0$	Std. Dev.	31.2^0	8.4^0	3.3^0	3.8^0
$E[\hat{\alpha}_\theta] = 25.4^0$	RMSE	35.1^0	15.7^0	13.0^0	12.5^0
	$E[\hat{\theta}]$ / $E[\hat{\bar{\theta}}]$	183.9^0	185.7^0	185.2^0	185.2^0
vcs_b/8K	Bias	2.4^0	4.2^0	3.7^0	3.7^0
$E[\hat{M}_0] = 3.2$	Std. Dev.	5.2^0	3.8^0	4.2^0	3.2^0
$E[\hat{\alpha}_\theta] = 7.0^0$	RMSE	5.7^0	5.7^0	5.6^0	4.8^0
	$E[\hat{\theta}]$ / $E[\hat{\bar{\theta}}]$	196.3^0	196.2^0	195.8^0	195.9^0
vcs_c/8K	Bias	14.8^0	14.8^0	14.3^0	14.4^0
$E[\hat{M}_0] = 4.0$	Std. Dev.	6.5^0	2.5^0	2.1^0	2.4^0
$E[\hat{\alpha}_\theta] = 12.3^0$	RMSE	16.2^0	15.0^0	14.5^0	14.6^0
	$E[\hat{\theta}]$ / $E[\hat{\bar{\theta}}]$	181.1^0	181.4^0	181.2^0	181.0^0
vcs_d/8K	Bias	-0.4^0	-0.1^0	-0.3^0	-0.5^0
$E[\hat{M}_0] = 3.3$	Std. Dev.	4.4^0	4.6^0	4.5^0	4.4^0
$E[\hat{\alpha}_\theta] = 7.5^0$	RMSE	4.4^0	4.6^0	4.5^0	4.5^0
Overall	Std. Dev.	13.0^0	4.6^0	3.3^0	3.4^0
Result	RMSE	16.4^0	9.9^0	9.0^0	8.9^0

Chapter 5

Fine Tuning of Parameter Settings

5.1 Grid Density

The parametric covariance $\bar{R}$ is found by using the Multiple Points Approximation Model. Obviously, if we use a larger number of points (or a finer grid), the $\bar{R}$ produced would be closer to the ideal one (from Eq.(2.10)). However, this is at the expense of a larger computation load. In this section, we study the effect of grid density.

Let us introduce the terms azimuth adjacent distance (aad) and elevation adjacent distance (ead): aad is the azimuth distance (in degree) between two azimuth adjacent points, and ead is the elevation distance accordingly. In the experiments of the last chapter, aad = 1^0 and ead = 2^0. We designate it as Grid Density Type 1. We believe that when α_θ is large, such grid density would give a good enough $\bar{R}$. However, for small α_θ, the $\bar{R}$ computed may differ too much from the ideal one (see Fig.3.1). In other words, should we adopt a finer grid when α_θ is small?

Here we suggest another grid density scheme, which we designate it as Grid Density Type 2: if $\hat{\alpha}_\theta \leq 10^0$, then aad = $\frac{1}{2}^0$ and ead = 1^0. If $\hat{\alpha}_\theta > 10^0$, then aad = 1^0 and ead = 2^0. In other words, we use a finer grid (than Type 1) at small $\hat{\alpha}_\theta$.

Experiment 5.1: Grid Density Type 2

Objective: To test Grid Density Type 2 and compare it with Grid Density Type 1 shown in Table 4.2.

Scenario: It is exactly the same as Experiment 4.1, and we use Distribution Type 2 (uniform distribution with square region) only.

Results: The results are listed in Tables 5.1.

Findings: Comparing with the results listed in Table 4.2, the estimation performance achieved here is roughly the same.

Remarks: As Grid Density Type 2 involves extra decisions and more computation but does not produce observable improvement, we keep using Grid Density Type 1.

Table 5.1: Grid Density Type 2

		MUSIC	DISP1	DISP2	MUDI	BFDI
	$E[\hat{\theta}]$ / $E[\hat{\tilde{\theta}}]$	181.0^0	183.8^0	183.2^0	184.2^0	185.2^0
cfh_a/8K	Bias	-0.9^0	1.9^0	1.3^0	2.3^0	3.3^0
$E[\tilde{M}_0] = 3.7$	Std. Dev.	3.2^0	1.8^0	1.9^0	1.5^0	3.0^0
$E[\tilde{\alpha}_\theta] = 7.9^0$	RMSE	3.4^0	2.6^0	2.4^0	2.7^0	4.5^0
	$E[\hat{\theta}]$ / $E[\hat{\tilde{\theta}}]$	112.4^0	109.1^0	108.8^0	107.3^0	109.3^0
iar_a/8K	Bias	14.0^0	10.7^0	10.4^0	8.9^0	10.9^0
$E[\tilde{M}_0] = 3.6$	Std. Dev.	5.8^0	5.4^0	8.2^0	4.0^0	4.6^0
$E[\tilde{\alpha}_\theta] = 18.8^0$	RMSE	15.1^0	12.0^0	13.2^0	9.8^0	11.9^0
	$E[\hat{\theta}]$ / $E[\hat{\tilde{\theta}}]$	254.3^0	247.2^0	248.2^0	246.4^0	247.3^0
vai_a/8K	Bias	5.2^0	-1.9^0	-0.8^0	-2.7^0	-1.8^0
$E[\tilde{M}_0] = 4.4$	Std. Dev.	8.4^0	5.0^0	5.7^0	2.4^0	2.1^0
$E[\tilde{\alpha}_\theta] = 10.8^0$	RMSE	9.9^0	5.4^0	5.8^0	3.6^0	2.8^0
	$E[\hat{\theta}]$ / $E[\hat{\tilde{\theta}}]$	197.6^0	170.2^0	172.0^0	163.6^0	167.6^0
vcs_a/8K	Bias	16.1^0	-11.3^0	-9.5^0	-17.9^0	-13.9^0
$E[\tilde{M}_0] = 4.0$	Std. Dev.	31.2^0	11.7^0	11.7^0	9.8^0	8.0^0
$E[\tilde{\alpha}_\theta] = 25.4^0$	RMSE	35.1^0	16.3^0	15.1^0	20.4^0	16.1^0
	$E[\hat{\theta}]$ / $E[\hat{\tilde{\theta}}]$	183.9^0	184.7^0	184.5^0	185.1^0	186.2^0
vcs_b/8K	Bias	2.4^0	3.2^0	3.0^0	3.6^0	4.7^0
$E[\tilde{M}_0] = 3.2$	Std. Dev.	5.2^0	3.0^0	3.1^0	6.7^0	5.8^0
$E[\tilde{\alpha}_\theta] = 7.0^0$	RMSE	5.7^0	4.4^0	4.3^0	7.6^0	7.4^0
	$E[\hat{\theta}]$ / $E[\hat{\tilde{\theta}}]$	196.3^0	196.2^0	199.3^0	195.0^0	196.7^0
vcs_c/8K	Bias	14.8^0	14.7^0	17.8^0	13.5^0	15.2^0
$E[\tilde{M}_0] = 4.0$	Std. Dev.	6.5^0	3.6^0	6.9^0	2.3^0	2.1^0
$E[\tilde{\alpha}_\theta] = 12.3^0$	RMSE	16.2^0	15.1^0	19.1^0	13.7^0	15.4^0
	$E[\hat{\theta}]$ / $E[\hat{\tilde{\theta}}]$	181.1^0	181.9^0	182.0^0	184.6^0	178.6^0
vcs_d/8K	Bias	-0.4^0	0.4^0	0.5^0	3.1^0	-2.9^0
$E[\tilde{M}_0] = 3.3$	Std. Dev.	4.4^0	5.2^0	6.9^0	8.0^0	4.2^0
$E[\tilde{\alpha}_\theta] = 7.5^0$	RMSE	4.4^0	5.2^0	6.9^0	8.5^0	5.1^0
Overall	Std. Dev.	13.0^0	5.9^0	7.0^0	5.8^0	4.7^0
Result	RMSE	16.4^0	10.1^0	11.2^0	11.0^0	10.3^0

5.2 Effective Signal Dimension

By assuming $K = 1$, we have $M_0 = m_0$. The current approach to estimating $\hat{M}_0$ is described in Subsection 2.4.2. There are several parameter settings that affect the estimation of $\hat{M}_0$, which in turn affect the estimation of $\hat{\theta}$. In this section, we adjust such parameter settings and investigate their effects.

5.2.1 Parameter Settings in Estimating $\hat{M}_0$

We adjust the following parameter settings.

(a) Currently $\hat{M}_0$ is derived from the estimated eigenvalues $\{\hat{\lambda}\}$. We try to derive it from:

(i) $\{\bar{\lambda}\}$, and

(ii) both $\{\hat{\lambda}\}$ and $\{\bar{\lambda}\}$

in Experiment 5.2. The set $\{\bar{\lambda}\}$ represents the eigenvalues of the parametric covariance $\bar{R}$ for a certain distribution type and a certain $\hat{\alpha}_\theta$. The criterion for estimating $\hat{M}_0$ by $\{\bar{\lambda}\}$ is similar to that described in Subsection 2.4.2, except replacing $\hat{\lambda}$ by $\bar{\lambda}$. For deriving $\hat{M}_0$ from both $\{\hat{\lambda}\}$ and $\{\bar{\lambda}\}$, there are some changes in Step 4 (of Subsection 2.4.2). The value of $\hat{M}_0$ would be determined as follows.

$$\sum_{i=1}^{\hat{M}_0} (\hat{\lambda}_i + \bar{\lambda}_i) \geq 2\gamma$$

$$\sum_{i=1}^{\hat{M}_0 - 1} (\hat{\lambda}_i + \bar{\lambda}_i) < 2\gamma$$

(b) Up until now a cp factor of 6 has been used. We try other numbers: 4, 2 and 0 in Experiment 5.3.

(c) A cv factor of 95% has been used until now. We try other coverages: 90%, 85% and 80% in Experiment 5.4.

(d) So far, we use $\bar{R}$ to estimate $\hat{M}_0$, thus $\hat{M}_0$ changes for each trial. Another approach is to fix $\hat{M}_0$ to a certain predetermined value. We try this in Experiment 5.5.

5.2.2 Testing

Experiment 5.2: Using Different Eigenvalue Sets

Objective: To test the dispersive methods by using different eigenvalue sets to estimate $\hat{M}_0$.

Scenario: To estimate $\hat{M}_0$ from (i) $\{\tilde{\lambda}\}$ and (ii) both $\{\hat{\lambda}\}$ and $\{\tilde{\lambda}\}$. Compensation factor = 6 and coverage factor = 95%.

Results: The results are shown in Tables 5.2 and 5.3. We compare them to Table 4.2, where $\hat{M}_0$ is estimated from $\{\hat{\lambda}\}$.

Findings: Using $\{\hat{\lambda}\}$ to estimate $\hat{M}_0$ yields marginally better estimation performance than the other approaches.

Experiment 5.3: Changing the Compensation (cp) Factor

Objective: To test the dispersive methods by using different cp factors.

Scenario: We derive $\hat{M}_0$ from $\{\hat{\lambda}\}$, cv = 95%. The compensation factors are set to 4, 2 and 0 in three tests. The selection cp = 0 simply means no compensation for noise.

Results: The results are shown in Tables 5.4 to 5.6. We compare them to Table 4.2, where cp = 6.

Findings: (a) The smaller the cp factor, the larger are the $\hat{M}_0$ and the $\hat{\alpha}_\delta$.

(b) cp = 6 gives marginally better results.

Remarks: We cannot use a cp factor larger than 6, as in many cases $\hat{M}_0$ is as large as 5 or 6.

Experiment 5.4: Changing the Coverage (cv) Factor

Objective: To test the dispersive methods by using different cv factors.

Scenario: We derive $\hat{M}_0$ from $\{\hat{\lambda}\}$, cp = 6. The coverage factors are set to 90%, 85% and 80% in three tests.

Results: The results are shown in Tables 5.7 to 5.9. We compare them to Table 4.2, where cv = 95%.

Findings: The coverage that yields the best estimation performance is around 90% to 95%.

Experiment 5.5: Fix $\hat{M}_0$ to a Predetermined Value

Objective: To test the dispersive methods with predetermined $\hat{M}_0$.

Scenario: $\hat{M}_0$ is fixed to 2, 4 and 6 in three tests.

Results: The results are shown in Tables 5.10 to 5.12.

Findings: The results shown in Table 4.2 are in general better than the above results. However, if $\hat{M}_0$ has to be fixed (say, for computation reason), it should be fixed between 2 and 4.

To conclude, the original parameter settings we choose in estimating $\hat{M}_0$ are good enough and need not be changed.

Table 5.2: $\hat{M}_0$ Estimated from $\{\bar{\lambda}\}$

		MUSIC	DISP1	DISP2	MUDI	BFDI
	$E[\hat{\theta}]$ / $E[\hat{\tilde{\theta}}]$	181.0^0	182.7^0	182.0^0	183.9^0	185.4^0
cfh_a/8K	Bias	-0.9^0	0.8^0	0.1^0	2.0^0	3.5^0
$E[\hat{M}_0] = 3.2$	Std. Dev.	3.2^0	2.7^0	4.1^0	3.7^0	3.4^0
$E[\hat{\alpha}_\theta] = 7.9^0$	RMSE	3.4^0	2.8^0	4.1^0	4.2^0	4.9^0
	$E[\hat{\theta}]$ / $E[\hat{\tilde{\theta}}]$	112.4^0	107.8^0	107.1^0	105.1^0	109.5^0
iar_a/8K	Bias	14.0^0	9.4^0	8.7^0	6.7^0	11.1^0
$E[\hat{M}_0] = 2.8$	Std. Dev.	5.8^0	3.9^0	6.2^0	4.5^0	4.0^0
$E[\hat{\alpha}_\theta] = 18.8^0$	RMSE	15.1^0	10.2^0	10.6^0	8.1^0	11.8^0
	$E[\hat{\theta}]$ / $E[\hat{\tilde{\theta}}]$	254.3^0	247.2^0	248.4^0	246.9^0	248.5^0
vai_a/8K	Bias	5.2^0	-1.9^0	-0.7^0	-2.2^0	-0.6^0
$E[\hat{M}_0] = 3.8$	Std. Dev.	8.4^0	5.1^0	5.3^0	3.6^0	2.9^0
$E[\hat{\alpha}_\theta] = 10.8^0$	RMSE	9.9^0	5.5^0	5.3^0	4.2^0	2.9^0
	$E[\hat{\theta}]$ / $E[\hat{\tilde{\theta}}]$	197.6^0	169.8^0	172.0^0	161.2^0	169.0^0
vcs_a/8K	Bias	16.1^0	-11.7^0	-9.5^0	-20.3^0	-12.5^0
$E[\hat{M}_0] = 3.8$	Std. Dev.	31.2^0	13.4^0	11.7^0	13.1^0	16.2^0
$E[\hat{\alpha}_\theta] = 25.4^0$	RMSE	35.1^0	17.8^0	15.1^0	24.2^0	20.4^0
	$E[\hat{\theta}]$ / $E[\hat{\tilde{\theta}}]$	183.9^0	184.9^0	183.6^0	184.5^0	186.9^0
vcs_b/8K	Bias	2.4^0	3.4^0	2.1^0	3.0^0	5.4^0
$E[\hat{M}_0] = 2.9$	Std. Dev.	5.2^0	4.2^0	5.8^0	4.9^0	6.1^0
$E[\hat{\alpha}_\theta] = 7.0^0$	RMSE	5.7^0	5.4^0	6.2^0	5.8^0	8.1^0
	$E[\hat{\theta}]$ / $E[\hat{\tilde{\theta}}]$	196.3^0	195.9^0	199.7^0	196.2^0	197.3^0
vcs_c/8K	Bias	14.8^0	14.4^0	18.2^0	14.7^0	15.8^0
$E[\hat{M}_0] = 4.4$	Std. Dev.	6.5^0	3.1^0	6.8^0	3.2^0	2.3^0
$E[\hat{\alpha}_\theta] = 12.3^0$	RMSE	16.2^0	14.7^0	19.4^0	15.1^0	16.0^0
	$E[\hat{\theta}]$ / $E[\hat{\tilde{\theta}}]$	181.1^0	181.1^0	181.3^0	182.5^0	181.0^0
vcs_d/8K	Bias	-0.4^0	-0.4^0	-0.2^0	1.0^0	-0.5^0
$E[\hat{M}_0] = 2.4$	Std. Dev.	4.4^0	4.2^0	4.4^0	6.6^0	3.3^0
$E[\hat{\alpha}_\theta] = 7.5^0$	RMSE	4.4^0	4.2^0	4.4^0	6.7^0	3.3^0
Overall	Std. Dev.	13.0^0	6.3^0	6.8^0	6.5^0	7.1^0
Result	RMSE	16.4^0	10.2^0	10.8^0	11.9^0	11.5^0

Table 5.3: $\hat{M}_0$ Estimated from both $\{\hat{\lambda}\}$ and $\{\bar{\lambda}\}$

		MUSIC	DISP1	DISP2	MUDI	BFDI
cfh_a/8K $E[\hat{M}_0] = 3.2$ $E[\hat{\alpha}_\theta] = 7.9^0$	$E[\bar{\theta}]$ / $E[\hat{\theta}]$	181.0^0	182.8^0	182.2^0	184.5^0	185.3^0
	Bias	-0.9^0	0.9^0	0.3^0	2.6^0	3.4^0
	Std. Dev.	3.2^0	2.7^0	4.1^0	3.5^0	3.2^0
	RMSE	3.4^0	2.8^0	4.1^0	4.4^0	4.7^0
iar_a/8K $E[\hat{M}_0] = 3.2$ $E[\hat{\alpha}_\theta] = 18.8^0$	$E[\bar{\theta}]$ / $E[\hat{\theta}]$	112.4^0	109.5^0	109.2^0	106.0^0	109.7^0
	Bias	14.0^0	11.1^0	10.8^0	7.6^0	11.3^0
	Std. Dev.	5.8^0	5.0^0	7.2^0	4.1^0	4.3^0
	RMSE	15.1^0	12.2^0	12.9^0	8.6^0	12.0^0
vai_a/8K $E[\hat{M}_0] = 4.0$ $E[\hat{\alpha}_\theta] = 10.8^0$	$E[\bar{\theta}]$ / $E[\hat{\theta}]$	254.3^0	247.6^0	243.4^0	247.9^0	248.1^0
	Bias	5.2^0	-1.5^0	-0.7^0	-1.2^0	-1.0^0
	Std. Dev.	8.4^0	4.8^0	4.7^0	2.2^0	1.4^0
	RMSE	9.9^0	5.0^0	4.7^0	2.5^0	1.7^0
vcs_a/8K $E[\hat{M}_0] = 3.8$ $E[\hat{\alpha}_\theta] = 25.4^0$	$E[\bar{\theta}]$ / $E[\hat{\theta}]$	197.6^0	169.7^0	171.9^0	161.5^0	169.1^0
	Bias	16.1^0	-11.9^0	-9.6^0	-20.0^0	-12.4^0
	Std. Dev.	31.2^0	13.4^0	11.7^0	13.3^0	16.2^0
	RMSE	35.1^0	17.9^0	15.1^0	24.0^0	20.4^0
vcs_b/8K $E[\hat{M}_0] = 3.0$ $E[\hat{\alpha}_\theta] = 7.0^0$	$E[\bar{\theta}]$ / $E[\hat{\theta}]$	183.9^0	184.7^0	184.3^0	184.2^0	186.8^0
	Bias	2.4^0	3.2^0	2.8^0	2.7^0	5.3^0
	Std. Dev.	5.2^0	4.2^0	4.7^0	5.2^0	6.2^0
	RMSE	5.7^0	5.3^0	5.4^0	5.9^0	8.2^0
vcs_c/8K $E[\hat{M}_0] = 4.2$ $E[\hat{\alpha}_\theta] = 12.3^0$	$E[\bar{\theta}]$ / $E[\hat{\theta}]$	196.3^0	195.9^0	199.1^0	196.3^0	197.1^0
	Bias	14.8^0	14.4^0	17.6^0	14.8^0	15.6^0
	Std. Dev.	6.5^0	3.1^0	6.7^0	3.1^0	2.3^0
	RMSE	16.2^0	14.7^0	18.8^0	15.1^0	15.8^0
vcs_d/8K $E[\hat{M}_0] = 2.7$ $E[\hat{\alpha}_\theta] = 7.5^0$	$E[\bar{\theta}]$ / $E[\hat{\theta}]$	181.1^0	182.0^0	181.9^0	184.1^0	179.8^0
	Bias	-0.4^0	0.5^0	0.4^0	2.6^0	-1.7^0
	Std. Dev.	4.4^0	5.4^0	6.9^0	7.0^0	4.0^0
	RMSE	4.4^0	5.4^0	6.9^0	7.4^0	4.3^0
Overall Result	Std. Dev.	13.0^0	6.4^0	7.0^0	6.5^0	7.1^0
	RMSE	16.4^0	10.5^0	11.1^0	11.9^0	11.5^0

Table 5.4: cp = 4

		MUSIC	DISP1	DISP2	MUDI	BFDI
cfh_a/8K $E[\hat{M}_0] = 4.0$ $E[\hat{\alpha}_\theta] = 8.1^0$	$E[\hat{\theta}]$ / $E[\hat{\theta}]$	181.0^0	183.1^0	182.1^0	182.5^0	185.5^0
	Bias	-0.9^0	1.2^0	0.2^0	0.6^0	3.6^0
	Std. Dev.	3.2^0	2.6^0	4.4^0	3.7^0	2.9^0
	RMSE	3.4^0	2.9^0	4.4^0	3.8^0	4.6^0
iar_a/8K $E[\hat{M}_0] = 3.8$ $E[\hat{\alpha}_\theta] = 19.0^0$	$E[\hat{\theta}]$ / $E[\hat{\theta}]$	112.4^0	108.7^0	109.1^0	108.4^0	109.0^0
	Bias	14.0^0	10.3^0	10.7^0	10.0^0	10.6^0
	Std. Dev.	5.8^0	5.1^0	9.2^0	4.3^0	4.6^0
	RMSE	15.1^0	11.5^0	14.1^0	10.9^0	11.6^0
vai_a/8K $E[\hat{M}_0] = 5.2$ $E[\hat{\alpha}_\theta] = 11.4^0$	$E[\hat{\theta}]$ / $E[\hat{\theta}]$	254.3^0	246.7^0	246.9^0	245.2^0	246.5^0
	Bias	5.2^0	-2.4^0	-2.2^0	-3.9^0	-2.6^0
	Std. Dev.	8.4^0	5.7^0	5.8^0	4.0^0	3.3^0
	RMSE	9.9^0	6.2^0	6.2^0	5.6^0	4.2^0
vcs_a/8K $E[\hat{M}_0] = 4.2$ $E[\hat{\alpha}_\theta] = 25.6^0$	$E[\hat{\theta}]$ / $E[\hat{\theta}]$	197.6^0	169.0^0	170.6^0	164.7^0	168.9^0
	bias	16.1^0	-12.5^0	-10.9^0	-16.8^0	-12.6^0
	Std. Dev.	31.2^0	11.3^0	11.5^0	10.3^0	11.2^0
	RMSE	35.1^0	16.9^0	15.8^0	19.7^0	16.8^0
vcs_b/8K $E[\hat{M}_0] = 3.4$ $E[\hat{\alpha}_\theta] = 7.1^0$	$E[\hat{\theta}]$ / $E[\hat{\theta}]$	183.9^0	184.8^0	183.9^0	184.8^0	185.9^0
	Bias	2.4^0	3.3^0	2.4^0	3.3^0	4.4^0
	Std. Dev.	5.2^0	3.1^0	4.8^0	6.8^0	6.1^0
	RMSE	5.7^0	4.5^0	5.4^0	7.5^0	7.5^0
vcs_c/8K $E[\hat{M}_0] = 4.5$ $E[\hat{\alpha}_\theta] = 12.4^0$	$E[\hat{\theta}]$ / $E[\hat{\theta}]$	196.3^0	196.2^0	200.0^0	195.3^0	197.3^0
	Bias	14.8^0	14.7^0	18.5^0	13.8^0	15.8^0
	Std. Dev.	6.5^0	3.4^0	6.8^0	2.5^0	2.1^0
	RMSE	16.2^0	15.1^0	19.7^0	14.0^0	15.9^0
vcs_d/8K $E[\hat{M}_0] = 3.6$ $E[\hat{\alpha}_\theta] = 7.7^0$	$E[\hat{\theta}]$ / $E[\hat{\theta}]$	181.1^0	182.4^0	183.3^0	182.5^0	178.7^0
	Bias	-0.4^0	0.9^0	1.8^0	1.0^0	-2.8^0
	Std. Dev.	4.4^0	4.5^0	7.4^0	7.5^0	3.6^0
	RMSE	4.4^0	4.6^0	7.6^0	7.6^0	4.5^0
Overall Result	Std. Dev.	13.0^0	5.8^0	7.5^0	6.1^0	5.6^0
	RMSE	16.4^0	10.2^0	11.8^0	11.1^0	10.6^0

Table 5.5: cp = 2

		MUSIC	DISP1	DISP2	MUDI	BFDI
	$E[\hat{\theta}]$ / $E[\hat{\tilde{\theta}}]$	181.0^0	183.0^0	182.1^0	182.2^0	185.6^0
cfh_a/8K	Bias	-0.9^0	1.1^0	0.2^0	0.3^0	3.7^0
$E[\hat{M}_0] = 4.1$	Std. Dev.	3.2^0	$\mathbf{2.6^0}$	4.4^0	3.9^0	3.1^0
$E[\hat{\alpha}_\theta] = 8.1^0$	RMSE	3.4^0	$\mathbf{2.9^0}$	4.4^0	3.9^0	4.8^0
	$E[\hat{\theta}]$ / $E[\hat{\tilde{\theta}}]$	112.4^0	108.8^0	109.0^0	108.4^0	109.0^0
iar_a/8K	Bias	14.0^0	10.3^0	10.6^0	10.0^0	10.6^0
$E[\hat{M}_0] = 3.8$	Std. Dev.	5.8^0	5.0^0	9.1^0	$\mathbf{4.3^0}$	4.7^0
$E[\hat{\alpha}_\theta] = 19.1^0$	RMSE	15.1^0	11.5^0	14.0^0	$\mathbf{10.9^0}$	11.6^0
	$E[\hat{\theta}]$ / $E[\hat{\tilde{\theta}}]$	254.3^0	246.8^0	247.7^0	247.8^0	246.8^0
vai_a/8K	Bias	5.2^0	-2.3^0	-1.4^0	-1.3^0	-2.3^0
$E[\hat{M}_0] = 5.6$	Std. Dev.	8.4^0	5.8^0	7.1^0	9.4^0	$\mathbf{4.1^0}$
$E[\hat{\alpha}_\theta] = 11.8^0$	RMSE	9.9^0	6.2^0	7.2^0	9.5^0	$\mathbf{4.7^0}$
	$E[\hat{\theta}]$ / $E[\hat{\tilde{\theta}}]$	197.6^0	168.8^0	170.3^0	166.2^0	168.8^0
vcs_a/8K	Bias	16.1^0	-12.7^0	-11.2^0	-15.3^0	-12.7^0
$E[\hat{M}_0] = 4.3$	Std. Dev.	31.2^0	$\mathbf{11.1^0}$	11.3^0	13.0^0	11.2^0
$E[\hat{\alpha}_\theta] = 25.9^0$	RMSE	35.1^0	16.9^0	$\mathbf{15.9^0}$	20.1^0	16.9^0
	$E[\hat{\theta}]$ / $E[\hat{\tilde{\theta}}]$	183.9^0	184.0^0	183.2^0	184.2^0	186.6^0
vcs_b/8K	Bias	2.4^0	2.5^0	1.7^0	2.7^0	5.1^0
$E[\hat{M}_0] = 3.6$	Std. Dev.	5.2^0	$\mathbf{3.5^0}$	5.2^0	7.0^0	5.9^0
$E[\hat{\alpha}_\theta] = 7.3^0$	RMSE	5.7^0	$\mathbf{4.3^0}$	5.4^0	7.5^0	7.8^0
	$E[\hat{\theta}]$ / $E[\hat{\tilde{\theta}}]$	196.3^0	196.1^0	199.7^0	195.4^0	197.7^0
vcs_c/8K	Bias	14.8^0	14.6^0	18.2^0	13.9^0	16.2^0
$E[\hat{M}_0] = 4.7$	Std. Dev.	6.5^0	2.9^0	6.5^0	2.9^0	$\mathbf{2.0^0}$
$E[\hat{\alpha}_\theta] = 12.6^0$	RMSE	16.2^0	14.9^0	19.3^0	$\mathbf{14.2^0}$	16.3^0
	$E[\hat{\theta}]$ / $E[\hat{\tilde{\theta}}]$	181.1^0	182.4^0	182.7^0	183.7^0	179.1^0
vcs_d/8K	Bias	-0.4^0	0.9^0	1.2^0	2.2^0	-2.4^0
$E[\hat{M}_0] = 3.8$	Std. Dev.	4.4^0	4.4^0	7.7^0	8.2^0	$\mathbf{3.8^0}$
$E[\hat{\alpha}_\theta] = 7.9^0$	RMSE	$\mathbf{4.4^0}$	4.5^0	7.8^0	8.5^0	4.5^0
Overall	Std. Dev.	13.0^0	5.7^0	7.6^0	7.7^0	$\mathbf{5.7^0}$
Result	RMSE	16.4^0	$\mathbf{10.2^0}$	11.9^0	11.7^0	10.8^0

Table 5.6: cp = 0

		MUSIC	DISP1	DISP2	MUDI	BFDI
	$E[\hat{\theta}]$ / $E[\hat{\tilde{\theta}}]$	181.0^0	183.2^0	182.1^0	183.7^0	186.6^0
cfh_a/8K	Bias	-0.9^0	1.3^0	0.2^0	1.8^0	4.7^0
$E[\hat{M}_0] = 4.5$	Std. Dev.	3.2^0	2.6^0	4.7^0	3.9^0	3.1^0
$E[\hat{\alpha}_\theta] = 8.4^0$	RMSE	3.4^0	2.9^0	4.7^0	4.3^0	5.6^0
	$E[\hat{\theta}]$ / $E[\hat{\tilde{\theta}}]$	112.4^0	106.3^0	105.5^0	110.0^0	107.9^0
iar_a/8K	Bias	14.0^0	7.9^0	7.1^0	11.6^0	9.5^0
$E[\hat{M}_0] = 4.2$	Std. Dev.	5.8^0	4.5^0	9.8^0	4.4^0	4.1^0
$E[\hat{\alpha}_\theta] = 19.6^0$	RMSE	15.1^0	9.1^0	12.1^0	12.4^0	10.4^0
	$E[\hat{\theta}]$ / $E[\hat{\tilde{\theta}}]$	254.3^0	247.9^0	248.8^0	252.0^0	248.1^0
vai_a/8K	Bias	5.2^0	-1.2^0	-0.3^0	2.9^0	-1.0^0
$E[\hat{M}_0] = 6.2$	Std. Dev.	8.4^0	5.9^0	7.3^0	12.1^0	6.9^0
$E[\hat{\alpha}_\theta] = 12.2^0$	RMSE	9.9^0	6.1^0	7.3^0	12.5^0	6.9^0
	$E[\hat{\theta}]$ / $E[\hat{\tilde{\theta}}]$	197.6^0	171.3^0	171.0^0	185.0^0	194.0^0
vcs_a/8K	Bias	16.1^0	-10.2^0	-10.5^0	3.5^0	12.5^0
$E[\hat{M}_0] = 6.8$	Std. Dev.	31.2^0	14.6^0	9.6^0	24.1^0	20.9^0
$E[\hat{\alpha}_\theta] = 28.6^0$	RMSE	35.1^0	17.8^0	14.3^0	24.4^0	24.3^0
	$E[\hat{\theta}]$ / $E[\hat{\tilde{\theta}}]$	183.9^0	183.3^0	182.5^0	182.5^0	187.2^0
vcs_b/8K	Bias	2.4^0	1.8^0	1.0^0	1.0^0	5.7^0
$E[\hat{M}_0] = 4.2$	Std. Dev.	5.2^0	3.2^0	4.2^0	5.5^0	5.7^0
$E[\hat{\alpha}_\theta] = 7.8^0$	RMSE	5.7^0	3.7^0	4.3^0	5.6^0	8.0^0
	$E[\hat{\theta}]$ / $E[\hat{\tilde{\theta}}]$	196.3^0	196.8^0	203.9^0	195.6^0	199.2^0
vcs_c/8K	Bias	14.8^0	15.3^0	22.4^0	14.1^0	17.8^0
$E[\hat{M}_0] = 5.4$	Std. Dev.	6.5^0	4.2^0	7.8^0	3.0^0	2.6^0
$E[\hat{\alpha}_\theta] = 13.1^0$	RMSE	16.2^0	15.9^0	23.7^0	14.5^0	17.9^0
	$E[\hat{\theta}]$ / $E[\hat{\tilde{\theta}}]$	181.1^0	183.5^0	183.9^0	182.4^0	179.6^0
vcs_d/8K	Bias	-0.4^0	2.0^0	2.4^0	0.9^0	-1.9^0
$E[\hat{M}_0] = 4.0$	Std. Dev.	4.4^0	4.9^0	7.8^0	7.6^0	3.0^0
$E[\hat{\alpha}_\theta] = 8.0^0$	RMSE	4.4^0	5.3^0	8.2^0	7.6^0	3.6^0
Overall	Std. Dev.	13.0^0	6.8^0	7.6^0	11.1^0	8.9^0
Result	RMSE	16.4^0	10.3^0	12.4^0	13.2^0	13.0^0

Table 5.7: cv = 90%

		MUSIC	DISP1	DISP2	MUDI	BFDI
cfh_a/8K $E[\hat{M}_0] = 2.7$ $E[\hat{\alpha}_\theta] = 7.9^0$	$E[\hat{\theta}]$ / $E[\hat{\tilde{\theta}}]$	181.0^0	183.3^0	182.9^0	184.4^0	184.7^0
	Bias	-0.9^0	1.4^0	1.0^0	2.5^0	2.8^0
	Std. Dev.	3.2^0	1.7^0	1.6^0	2.5^0	2.5^0
	RMSE	3.4^0	2.2^0	1.9^0	3.6^0	3.7^0
iar_a/8K $E[\hat{M}_0] = 2.9$ $E[\hat{\alpha}_\theta] = 18.8^0$	$E[\hat{\theta}]$ / $E[\hat{\tilde{\theta}}]$	112.4^0	108.2^0	107.1^0	104.5^0	109.6^0
	Bias	14.0^0	9.8^0	8.7^0	6.1^0	11.2^0
	Std. Dev.	5.8^0	4.7^0	6.8^0	5.2^0	4.2^0
	RMSE	15.1^0	10.9^0	11.0^0	8.0^0	12.0^0
vai_a/8K $E[\hat{M}_0] = 3.3$ $E[\hat{\alpha}_\theta] = 10.8^0$	$E[\hat{\theta}]$ / $E[\hat{\tilde{\theta}}]$	254.3^0	248.1^0	250.1^0	246.2^0	247.4^0
	Bias	5.2^0	-1.0^0	1.0^0	-2.9^0	-1.7^0
	Std. Dev.	8.4^0	4.4^0	5.2^0	3.4^0	2.0^0
	RMSE	9.9^0	4.5^0	5.3^0	4.4^0	2.6^0
vcs_a/8K $E[\hat{M}_0] = 3.0$ $E[\hat{\alpha}_\theta] = 25.4^0$	$E[\hat{\theta}]$ / $E[\hat{\tilde{\theta}}]$	197.6^0	170.3^0	172.9^0	160.4^0	164.0^0
	Bias	16.1^0	-11.2^0	-8.6^0	-21.1^0	-17.5^0
	Std. Dev.	31.2^0	13.0^0	10.9^0	11.8^0	8.3^0
	RMSE	35.1^0	17.2^0	13.9^0	24.2^0	19.4^0
vcs_b/8K $E[\hat{M}_0] = 2.4$ $E[\hat{\alpha}_\theta] = 7.0^0$	$E[\hat{\theta}]$ / $E[\hat{\tilde{\theta}}]$	183.9^0	185.3^0	184.5^0	185.3^0	185.9^0
	Bias	2.4^0	3.8^0	3.0^0	3.8^0	4.4^0
	Std. Dev.	5.2^0	4.1^0	4.1^0	3.8^0	5.8^0
	RMSE	5.7^0	5.6^0	5.1^0	5.4^0	7.3^0
vcs_c/8K $E[\hat{M}_0] = 3.0$ $E[\hat{\alpha}_\theta] = 12.3^0$	$E[\hat{\theta}]$ / $E[\hat{\tilde{\theta}}]$	196.3^0	196.7^0	198.0^0	196.1^0	196.1^0
	Bias	14.8^0	15.2^0	16.5^0	14.6^0	14.6^0
	Std. Dev.	6.5^0	3.5^0	5.9^0	2.6^0	3.0^0
	RMSE	16.2^0	15.6^0	17.5^0	14.8^0	14.9^0
vcs_d/8K $E[\hat{M}_0] = 2.5$ $E[\hat{\alpha}_\theta] = 7.5^0$	$E[\hat{\theta}]$ / $E[\hat{\tilde{\theta}}]$	181.1^0	181.7^0	182.2^0	182.8^0	181.1^0
	Bias	-0.4^0	0.2^0	0.7^0	1.3^0	-0.4^0
	Std. Dev.	4.4^0	5.2^0	5.4^0	6.5^0	3.1^0
	RMSE	4.4^0	5.2^0	5.4^0	6.6^0	3.1^0
Overall Result	Std. Dev.	13.0^0	6.2^0	6.3^0	6.0^0	4.6^0
	RMSE	16.4^0	10.3^0	10.1^0	11.8^0	10.9^0

Table 5.8: cv = 85%

		MUSIC	DISP1	DISP2	MUDI	BFDI
	$E[\hat{\theta}]$ / $E[\hat{\tilde{\theta}}]$	181.0^0	183.2^0	182.7^0	183.5^0	184.0^0
cfh_a/8K	Bias	-0.9^0	1.3^0	0.8^0	1.6^0	2.1^0
$E[\hat{M}_0] = 2.3$	Std. Dev.	3.2^0	1.5^0	$\mathbf{1.4^0}$	2.8^0	2.9^0
$E[\hat{\alpha}_\theta] = 7.9^0$	RMSE	3.4^0	2.0^0	$\mathbf{1.6^0}$	3.2^0	3.5^0
	$E[\hat{\theta}]$ / $E[\hat{\tilde{\theta}}]$	112.4^0	108.7^0	108.7^0	108.8^0	109.9^0
iar_a/8K	Bias	14.0^0	10.3^0	10.3^0	10.4^0	11.5^0
$E[\hat{M}_0] = 2.3$	Std. Dev.	5.8^0	$\mathbf{3.3^0}$	4.5^0	7.0^0	4.9^0
$E[\hat{\alpha}_\theta] = 18.8^0$	RMSE	15.1^0	$\mathbf{10.8^0}$	11.2^0	12.5^0	12.5^0
	$E[\hat{\theta}]$ / $E[\hat{\tilde{\theta}}]$	254.3^0	249.6^0	252.2^0	247.8^0	248.8^0
vai_a/8K	Bias	5.2^0	0.5^0	3.1^0	-1.3^0	-0.3^0
$E[\hat{M}_0] = 2.7$	Std. Dev.	8.4^0	5.5^0	5.5^0	6.5^0	$\mathbf{5.3^0}$
$E[\hat{\alpha}_\theta] = 10.8^0$	RMSE	9.9^0	5.5^0	6.3^0	6.6^0	$\mathbf{5.3^0}$
	$E[\hat{\theta}]$ / $E[\hat{\tilde{\theta}}]$	197.6^0	169.4^0	174.0^0	163.2^0	163.4^0
vcs_a/8K	Bias	16.1^0	-12.1^0	-7.5^0	-18.3^0	-18.1^0
$E[\hat{M}_0] = 2.5$	Std. Dev.	31.2^0	12.6^0	13.4^0	$\mathbf{8.8^0}$	9.4^0
$E[\hat{\alpha}_\theta] = 25.4^0$	RMSE	35.1^0	17.4^0	$\mathbf{15.3^0}$	20.3^0	20.4^0
	$E[\hat{\theta}]$ / $E[\hat{\tilde{\theta}}]$	183.9^0	185.1^0	184.3^0	185.1^0	185.6^0
vcs_b/8K	Bias	2.4^0	3.6^0	2.8^0	3.6^0	4.1^0
$E[\hat{M}_0] = 2.2$	Std. Dev.	5.2^0	4.3^0	4.3^0	$\mathbf{3.9^0}$	5.5^0
$E[\hat{\alpha}_\theta] = 7.0^0$	RMSE	5.7^0	5.6^0	$\mathbf{5.1^0}$	5.2^0	6.9^0
	$E[\hat{\theta}]$ / $E[\hat{\tilde{\theta}}]$	196.3^0	195.2^0	196.2^0	197.1^0	196.9^0
vcs_c/8K	Bias	14.8^0	13.7^0	14.7^0	15.6^0	15.4^0
$E[\hat{M}_0] = 2.5$	Std. Dev.	6.5^0	3.8^0	6.4^0	$\mathbf{3.4^0}$	4.1^0
$E[\hat{\alpha}_\theta] = 12.3^0$	RMSE	16.2^0	$\mathbf{14.2^0}$	16.0^0	16.0^0	16.0^0
	$E[\hat{\theta}]$ / $E[\hat{\tilde{\theta}}]$	181.1^0	180.5^0	180.8^0	180.9^0	181.4^0
vcs_d/8K	Bias	-0.4^0	-1.0^0	-0.7^0	-0.6^0	-0.1^0
$E[\hat{M}_0] = 2.1$	Std. Dev.	4.4^0	3.5^0	3.6^0	5.2^0	$\mathbf{3.2^0}$
$E[\hat{\alpha}_\theta] = 7.5^0$	RMSE	4.4^0	3.7^0	3.6^0	5.3^0	$\mathbf{3.2^0}$
Overall	Std. Dev.	13.0^0	5.9^0	6.6^0	5.7^0	$\mathbf{5.4^0}$
Result	RMSE	16.4^0	10.0^0	$\mathbf{10.0^0}$	11.5^0	11.5^0

Table 5.9: cv = 80%

		MUSIC	DISP1	DISP2	MUDI	BFDI
	$E[\hat{\theta}]$ / $E[\hat{\tilde{\theta}}]$	181.0^0	183.3^0	182.6^0	183.0^0	183.2^0
cfh_a/8K	Bias	-0.9^0	1.4^0	0.7^0	1.1^0	1.3^0
$E[\hat{M}_0] = 2.1$	Std. Dev.	3.2^0	1.6^0	$\mathbf{1.3^0}$	2.7^0	2.8^0
$E[\hat{\alpha}_\theta] = 7.9^0$	RMSE	3.4^0	2.1^0	$\mathbf{1.5^0}$	2.9^0	3.1^0
	$E[\hat{\theta}]$ / $E[\hat{\tilde{\theta}}]$	112.4^0	109.5^0	109.8^0	109.6^0	110.4^0
iar_a/8K	Bias	14.0^0	11.1^0	11.4^0	11.2^0	12.0^0
$E[\hat{M}_0] = 2.0$	Std. Dev.	5.8^0	$\mathbf{4.3^0}$	4.4^0	6.5^0	4.9^0
$E[\hat{\alpha}_\theta] = 18.8^0$	RMSE	15.1^0	$\mathbf{11.9^0}$	12.3^0	13.0^0	13.0^0
	$E[\hat{\theta}]$ / $E[\hat{\tilde{\theta}}]$	254.3^0	249.7^0	253.2^0	252.4^0	251.4^0
vai_a/8K	Bias	5.2^0	0.6^0	4.1^0	3.3^0	2.3^0
$E[\hat{M}_0] = 2.2$	Std. Dev.	8.4^0	6.4^0	$\mathbf{6.1^0}$	8.4^0	7.7^0
$E[\hat{\alpha}_\theta] = 10.8^0$	RMSE	9.9^0	$\mathbf{6.5^0}$	7.4^0	9.0^0	8.1^0
	$E[\hat{\theta}]$ / $E[\hat{\tilde{\theta}}]$	197.6^0	168.0^0	171.1^0	164.0^0	164.0^0
vcs_a/8K	Bias	16.1^0	-13.5^0	-10.4^0	-17.5^0	-17.5^0
$E[\hat{M}_0] = 2.2$	Std. Dev.	31.2^0	11.9^0	15.4^0	$\mathbf{6.7^0}$	7.7^0
$E[\hat{\alpha}_\theta] = 25.4^0$	RMSE	35.1^0	$\mathbf{18.0^0}$	18.6^0	18.7^0	19.1^0
	$E[\hat{\theta}]$ / $E[\hat{\tilde{\theta}}]$	183.9^0	185.4^0	184.5^0	185.9^0	185.3^0
vcs_b/8K	Bias	2.4^0	3.9^0	3.0^0	4.4^0	3.8^0
$E[\hat{M}_0] = 1.8$	Std. Dev.	5.2^0	5.0^0	$\mathbf{4.9^0}$	5.3^0	5.2^0
$E[\hat{\alpha}_\theta] = 7.0^0$	RMSE	$\mathbf{5.7^0}$	6.3^0	5.7^0	6.9^0	6.4^0
	$E[\hat{\theta}]$ / $E[\hat{\tilde{\theta}}]$	196.3^0	193.1^0	192.0^0	198.2^0	197.9^0
vcs_c/8K	Bias	14.8^0	11.6^0	10.5^0	16.7^0	16.4^0
$E[\hat{M}_0] = 2.1$	Std. Dev.	6.5^0	$\mathbf{2.2^0}$	2.8^0	3.3^0	4.0^0
$E[\hat{\alpha}_\theta] = 12.3^0$	RMSE	16.2^0	11.8^0	$\mathbf{10.8^0}$	17.0^0	16.8^0
	$E[\hat{\theta}]$ / $E[\hat{\tilde{\theta}}]$	181.1^0	180.2^0	180.6^0	179.4^0	180.5^0
vcs_d/8K	Bias	-0.4^0	-1.3^0	-0.9^0	-2.1^0	-1.0^0
$E[\hat{M}_0] = 1.5$	Std. Dev.	4.4^0	$\mathbf{2.8^0}$	3.1^0	4.3^0	3.5^0
$E[\hat{\alpha}_\theta] = 7.5^0$	RMSE	4.4^0	$\mathbf{3.1^0}$	3.3^0	4.8^0	3.7^0
Overall	Std. Dev.	13.0^0	5.9^0	6.9^0	5.6^0	$\mathbf{5.4^0}$
Result	RMSE	16.4^0	$\mathbf{10.0^0}$	10.1^0	11.7^0	11.6^0

Table 5.10: $\hat{M}_0 = 2$

		MUSIC	DISP1	DISP2	MUDI	BFDI
cfh_a/8K $E[\hat{M}_0] = 2.0$ $E[\hat{\alpha}_\theta] = 7.9^0$	$E[\hat{\theta}]$ / $E[\hat{\tilde{\theta}}]$	181.0^0	183.6^0	182.8^0	183.7^0	183.5^0
	Bias	-0.9^0	1.7^0	0.8^0	1.8^0	1.6^0
	Std. Dev.	3.2^0	2.1^0	$\mathbf{1.7^0}$	3.1^0	2.8^0
	RMSE	3.4^0	2.7^0	$\mathbf{1.9^0}$	3.6^0	3.2^0
iar_a/8K $E[\hat{M}_0] = 2.0$ $E[\hat{\alpha}_\theta] = 18.8^0$	$E[\hat{\theta}]$ / $E[\hat{\tilde{\theta}}]$	112.4^0	109.2^0	109.6^0	108.3^0	109.7^0
	Bias	14.0^0	10.8^0	11.2^0	9.9^0	11.3^0
	Std. Dev.	5.8^0	4.1^0	4.6^0	4.8^0	$\mathbf{3.9^0}$
	RMSE	15.1^0	11.6^0	12.1^0	$\mathbf{11.0^0}$	12.0^0
vai_a/8K $E[\hat{M}_0] = 2.0$ $E[\hat{\alpha}_\theta] = 10.8^0$	$E[\hat{\theta}]$ / $E[\hat{\tilde{\theta}}]$	254.3^0	249.9^0	252.9^0	253.6^0	253.1^0
	Bias	5.2^0	0.8^0	3.8^0	4.5^0	4.0^0
	Std. Dev.	8.4^0	6.8^0	$\mathbf{6.2^0}$	8.4^0	7.4^0
	RMSE	9.9^0	$\mathbf{6.8^0}$	7.3^0	9.5^0	8.4^0
vcs_a/8K $E[\hat{M}_0] = 2.0$ $E[\hat{\alpha}_\theta] = 25.4^0$	$E[\hat{\theta}]$ / $E[\hat{\tilde{\theta}}]$	197.6^0	170.6^0	170.8^0	163.5^0	162.0^0
	Bias	16.1^0	-10.9^0	-10.7^0	-18.0^0	-19.5^0
	Std. Dev.	31.2^0	11.6^0	15.5^0	$\mathbf{7.8^0}$	11.9^0
	RMSE	35.1^0	$\mathbf{15.9^0}$	18.8^0	19.6^0	22.9^0
vcs_b/8K $E[\hat{M}_0] = 2.0$ $E[\hat{\alpha}_\theta] = 7.0^0$	$E[\hat{\theta}]$ / $E[\hat{\tilde{\theta}}]$	183.9^0	185.4^0	184.4^0	185.9^0	185.4^0
	Bias	2.4^0	3.9^0	2.9^0	4.4^0	3.9^0
	Std. Dev.	5.2^0	4.7^0	4.6^0	$\mathbf{4.6^0}$	5.4^0
	RMSE	5.7^0	6.1^0	$\mathbf{5.4^0}$	6.3^0	6.7^0
vcs_c/8K $E[\hat{M}_0] = 2.0$ $E[\hat{\alpha}_\theta] = 12.3^0$	$E[\hat{\theta}]$ / $E[\hat{\tilde{\theta}}]$	196.3^0	193.0^0	191.4^0	198.2^0	197.9^0
	Bias	14.8^0	11.5^0	9.9^0	16.7^0	16.4^0
	Std. Dev.	6.5^0	$\mathbf{1.9^0}$	2.1^0	3.3^0	4.0^0
	RMSE	16.2^0	11.7^0	$\mathbf{10.1^0}$	17.0^0	16.8^0
vcs_d/8K $E[\hat{M}_0] = 2.0$ $E[\hat{\alpha}_\theta] = 7.5^0$	$E[\hat{\theta}]$ / $E[\hat{\tilde{\theta}}]$	181.1^0	180.2^0	180.7^0	179.2^0	180.6^0
	Bias	-0.4^0	-1.3^0	-0.8^0	-2.3^0	-0.9^0
	Std. Dev.	4.4^0	3.6^0	3.8^0	4.7^0	$\mathbf{3.3^0}$
	RMSE	4.4^0	3.9^0	3.9^0	5.2^0	$\mathbf{3.4^0}$
Overall Result	Std. Dev.	13.0^0	5.9^0	7.0^0	5.6^0	6.3^0
	RMSE	16.4^0	$\mathbf{9.5^0}$	10.0^0	11.7^0	12.5^0

Table 5.11: $\hat{M}_0 = 4$

		MUSIC	DISP1	DISP2	MUDI	BFDI
	$E[\hat{\theta}]$ / $E[\hat{\bar{\theta}}]$	181.0^0	183.9^0	183.2^0	183.8^0	185.5^0
cfh_a/8K	Bias	-0.9^0	2.0^0	1.3^0	1.9^0	3.6^0
$E[\hat{M}_0] = 4.0$	Std. Dev.	3.2^0	1.4^0	1.9^0	$\mathbf{1.1^0}$	2.8^0
$E[\hat{\alpha}_\theta] = 7.9^0$	RMSE	3.4^0	2.5^0	2.3^0	$\mathbf{2.2^0}$	4.6^0
	$E[\hat{\theta}]$ / $E[\hat{\bar{\theta}}]$	112.4^0	106.2^0	107.1^0	110.4^0	109.4^0
iar_a/8K	Bias	14.0^0	7.8^0	8.7^0	12.0^0	11.0^0
$E[\hat{M}_0] = 4.0$	Std. Dev.	5.8^0	6.0^0	9.3^0	$\mathbf{3.1^0}$	4.2^0
$E[\hat{\alpha}_\theta] = 18.8^0$	RMSE	15.1^0	$\mathbf{9.8^0}$	12.8^0	12.4^0	11.8^0
	$E[\hat{\theta}]$ / $E[\hat{\bar{\theta}}]$	254.3^0	247.9^0	248.7^0	247.8^0	248.1^0
vai_a/8K	Bias	5.2^0	-1.2^0	-0.4^0	-1.3^0	-1.0^0
$E[\hat{M}_0] = 4.0$	Std. Dev.	8.4^0	4.6^0	4.6^0	2.7^0	$\mathbf{1.4^0}$
$E[\hat{\alpha}_\theta] = 10.8^0$	RMSE	9.9^0	4.8^0	4.6^0	3.0^0	$\mathbf{1.7^0}$
	$E[\hat{\theta}]$ / $E[\hat{\bar{\theta}}]$	197.6^0	169.7^0	171.8^0	160.9^0	166.6^0
vcs_a/8K	Bias	16.1^0	-11.8^0	-9.7^0	-20.6^0	-14.9^0
$E[\hat{M}_0] = 4.0$	Std. Dev.	31.2^0	13.4^0	11.7^0	13.7^0	$\mathbf{9.0^0}$
$E[\hat{\alpha}_\theta] = 25.4^0$	RMSE	35.1^0	17.8^0	$\mathbf{15.2^0}$	24.7^0	17.4^0
	$E[\hat{\theta}]$ / $E[\hat{\bar{\theta}}]$	183.9^0	184.2^0	184.0^0	185.4^0	185.8^0
vcs_b/8K	Bias	2.4^0	2.7^0	2.5^0	3.9^0	4.3^0
$E[\hat{M}_0] = 4.0$	Std. Dev.	5.2^0	$\mathbf{2.1^0}$	2.2^0	9.2^0	5.5^0
$E[\hat{\alpha}_\theta] = 7.0^0$	RMSE	5.7^0	3.5^0	$\mathbf{3.3^0}$	10.0^0	7.0^0
	$E[\hat{\theta}]$ / $E[\hat{\bar{\theta}}]$	196.3^0	196.2^0	199.3^0	194.9^0	196.7^0
vcs_c/8K	Bias	14.8^0	14.7^0	17.8^0	13.4^0	15.2^0
$E[\hat{M}_0] = 4.0$	Std. Dev.	6.5^0	3.6^0	6.9^0	2.4^0	$\mathbf{2.2^0}$
$E[\hat{\alpha}_\theta] = 12.3^0$	RMSE	16.2^0	15.1^0	19.1^0	$\mathbf{13.6^0}$	15.3^0
	$E[\hat{\theta}]$ / $E[\hat{\bar{\theta}}]$	181.1^0	183.9^0	184.5^0	183.3^0	178.1^0
vcs_d/8K	Bias	-0.4^0	2.4^0	3.0^0	1.8^0	-3.4^0
$E[\hat{M}_0] = 4.0$	Std. Dev.	4.4^0	5.4^0	7.6^0	6.3^0	$\mathbf{3.9^0}$
$E[\hat{\alpha}_\theta] = 7.5^0$	RMSE	$\mathbf{4.4^0}$	5.9^0	8.1^0	6.5^0	5.2^0
Overall	Std. Dev.	13.0^0	6.4^0	7.1^0	6.9^0	$\mathbf{4.8^0}$
Result	RMSE	16.4^0	$\mathbf{10.1^0}$	11.1^0	12.6^0	10.5^0

Table 5.12: $\hat{M}_0 = 6$

		MUSIC	DISP1	DISP2	MUDI	BFDI
	$E[\hat{\theta}]$ / $E[\hat{\bar{\theta}}]$	181.0^0	183.4^0	182.6^0	190.3^0	191.9^0
cfh_a/8K	Bias	-0.9^0	1.5^0	0.7^0	8.4^0	10.0^0
$E[\hat{M}_0] = 6.0$	Std. Dev.	3.2^0	2.4^0	4.6^0	2.5^0	$\mathbf{0.7^0}$
$E[\hat{\alpha}_\theta] = 7.9^0$	RMSE	3.4^0	$\mathbf{2.8^0}$	4.7^0	8.8^0	10.0^0
	$E[\hat{\theta}]$ / $E[\hat{\bar{\theta}}]$	112.4^0	94.8^0	79.1^0	96.6^0	114.6^0
iar_a/8K	Bias	14.0^0	-3.6^0	-19.3^0	-1.8^0	16.2^0
$E[\hat{M}_0] = 6.0$	Std. Dev.	5.8^0	$\mathbf{12.2^0}$	13.6^0	5.4^0	$\mathbf{4.9^0}$
$E[\hat{\alpha}_\theta] = 18.8^0$	RMSE	15.1^0	12.7^0	23.6^0	$\mathbf{5.7^0}$	16.9^0
	$E[\hat{\theta}]$ / $E[\hat{\bar{\theta}}]$	254.3^0	248.4^0	248.4^0	246.8^0	246.2^0
vai_a/8K	Bias	5.2^0	-0.7^0	-0.7^0	-2.3^0	-2.9^0
$E[\hat{M}_0] = 6.0$	Std. Dev.	8.4^0	6.5^0	7.8^0	9.5^0	$\mathbf{4.3^0}$
$E[\hat{\alpha}_\theta] = 10.8^0$	RMSE	9.9^0	6.6^0	7.8^0	9.8^0	$\mathbf{5.2^0}$
	$E[\hat{\theta}]$ / $E[\hat{\bar{\theta}}]$	197.6^0	171.0^0	173.4^0	169.8^0	188.4^0
vcs_a/8K	Bias	16.1^0	-10.5^0	-8.1^0	-11.7^0	6.9^0
$E[\hat{M}_0] = 6.0$	Std. Dev.	31.2^0	15.1^0	$\mathbf{10.1^0}$	26.1^0	27.4^0
$E[\hat{\alpha}_\theta] = 25.4^0$	RMSE	35.1^0	18.4^0	$\mathbf{13.0^0}$	28.6^0	28.3^0
	$E[\hat{\theta}]$ / $E[\hat{\bar{\theta}}]$	183.9^0	182.3^0	182.7^0	182.4^0	194.9^0
vcs_b/8K	Bias	2.4^0	0.8^0	1.2^0	0.9^0	13.4^0
$E[\hat{M}_0] = 6.0$	Std. Dev.	$\mathbf{5.2^0}$	8.4^0	8.9^0	10.4^0	7.0^0
$E[\hat{\alpha}_\theta] = 7.0^0$	RMSE	$\mathbf{5.7^0}$	8.4^0	9.0^0	10.4^0	15.1^0
	$E[\hat{\theta}]$ / $E[\hat{\bar{\theta}}]$	196.3^0	197.5^0	205.6^0	196.1^0	200.4^0
vcs_c/8K	Bias	14.8^0	16.0^0	24.1^0	14.6^0	18.9^0
$E[\hat{M}_0] = 6.0$	Std. Dev.	6.5^0	5.6^0	8.2^0	3.1^0	$\mathbf{2.8^0}$
$E[\hat{\alpha}_\theta] = 12.3^0$	RMSE	16.2^0	16.9^0	25.5^0	$\mathbf{14.9^0}$	19.1^0
	$E[\hat{\theta}]$ / $E[\hat{\bar{\theta}}]$	181.1^0	189.2^0	187.5^0	179.2^0	179.6^0
vcs_d/8K	Bias	-0.4^0	7.7^0	6.0^0	-2.3^0	-1.9^0
$E[\hat{M}_0] = 6.0$	Std. Dev.	$\mathbf{4.4^0}$	5.4^0	8.0^0	10.8^0	4.4^0
$E[\hat{\alpha}_\theta] = 7.5^0$	RMSE	$\mathbf{4.4^0}$	9.4^0	10.0^0	11.1^0	4.8^0
Overall	Std. Dev.	13.0^0	$\mathbf{8.9^0}$	9.1^0	12.2^0	11.2^0
Result	RMSE	16.4^0	$\mathbf{11.9^0}$	15.3^0	14.5^0	16.2^0

5.3 Spread

Although the azimuth spread $\hat{\alpha}_\theta$ is not the primary parameter of interest, its accuracy will directly affect the accuracy of $\hat{\bar{\theta}}$ (see Finding (a) of Experiment 3.6). In this section, we suggest some approaches to estimate $\hat{\alpha}_\theta$.

5.3.1 Four Approaches to Estimate $\hat{\alpha}_\theta$

The current approach for estimating $\hat{\alpha}_\theta$ is described in Subsection 3.2.4. We designate it as Approach A[1], and is repeated below.

Approach A: Estimate $\hat{\alpha}_\theta$ from $\{\hat{\lambda}\}$

Steps 1 By employing certain distribution type, we pre-store a file containing the mean eigenvalues of $\tilde{\boldsymbol{R}}$ at $\alpha_\theta = 1^0 : 30^0$. The way to find the mean eigenvalues is

```
for α_θ = 1^0 : 30^0
    for θ̄ = 0^0 : 30^0 : 150^0
        compute R̃, then {λ̃}
    end
    find the average {λ̃} at that particular α_θ
end
```

Note that the pre-stored files differ for different array geometries, which in turn differ for different signal wavelengths.

Step 2 From $\hat{\boldsymbol{R}}$, compute $\hat{M}_0$ and $\{\hat{\lambda}\}$.

Step 3 Compare $\{\hat{\lambda}\}$ with the $\{\tilde{\lambda}\}$s of the pre-stored file. Pick out the nearest $\{\tilde{\lambda}\}$, i.e. the one whose difference with $\{\hat{\lambda}\}$ gives the smallest norm. The corresponding α_θ is $\hat{\alpha}_\theta$.

[1] The approaches are named alphabetically rather than numerically so as to differentiate them from the approaches for estimating $\hat{\bar{\theta}}$ described in Section 3.2.

We suggest three other approaches, which are listed below.

Approach B: Limit $\hat{\alpha}_\theta$ by $\hat{M}_0$

Steps 1-3 Exactly the same as Approach A.

Step 4 From $\{\tilde{\lambda}\}$, compute $\tilde{M}_0$.

Step 5 If $\tilde{M}_0 > \hat{M}_0$, $\hat{\alpha}_\theta$ is decremented by 1. If $\tilde{M}_0 < \hat{M}_0$, $\hat{\alpha}_\theta$ is incremented by 1. The corresponding $\{\tilde{\lambda}\}$ (of that $\hat{\alpha}_\theta$) is chosen. Go back to Step 4 until $\tilde{M}_0 = \hat{M}_0$.

Approach C: $\hat{\alpha}_\theta$ estimated from $\hat{m}_0$

Step 1 The pre-stored file contains 30 eigenvalue vectors, which corresponds to $\alpha_\theta = 1^0 : 30^0$. We pre-calculate $\tilde{m}_0$ for each eigenvalue vector. The result is a vector denoted as $\boldsymbol{n}$, which should have non-descending elements. That is, $n_i \geq n_j$ if $i > j$, where n_i, n_j are the ith and jth element of $\boldsymbol{n}$.

From the non-descending property of $\boldsymbol{n}$, we can say that the first x_1 elements of $\boldsymbol{n}$ are equal to 1, the next x_2 elements are equal to 2, and so on. As the compensation factor is set to 6, $n_i \leq 6$ for all i. Thus,

$$\sum_{i=1}^{6} x_i = 30$$

where 30 is the number of entries we have in the pre-stored file.

Step 2 From $\hat{m}_0$ (which is equal to $\hat{M}_0$ for $K = 1$), we search for the same value in the vector $\boldsymbol{n}$ generated above. We get a consecutive range having $n_i = n_{i+1} = \cdots = n_j = \hat{m}_0$. We pick up the middle element $n_{\frac{i+j}{2}}$. The location $\frac{i+j}{2}$ is $\hat{\alpha}_\theta$.

Note that in this approach, we estimate $\hat{\alpha}_\theta$ from $\hat{m}_0$ rather than from $\{\hat{\lambda}\}$. This is necessary if K is assumed larger than 1, as will be discussed in Chapter 6.

Approach D: Pre-determined $\hat{\alpha}_\theta$

This is the simplest approach: we just fix $\hat{\alpha}_\theta$ to a pre-determined value.

5.3.2 Testing

Experiment 5.6: $\hat{\alpha}_\theta$ Limited by $\tilde{M}_0$

Objective: To test the dispersive methods by using Approach B to estimate $\hat{\alpha}_\theta$.

Results: The results are shown in Tables 5.13.

Findings: The estimation performance is similar to the results of Approach A shown in Table 4.2.

Experiment 5.7: $\hat{\alpha}_\theta$ Estimated from $\hat{m}_0$

Objective: To test the dispersive methods by using Approach C to estimate $\hat{\alpha}_\theta$.

Results: The results are shown in Tables 5.14.

Findings: The estimation performance is similar to the results of Approach A shown in Table 4.2.

Experiment 5.8: Pre-determined $\hat{\alpha}_\theta$

Objective: To test the dispersive methods by using Approach D to estimate $\hat{\alpha}_\theta$.

Scenario: $\hat{\alpha}_\theta$ is fixed to 5^0, 10^0, 15^0 and 20^0 in 4 tests.

Results: The results are shown in Tables 5.15 to 5.18.

Findings: When comparing with the results of Approach A shown in Table 4.2, the estimation performances of DISPARE I, DISPARE II and MUSIC DISC are worse here. However, for BF DISC, the performance is better than before when $\hat{\alpha}_\theta$ is around 10^0.

Overall speaking, using Approach A yields the best $\hat{\tilde{\theta}}$ estimates. Thus, Approach A is used unless otherwise stated.

Table 5.13: $\hat{\alpha}_\theta$ Limited by $\hat{M}_0$

		MUSIC	DISP1	DISP2	MUDI	BFDI
	$E[\hat{\theta}]$ / $E[\hat{\tilde{\theta}}]$	181.0^0	184.1^0	183.7^0	184.4^0	185.9^0
cfh_a/8K	Bias	-0.9^0	2.2^0	1.8^0	2.5^0	4.0^0
$E[\hat{M}_0] = 3.7$	Std. Dev.	3.2^0	1.6^0	$\mathbf{1.4^0}$	2.2^0	2.7^0
$E[\hat{\alpha}_\theta] = 9.1^0$	RMSE	3.4^0	2.8^0	$\mathbf{2.2^0}$	3.3^0	4.9^0
	$E[\hat{\theta}]$ / $E[\hat{\tilde{\theta}}]$	112.4^0	110.2^0	108.4^0	107.2^0	108.7^0
iar_a/8K	Bias	14.0^0	11.8^0	10.0^0	8.8^0	10.3^0
$E[\hat{M}_0] = 3.6$	Std. Dev.	5.8^0	4.5^0	7.9^0	$\mathbf{4.3^0}$	5.3^0
$E[\hat{\alpha}_\theta] = 21.2^0$	RMSE	15.1^0	12.6^0	12.8^0	$\mathbf{9.8^0}$	11.6^0
	$E[\hat{\theta}]$ / $E[\hat{\tilde{\theta}}]$	254.3^0	246.6^0	247.2^0	246.6^0	247.1^0
vai_a/8K	Bias	5.2^0	-2.5^0	-1.9^0	-2.5^0	-2.0^0
$E[\hat{M}_0] = 4.4$	Std. Dev.	8.4^0	4.6^0	5.1^0	2.8^0	$\mathbf{2.5^0}$
$E[\hat{\alpha}_\theta] = 11.9^0$	RMSE	9.9^0	5.3^0	5.4^0	3.8^0	$\mathbf{3.2^0}$
	$E[\hat{\theta}]$ / $E[\hat{\tilde{\theta}}]$	197.6^0	169.9^0	170.9^0	164.1^0	167.5^0
vcs_a/8K	Bias	16.1^0	-11.6^0	-10.6^0	-17.4^0	-14.0^0
$E[\hat{M}_0] = 4.0$	Std. Dev.	31.2^0	11.6^0	12.0^0	9.6^0	$\mathbf{8.0^0}$
$E[\hat{\alpha}_\theta] = 25.7^0$	RMSE	35.1^0	16.4^0	$\mathbf{16.0^0}$	19.8^0	16.1^0
	$E[\hat{\theta}]$ / $E[\hat{\tilde{\theta}}]$	183.9^0	184.5^0	184.2^0	184.9^0	187.2^0
vcs_b/8K	Bias	2.4^0	3.0^0	2.7^0	3.4^0	5.7^0
$E[\hat{M}_0] = 3.2$	Std. Dev.	5.2^0	$\mathbf{2.3^0}$	2.9^0	7.0^0	5.5^0
$E[\hat{\alpha}_\theta] = 7.5^0$	RMSE	5.7^0	$\mathbf{3.8^0}$	4.0^0	7.7^0	7.9^0
	$E[\hat{\theta}]$ / $E[\hat{\tilde{\theta}}]$	196.3^0	195.4^0	198.0^0	194.6^0	196.7^0
vcs_c/8K	Bias	14.8^0	13.9^0	16.5^0	13.1^0	15.2^0
$E[\hat{M}_0] = 4.0$	Std. Dev.	6.5^0	2.7^0	6.2^0	2.1^0	$\mathbf{1.9^0}$
$E[\hat{\alpha}_\theta] = 11.3^0$	RMSE	16.2^0	14.2^0	17.7^0	$\mathbf{13.3^0}$	15.3^0
	$E[\hat{\theta}]$ / $E[\hat{\tilde{\theta}}]$	181.1^0	182.6^0	181.9^0	184.6^0	179.7^0
vcs_d/8K	Bias	-0.4^0	1.1^0	0.4^0	3.1^0	-1.8^0
$E[\hat{M}_0] = 3.3$	Std. Dev.	4.4^0	$\mathbf{4.1^0}$	6.7^0	8.2^0	5.2^0
$E[\hat{\alpha}_\theta] = 10.5^0$	RMSE	4.4^0	$\mathbf{4.3^0}$	6.7^0	8.8^0	5.5^0
Overall	Std. Dev.	13.0^0	5.5^0	6.8^0	5.9^0	$\mathbf{4.9^0}$
Result	RMSE	16.4^0	$\mathbf{10.0^0}$	10.9^0	10.9^0	10.4^0

Table 5.14: $\hat{\alpha}_\theta$ Estimated from $\hat{m}_0$

		MUSIC	DISP1	DISP2	MUDI	BFDI
	$E[\hat{\theta}]$ / $E[\hat{\tilde{\theta}}]$	181.0^0	184.5^0	183.9^0	184.7^0	185.9^0
cfh_a/8K	Bias	-0.9^0	2.6^0	2.0^0	2.8^0	4.0^0
$E[\hat{M}_0] = 3.7$	Std. Dev.	3.2^0	1.2^0	$\mathbf{1.0^0}$	2.3^0	2.3^0
$E[\hat{\alpha}_\theta] = 9.9^0$	RMSE	3.4^0	2.9^0	$\mathbf{2.2^0}$	3.6^0	4.6^0
	$E[\hat{\theta}]$ / $E[\hat{\tilde{\theta}}]$	112.4^0	109.5^0	107.5^0	107.7^0	107.7^0
iar_a/8K	Bias	14.0^0	11.1^0	9.1^0	9.3^0	9.3^0
$E[\hat{M}_0] = 3.6$	Std. Dev.	5.8^0	$\mathbf{4.2^0}$	8.2^0	5.7^0	6.4^0
$E[\hat{\alpha}_\theta] = 23.6^0$	RMSE	15.1^0	11.9^0	12.2^0	$\mathbf{10.9^0}$	11.3^0
	$E[\hat{\theta}]$ / $E[\hat{\tilde{\theta}}]$	254.3^0	247.5^0	246.9^0	246.6^0	246.6^0
vai_a/8K	Bias	5.2^0	-1.6^0	-2.2^0	-2.5^0	-2.5^0
$E[\hat{M}_0] = 4.4$	Std. Dev.	8.4^0	5.9^0	4.4^0	2.9^0	$\mathbf{2.6^0}$
$E[\hat{\alpha}_\theta] = 13.0^0$	RMSE	9.9^0	6.2^0	4.9^0	3.9^0	$\mathbf{3.6^0}$
	$E[\hat{\theta}]$ / $E[\hat{\tilde{\theta}}]$	197.6^0	167.0^0	168.2^0	165.5^0	167.2^0
vcs_a/8K	Bias	16.1^0	-14.5^0	-13.3^0	-16.0^0	-14.3^0
$E[\hat{M}_0] = 4.0$	Std. Dev.	31.2^0	10.9^0	12.2^0	8.6^0	$\mathbf{7.9^0}$
$E[\hat{\alpha}_\theta] = 26.3^0$	RMSE	35.1^0	18.1^0	18.1^0	18.2^0	$\mathbf{16.4^0}$
	$E[\hat{\theta}]$ / $E[\hat{\tilde{\theta}}]$	183.9^0	184.3^0	184.2^0	184.3^0	186.5^0
vcs_b/8K	Bias	2.4^0	2.8^0	2.7^0	2.8^0	5.0^0
$E[\hat{M}_0] = 3.2$	Std. Dev.	5.2^0	$\mathbf{2.8^0}$	2.9^0	5.7^0	5.5^0
$E[\hat{\alpha}_\theta] = 7.8^0$	RMSE	5.7^0	4.0^0	$\mathbf{3.9^0}$	6.3^0	7.5^0
	$E[\hat{\theta}]$ / $E[\hat{\tilde{\theta}}]$	196.3^0	195.6^0	198.1^0	194.3^0	196.5^0
vcs_c/8K	Bias	14.8^0	14.1^0	16.6^0	12.8^0	15.0^0
$E[\hat{M}_0] = 4.0$	Std. Dev.	6.5^0	2.9^0	6.3^0	2.2^0	$\mathbf{1.9^0}$
$E[\hat{\alpha}_\theta] = 10.9^0$	RMSE	16.2^0	14.4^0	17.7^0	$\mathbf{13.0^0}$	15.1^0
	$E[\hat{\theta}]$ / $E[\hat{\tilde{\theta}}]$	181.1^0	182.9^0	182.5^0	185.3^0	180.1^0
vcs_d/8K	Bias	-0.4^0	1.4^0	1.0^0	3.8^0	-1.4^0
$E[\hat{M}_0] = 3.3$	Std. Dev.	4.4^0	$\mathbf{4.2^0}$	5.5^0	9.0^0	5.0^0
$E[\hat{\alpha}_\theta] = 12.2^0$	RMSE	$\mathbf{4.4^0}$	4.4^0	5.6^0	9.8^0	5.2^0
Overall	Std. Dev.	13.0^0	5.4^0	6.7^0	5.8^0	$\mathbf{5.0^0}$
Result	RMSE	16.4^0	10.4^0	11.1^0	10.6^0	$\mathbf{10.3^0}$

Table 5.15: $\hat{\alpha}_\theta = 5^0$

		MUSIC	DISP1	DISP2	MUDI	BFDI
	$E[\hat{\theta}]$ / $E[\hat{\tilde{\theta}}]$	181.0^0	184.1^0	184.3^0	184.2^0	184.0^0
cfh_a/8K	Bias	-0.9^0	2.2^0	2.4^0	2.3^0	2.1^0
$E[\hat{M}_0] = 3.7$	Std. Dev.	3.2^0	2.4^0	3.6^0	1.3^0	$\mathbf{1.0^0}$
$E[\hat{\alpha}_\theta] = 5.0^0$	RMSE	3.4^0	3.3^0	4.3^0	2.6^0	$\mathbf{2.3^0}$
	$E[\hat{\theta}]$ / $E[\hat{\tilde{\theta}}]$	112.4^0	104.7^0	106.5^0	108.0^0	111.2^0
iar_a/8K	Bias	14.0^0	6.3^0	8.1^0	9.6^0	12.8^0
$E[\hat{M}_0] = 3.6$	Std. Dev.	5.8^0	9.9^0	10.9^0	3.1^0	$\mathbf{2.9^0}$
$E[\hat{\alpha}_\theta] = 5.0^0$	RMSE	15.1^0	11.7^0	13.6^0	$\mathbf{10.1^0}$	13.1^0
	$E[\hat{\theta}]$ / $E[\hat{\tilde{\theta}}]$	254.3^0	246.3^0	246.8^0	249.5^0	248.4^0
vai_a/8K	Bias	5.2^0	-2.8^0	-2.3^0	0.4^0	-0.7^0
$E[\hat{M}_0] = 4.4$	Std. Dev.	8.4^0	8.2^0	8.5^0	5.5^0	$\mathbf{4.4^0}$
$E[\hat{\alpha}_\theta] = 5.0^0$	RMSE	9.9^0	8.6^0	8.8^0	5.5^0	$\mathbf{4.5^0}$
	$E[\hat{\theta}]$ / $E[\hat{\tilde{\theta}}]$	197.6^0	167.0^0	167.0^0	165.2^0	174.8^0
vcs_a/8K	Bias	16.1^0	-14.5^0	-14.5^0	-16.3^0	-6.7^0
$E[\hat{M}_0] = 4.0$	Std. Dev.	31.2^0	14.2^0	14.2^0	19.7^0	$\mathbf{4.1^0}$
$E[\hat{\alpha}_\theta] = 5.0^0$	RMSE	35.1^0	20.3^0	20.3^0	25.5^0	$\mathbf{7.9^0}$
	$E[\hat{\theta}]$ / $E[\hat{\tilde{\theta}}]$	183.9^0	184.1^0	184.1^0	183.8^0	184.8^0
vcs_b/8K	Bias	2.4^0	2.6^0	2.6^0	2.3^0	3.3^0
$E[\hat{M}_0] = 3.2$	Std. Dev.	5.2^0	$\mathbf{3.4^0}$	3.7^0	7.1^0	6.4^0
$E[\hat{\alpha}_\theta] = 5.0^0$	RMSE	5.7^0	$\mathbf{4.3^0}$	4.5^0	7.5^0	7.2^0
	$E[\hat{\theta}]$ / $E[\hat{\tilde{\theta}}]$	196.3^0	192.0^0	192.9^0	193.2^0	197.3^0
vcs_c/8K	Bias	14.8^0	10.5^0	11.4^0	11.8^0	15.8^0
$E[\hat{M}_0] = 4.0$	Std. Dev.	6.5^0	$\mathbf{3.1^0}$	3.3^0	3.2^0	3.8^0
$E[\hat{\alpha}_\theta] = 5.0^0$	RMSE	16.2^0	$\mathbf{10.9^0}$	11.8^0	12.2^0	16.3^0
	$E[\hat{\theta}]$ / $E[\hat{\tilde{\theta}}]$	181.1^0	182.8^0	183.0^0	183.3^0	178.3^0
vcs_d/8K	Bias	-0.4^0	1.3^0	1.5^0	1.8^0	-3.2^0
$E[\hat{M}_0] = 3.3$	Std. Dev.	4.4^0	6.0^0	6.7^0	7.5^0	$\mathbf{3.8^0}$
$E[\hat{\alpha}_\theta] = 5.0^0$	RMSE	$\mathbf{4.4^0}$	6.1^0	6.9^0	7.7^0	4.9^0
Overall	Std. Dev.	13.0^0	7.8^0	8.2^0	8.8^0	$\mathbf{4.1^0}$
Result	RMSE	16.4^0	10.8^0	11.3^0	12.3^0	$\mathbf{9.3^0}$

Table 5.16: $\hat{\alpha}_\theta = 10^0$

		MUSIC	DISP1	DISP2	MUDI	BFDI
cfh_a/8K $E[\hat{M}_0] = 3.7$ $E[\hat{\alpha}_\theta] = 10.0^0$	$E[\hat{\theta}]$ / $E[\hat{\tilde{\theta}}]$	181.0^0	184.8^0	184.2^0	184.4^0	186.7^0
	Bias	-0.9^0	2.9^0	2.3^0	2.5^0	4.8^0
	Std. Dev.	3.2^0	1.1^0	$\mathbf{0.8^0}$	2.2^0	2.9^0
	RMSE	3.4^0	3.1^0	$\mathbf{2.4^0}$	3.4^0	5.6^0
iar_a/8K $E[\hat{M}_0] = 3.6$ $E[\hat{\alpha}_\theta] = 10.0^0$	$E[\hat{\theta}]$ / $E[\hat{\tilde{\theta}}]$	112.4^0	105.0^0	109.1^0	107.7^0	110.7^0
	Bias	14.0^0	6.6^0	10.7^0	9.3^0	12.3^0
	Std. Dev.	5.8^0	8.0^0	11.2^0	3.4^0	$\mathbf{3.1^0}$
	RMSE	15.1^0	10.4^0	15.5^0	$\mathbf{9.9^0}$	12.7^0
vai_a/8K $E[\hat{M}_0] = 4.4$ $E[\hat{\alpha}_\theta] = 10.0^0$	$E[\hat{\theta}]$ / $E[\hat{\tilde{\theta}}]$	254.3^0	247.6^0	247.8^0	246.7^0	247.6^0
	Bias	5.2^0	-1.5^0	-1.3^0	-2.4^0	-1.5^0
	Std. Dev.	8.4^0	5.4^0	6.1^0	3.1^0	$\mathbf{1.8^0}$
	RMSE	9.9^0	5.6^0	6.2^0	3.9^0	$\mathbf{2.3^0}$
vcs_a/8K $E[\hat{M}_0] = 4.0$ $E[\hat{\alpha}_\theta] = 10.0^0$	$E[\hat{\theta}]$ / $E[\hat{\tilde{\theta}}]$	197.6^0	168.8^0	168.5^0	163.4^0	173.6^0
	Bias	16.1^0	-12.7^0	-13.0^0	-18.1^0	-7.9^0
	Std. Dev.	31.2^0	13.7^0	13.8^0	18.9^0	$\mathbf{3.4^0}$
	RMSE	35.1^0	18.7^0	19.0^0	26.1^0	$\mathbf{8.6^0}$
vcs_b/8K $E[\hat{M}_0] = 3.2$ $E[\hat{\alpha}_\theta] = 10.0^0$	$E[\hat{\theta}]$ / $E[\hat{\tilde{\theta}}]$	183.9^0	185.5^0	184.1^0	186.0^0	190.0^0
	Bias	2.4^0	4.0^0	2.6^0	4.5^0	8.5^0
	Std. Dev.	5.2^0	$\mathbf{3.2^0}$	4.1^0	5.2^0	5.8^0
	RMSE	5.7^0	5.1^0	$\mathbf{4.8^0}$	6.8^0	10.3^0
vcs_c/8K $E[\hat{M}_0] = 4.0$ $E[\hat{\alpha}_\theta] = 10.0^0$	$E[\hat{\theta}]$ / $E[\hat{\tilde{\theta}}]$	196.3^0	194.0^0	196.5^0	193.8^0	196.1^0
	Bias	14.8^0	12.5^0	15.0^0	12.3^0	14.6^0
	Std. Dev.	6.5^0	2.5^0	6.0^0	$\mathbf{2.4^0}$	2.5^0
	RMSE	16.2^0	12.8^0	16.2^0	$\mathbf{12.6^0}$	14.8^0
vcs_d/8K $E[\hat{M}_0] = 3.3$ $E[\hat{\alpha}_\theta] = 10.0^0$	$E[\hat{\theta}]$ / $E[\hat{\tilde{\theta}}]$	181.1^0	183.0^0	183.0^0	184.6^0	178.9^0
	Bias	-0.4^0	1.5^0	1.5^0	3.1^0	-2.6^0
	Std. Dev.	4.4^0	$\mathbf{4.3^0}$	6.1^0	8.3^0	4.9^0
	RMSE	$\mathbf{4.4^0}$	4.5^0	6.3^0	8.9^0	5.6^0
Overall Result	Std. Dev.	13.0^0	6.7^0	8.0^0	8.3^0	$\mathbf{3.7^0}$
	RMSE	16.4^0	10.1^0	11.8^0	12.5^0	$\mathbf{9.5^0}$

Table 5.17: $\hat{\alpha}_\theta = 15^0$

		MUSIC	DISP1	DISP2	MUDI	BFDI
	$E[\hat{\theta}]$ / $E[\hat{\tilde{\theta}}]$	181.0^0	186.5^0	182.7^0	185.6^0	189.9^0
cfh_a/8K	Bias	-0.9^0	4.6^0	0.8^0	3.7^0	8.0^0
$E[\hat{M}_0] = 3.7$	Std. Dev.	3.2^0	2.5^0	5.2^0	9.7^0	$\mathbf{1.1^0}$
$E[\hat{\alpha}_\theta] = 15.0^0$	RMSE	$\mathbf{3.4^0}$	5.2^0	5.3^0	10.4^0	8.1^0
	$E[\hat{\theta}]$ / $E[\hat{\tilde{\theta}}]$	112.4^0	107.2^0	109.7^0	107.2^0	109.8^0
iar_a/8K	Bias	14.0^0	8.8^0	11.3^0	8.8^0	11.4^0
$E[\hat{M}_0] = 3.6$	Std. Dev.	5.8^0	5.9^0	8.5^0	4.0^0	$\mathbf{4.0^0}$
$E[\hat{\alpha}_\theta] = 15.0^0$	RMSE	15.1^0	10.6^0	14.1^0	$\mathbf{9.7^0}$	12.1^0
	$E[\hat{\theta}]$ / $E[\hat{\tilde{\theta}}]$	254.3^0	246.4^0	246.5^0	245.4^0	246.3^0
vai_a/8K	Bias	5.2^0	-2.7^0	-2.6^0	-3.7^0	-2.8^0
$E[\hat{M}_0] = 4.4$	Std. Dev.	8.4^0	4.0^0	3.5^0	$\mathbf{2.1^0}$	2.3^0
$E[\hat{\alpha}_\theta] = 15.0^0$	RMSE	9.9^0	4.8^0	4.3^0	4.2^0	$\mathbf{3.7^0}$
	$E[\hat{\theta}]$ / $E[\hat{\tilde{\theta}}]$	197.6^0	172.8^0	170.1^0	163.9^0	172.1^0
vcs_a/8K	Bias	16.1^0	-8.7^0	-11.4^0	-17.6^0	-9.4^0
$E[\hat{M}_0] = 4.0$	Std. Dev.	31.2^0	12.7^0	12.3^0	10.1^0	$\mathbf{2.6^0}$
$E[\hat{\alpha}_\theta] = 15.0^0$	RMSE	35.1^0	15.4^0	16.8^0	20.3^0	$\mathbf{9.8^0}$
	$E[\hat{\theta}]$ / $E[\hat{\tilde{\theta}}]$	183.9^0	184.9^0	181.9^0	189.4^0	192.8^0
vcs_b/8K	Bias	2.4^0	3.4^0	0.4^0	7.9^0	11.3^0
$E[\hat{M}_0] = 3.2$	Std. Dev.	5.2^0	4.4^0	4.3^0	6.4^0	$\mathbf{2.3^0}$
$E[\hat{\alpha}_\theta] = 15.0^0$	RMSE	5.7^0	5.6^0	$\mathbf{4.3^0}$	10.2^0	11.5^0
	$E[\hat{\theta}]$ / $E[\hat{\tilde{\theta}}]$	196.3^0	198.2^0	201.3^0	196.4^0	197.5^0
vcs_c/8K	Bias	14.8^0	16.7^0	19.8^0	14.9^0	16.0^0
$E[\hat{M}_0] = 4.0$	Std. Dev.	6.5^0	2.2^0	5.4^0	2.3^0	$\mathbf{1.4^0}$
$E[\hat{\alpha}_\theta] = 15.0^0$	RMSE	16.2^0	16.8^0	20.5^0	$\mathbf{15.1^0}$	16.0^0
	$E[\hat{\theta}]$ / $E[\hat{\tilde{\theta}}]$	181.1^0	183.4^0	182.0^0	184.7^0	182.4^0
vcs_d/8K	Bias	-0.4^0	1.9^0	0.5^0	3.2^0	0.9^0
$E[\hat{M}_0] = 3.3$	Std. Dev.	4.4^0	$\mathbf{4.3^0}$	6.1^0	7.0^0	8.6^0
$E[\hat{\alpha}_\theta] = 15.0^0$	RMSE	$\mathbf{4.4^0}$	4.7^0	6.1^0	7.8^0	8.7^0
Overall	Std. Dev.	13.0^0	6.1^0	7.0^0	6.7^0	$\mathbf{4.0^0}$
Result	RMSE	16.4^0	$\mathbf{10.3^0}$	12.0^0	12.1^0	10.6^0

Table 5.18: $\hat{\alpha}_\theta = 20^0$

		MUSIC	DISP1	DISP2	MUDI	BFDI
	$E[\hat{\theta}]$ / $E[\hat{\tilde{\theta}}]$	181.0^0	183.7^0	181.2^0	187.8^0	195.4^0
cfh_a/8K	Bias	-0.9^0	1.8^0	-0.7^0	5.9^0	13.5^0
$E[\hat{M}_0] = 3.7$	Std. Dev.	3.2^0	4.5^0	5.1^0	16.2^0	$\mathbf{1.3^0}$
$E[\hat{\alpha}_\theta] = 20.0^0$	RMSE	$\mathbf{3.4^0}$	4.8^0	5.1^0	17.2^0	13.6^0
	$E[\hat{\theta}]$ / $E[\hat{\tilde{\theta}}]$	112.4^0	108.2^0	108.4^0	107.4^0	108.8^0
iar_a/8K	Bias	14.0^0	9.8^0	10.0^0	9.0^0	10.4^0
$E[\hat{M}_0] = 3.6$	Std. Dev.	5.8^0	$\mathbf{4.2^0}$	7.1^0	5.7^0	4.9^0
$E[\hat{\alpha}_\theta] = 20.0^0$	RMSE	15.1^0	10.7^0	$\mathbf{12.3^0}$	$\mathbf{10.7^0}$	11.5^0
	$E[\hat{\theta}]$ / $E[\hat{\tilde{\theta}}]$	254.3^0	248.2^0	248.8^0	245.5^0	247.1^0
vai_a/8K	Bias	5.2^0	-0.9^0	-0.3^0	-3.6^0	-2.0^0
$E[\hat{M}_0] = 4.4$	Std. Dev.	8.4^0	5.3^0	3.2^0	7.7^0	$\mathbf{1.3^0}$
$E[\hat{\alpha}_\theta] = 20.0^0$	RMSE	9.9^0	5.3^0	3.2^0	8.5^0	$\mathbf{2.4^0}$
	$E[\hat{\theta}]$ / $E[\hat{\tilde{\theta}}]$	197.6^0	174.3^0	174.8^0	165.1^0	170.4^0
vcs_a/8K	Bias	16.1^0	-7.2^0	-6.7^0	-16.4^0	-11.1^0
$E[\hat{M}_0] = 4.0$	Std. Dev.	31.2^0	12.2^0	10.2^0	8.0^0	$\mathbf{2.0^0}$
$E[\hat{\alpha}_\theta] = 20.0^0$	RMSE	35.1^0	14.2^0	12.2^0	18.2^0	$\mathbf{11.3^0}$
	$E[\hat{\theta}]$ / $E[\hat{\tilde{\theta}}]$	183.9^0	187.2^0	182.2^0	195.7^0	196.0^0
vcs_b/8K	Bias	2.4^0	5.7^0	0.7^0	14.2^0	14.5^0
$E[\hat{M}_0] = 3.2$	Std. Dev.	5.2^0	6.3^0	7.6^0	4.5^0	$\mathbf{2.2^0}$
$E[\hat{\alpha}_\theta] = 20.0^0$	RMSE	$\mathbf{5.7^0}$	8.5^0	7.6^0	14.9^0	14.7^0
	$E[\hat{\theta}]$ / $E[\hat{\tilde{\theta}}]$	196.3^0	200.7^0	203.0^0	200.4^0	201.0^0
vcs_c/8K	Bias	14.8^0	19.2^0	21.5^0	18.9^0	19.5^0
$E[\hat{M}_0] = 4.0$	Std. Dev.	6.5^0	1.4^0	2.8^0	4.4^0	$\mathbf{1.1^0}$
$E[\hat{\alpha}_\theta] = 20.0^0$	RMSE	$\mathbf{16.2^0}$	19.3^0	21.7^0	19.4^0	19.6^0
	$E[\hat{\theta}]$ / $E[\hat{\tilde{\theta}}]$	181.1^0	185.7^0	183.2^0	187.8^0	191.5^0
vcs_d/8K	Bias	-0.4^0	4.2^0	1.7^0	6.3^0	10.0^0
$E[\hat{M}_0] = 3.3$	Std. Dev.	4.4^0	4.2^0	4.6^0	4.0^0	$\mathbf{3.8^0}$
$E[\hat{\alpha}_\theta] = 20.0^0$	RMSE	$\mathbf{4.4^0}$	5.9^0	4.9^0	7.5^0	10.7^0
Overall	Std. Dev.	13.0^0	6.3^0	6.3^0	8.2^0	$\mathbf{2.7^0}$
Result	RMSE	16.4^0	$\mathbf{11.0^0}$	11.3^0	14.5^0	12.9^0

Chapter 6

Changing M and K

6.1 Changing the Number of Sensors M

According to [3], employing an array with a larger spatial coverage *may not* produce a more accurate DOA estimate for a dispersive signal. On the contrary, computer simulations show that if the signal dispersion is large, then an array with larger aperture may give worse results.

A brief explanation is given here. Let us consider a uniform distribution and the approximated Model 1a (Subsection 3.1.1). The modulus of $\tilde{r}_{mn}$ (the mnth element of $\tilde{\boldsymbol{R}}$), as shown in Eq.(3.10), is a sinc function depending on the dispersiveness and the distance of the mth and the nth antennas. As sinc is monotonically decreasing in the interval [0,π], the farther apart between the mth and the nth antennas, the larger z is and thus the smaller the modulus. Small modulus means that the element is more susceptible to being corrupted (due to noise or a limited number of sampling). As an antenna array with a larger aperture contains more pairs with larger spacings, the resulting estimated covariance $\hat{\boldsymbol{R}}$ would be more susceptible to error than for an array with a smaller aperture.

From Eq.(3.10), we also observe that the modulus of $\tilde{r}_{mn}$ decreases as α_θ increases. This is the effect of signal dispersion. The extent of such effect, which also depends on the antenna pair

distance, is different among the elements of $\tilde{R}$. This explains why it is so difficult to accurately estimate the DOA of a dispersed signal.

In this project, the Vortex sensor array consists of 12 sensors, where the first 8 form a circle and the last 4 are far apart from them (Fig.1.1). Given the previous discussion, we try to use 10 sensors (Sensors 1 to 10) and 8 sensors (Sensors 1 to 8) to estimate the DOAs.

Experiment 6.1: Changing M

Objective: To test the DF methods by using a smaller M.

Scenario: We test for $M = 10$ and $M = 8$. For $M = 10$ case, cp $= 5$ for the dispersive methods. For $M = 8$, cp $= 4$.

Results: The results are shown in Table 6.1 and Table 6.2.

Findings: MUSIC gives more accurate estimates when compared to using $M = 12$. However, the dispersive methods give worse results than before.

Remarks:

(a) One possible explanation is: the dispersive methods are designed for signal dispersion. Using an array with smaller aperture reduces the dispersive effect, which does not help much to the dispersive methods. However, a smaller array collects less signal energy, and such adverse effect bypass the benefit for the dispersive methods.

(b) We also tested different cp for $M = 10$ and $M = 8$. The performance remains roughly the same. The results are not listed here.

Table 6.1: Number of Sensor $M = 10$

		MUSIC	DISP1	DISP2	MUDI	BFDI
	$E[\hat{\theta}]$ / $E[\hat{\tilde{\theta}}]$	181.5^0	184.2^0	183.1^0	186.6^0	189.3^0
cfh_a/8K	Bias	-0.4^0	2.3^0	1.2^0	4.7^0	7.4^0
$E[\hat{M}_0] = 3.0$	Std. Dev.	3.0^0	$\mathbf{2.1^0}$	2.5^0	3.2^0	2.3^0
$E[\hat{\alpha}_\theta] = 10.2^0$	RMSE	3.0^0	3.1^0	$\mathbf{2.8^0}$	5.7^0	7.7^0
	$E[\hat{\theta}]$ / $E[\hat{\tilde{\theta}}]$	112.2^0	106.1^0	101.5^0	111.7^0	107.3^0
iar_a/8K	Bias	13.8^0	7.7^0	3.1^0	13.3^0	8.9^0
$E[\hat{M}_0] = 3.3$	Std. Dev.	$\mathbf{4.9^0}$	8.3^0	13.7^0	17.5^0	5.2^0
$E[\hat{\alpha}_\theta] = 24.1^0$	RMSE	14.7^0	11.3^0	14.0^0	22.0^0	$\mathbf{10.3^0}$
	$E[\hat{\theta}]$ / $E[\hat{\tilde{\theta}}]$	254.2^0	244.9^0	246.7^0	245.2^0	245.9^0
vai_a/8K	Bias	5.1^0	-4.2^0	-2.4^0	-3.9^0	-3.2^0
$E[\hat{M}_0] = 3.7$	Std. Dev.	8.7^0	3.8^0	5.0^0	2.1^0	$\mathbf{1.4^0}$
$E[\hat{\alpha}_\theta] = 13.6^0$	RMSE	10.1^0	5.7^0	5.5^0	4.4^0	$\mathbf{3.5^0}$
	$E[\hat{\theta}]$ / $E[\hat{\tilde{\theta}}]$	201.5^0	167.0^0	167.4^0	166.3^0	177.3^0
vcs_a/8K	Bias	20.0^0	-14.5^0	-14.1^0	-15.2^0	-4.2^0
$E[\hat{M}_0] = 3.4$	Std. Dev.	28.7^0	$\mathbf{10.6^0}$	13.2^0	12.8^0	19.8^0
$E[\hat{\alpha}_\theta] = 29.2^0$	RMSE	35.0^0	$\mathbf{17.9^0}$	19.3^0	19.8^0	20.3^0
	$E[\hat{\theta}]$ / $E[\hat{\tilde{\theta}}]$	183.6^0	183.7^0	183.0^0	186.7^0	190.4^0
vcs_b/8K	Bias	2.1^0	2.2^0	1.5^0	5.2^0	8.9^0
$E[\hat{M}_0] = 2.9$	Std. Dev.	5.8^0	4.3^0	$\mathbf{4.2^0}$	10.0^0	4.3^0
$E[\hat{\alpha}_\theta] = 10.0^0$	RMSE	6.2^0	4.8^0	$\mathbf{4.5^0}$	11.3^0	9.8^0
	$E[\hat{\theta}]$ / $E[\hat{\tilde{\theta}}]$	196.7^0	198.4^0	198.5^0	198.0^0	198.9^0
vcs_c/8K	Bias	15.2^0	16.9^0	17.0^0	16.5^0	17.4^0
$E[\hat{M}_0] = 3.5$	Std. Dev.	6.4^0	2.7^0	4.9^0	2.6^0	$\mathbf{1.7^0}$
$E[\hat{\alpha}_\theta] = 15.8^0$	RMSE	$\mathbf{16.4^0}$	17.2^0	17.7^0	16.7^0	17.5^0
	$E[\hat{\theta}]$ / $E[\hat{\tilde{\theta}}]$	179.4^0	181.4^0	181.2^0	184.5^0	180.3^0
vcs_d/8K	Bias	-2.1^0	-0.1^0	-0.3^0	3.0^0	-1.2^0
$E[\hat{M}_0] = 3.1$	Std. Dev.	$\mathbf{4.2^0}$	6.5^0	7.7^0	10.6^0	7.4^0
$E[\hat{\alpha}_\theta] = 10.6^0$	RMSE	$\mathbf{4.7^0}$	6.5^0	7.7^0	11.0^0	7.5^0
Overall	Std. Dev.	12.1^0	$\mathbf{6.2^0}$	8.4^0	10.0^0	8.5^0
Result	RMSE	16.4^0	$\mathbf{11.0^0}$	12.0^0	14.4^0	12.2^0

Table 6.2: Number of Sensor $M = 8$

		MUSIC	DISP1	DISP2	MUDI	BFDI
	$E[\hat{\theta}]$ / $E[\hat{\tilde{\theta}}]$	182.1^0	182.4^0	181.7^0	182.5^0	191.1^0
cfh_a/8K	Bias	0.2^0	0.5^0	-0.2^0	0.6^0	9.2^0
$E[\hat{M}_0] = 2.8$	Std. Dev.	2.2^0	2.4^0	2.8^0	7.9^0	$\mathbf{2.1^0}$
$E[\hat{\alpha}_\theta] = 14.1^0$	RMSE	$\mathbf{2.2^0}$	2.5^0	2.8^0	7.9^0	9.4^0
	$E[\hat{\theta}]$ / $E[\hat{\tilde{\theta}}]$	111.1^0	98.9^0	97.7^0	92.2^0	91.8^0
iar_a/8K	Bias	12.7^0	0.5^0	-0.7^0	-6.2^0	-6.7^0
$E[\hat{M}_0] = 2.2$	Std. Dev.	$\mathbf{3.5^0}$	11.8^0	13.3^0	22.2^0	18.9^0
$E[\hat{\alpha}_\theta] = 28.2^0$	RMSE	13.2^0	$\mathbf{11.8^0}$	13.3^0	23.0^0	20.0^0
	$E[\hat{\theta}]$ / $E[\hat{\tilde{\theta}}]$	254.8^0	243.9^0	247.1^0	235.8^0	241.3^0
vai_a/8K	Bias	5.7^0	-5.2^0	-2.0^0	-13.3^0	-7.8^0
$E[\hat{M}_0] = 2.9$	Std. Dev.	8.9^0	$\mathbf{1.8^0}$	2.5^0	5.4^0	2.3^0
$E[\hat{\alpha}_\theta] = 16.0^0$	RMSE	10.6^0	5.5^0	$\mathbf{3.2^0}$	14.3^0	8.1^0
	$E[\hat{\theta}]$ / $E[\hat{\tilde{\theta}}]$	189.8^0	172.5^0	171.6^0	192.2^0	184.9^0
vcs_a/8K	Bias	8.3^0	-9.0^0	-9.9^0	10.7^0	3.4^0
$E[\hat{M}_0] = 3.0$	Std. Dev.	21.2^0	15.3^0	11.7^0	$\mathbf{8.4^0}$	21.5^0
$E[\hat{\alpha}_\theta] = 30.0^0$	RMSE	22.8^0	17.8^0	15.3^0	$\mathbf{13.6^0}$	21.8^0
	$E[\hat{\theta}]$ / $E[\hat{\tilde{\theta}}]$	183.4^0	182.7^0	182.3^0	187.6^0	194.3^0
vcs_b/8K	Bias	1.9^0	1.2^0	0.8^0	6.1^0	12.8^0
$E[\hat{M}_0] = 2.5$	Std. Dev.	6.3^0	5.9^0	5.8^0	10.6^0	$\mathbf{5.1^0}$
$E[\hat{\alpha}_\theta] = 14.1^0$	RMSE	6.6^0	6.0^0	$\mathbf{5.8^0}$	12.2^0	13.7^0
	$E[\hat{\theta}]$ / $E[\hat{\tilde{\theta}}]$	197.5^0	200.6^0	199.3^0	201.1^0	201.9^0
vcs_c/8K	Bias	16.0^0	19.1^0	17.8^0	19.6^0	20.4^0
$E[\hat{M}_0] = 3.0$	Std. Dev.	6.9^0	2.8^0	3.4^0	1.8^0	$\mathbf{1.5^0}$
$E[\hat{\alpha}_\theta] = 20.1^0$	RMSE	$\mathbf{17.4^0}$	19.3^0	18.1^0	19.7^0	20.5^0
	$E[\hat{\theta}]$ / $E[\hat{\tilde{\theta}}]$	181.1^0	184.7^0	184.4^0	184.4^0	185.6^0
vcs_d/8K	Bias	-0.4^0	3.2^0	2.9^0	2.9^0	4.1^0
$E[\hat{M}_0] = 2.4$	Std. Dev.	$\mathbf{1.8^0}$	8.0^0	10.5^0	7.4^0	4.8^0
$E[\hat{\alpha}_\theta] = 12.5^0$	RMSE	$\mathbf{1.8^0}$	8.6^0	10.9^0	8.0^0	6.3^0
Overall	Std. Dev.	9.5^0	8.4^0	$\mathbf{8.3^0}$	10.8^0	11.2^0
Result	RMSE	12.9^0	11.8^0	$\mathbf{11.4^0}$	15.0^0	15.5^0

6.2 Changing the Number of Signals K

Although dispersive methods give better estimates than MUSIC in general (at least for $M = 12$), in some cases the values of $\hat{\bar{\theta}}$ are still far from θ_s. One possible reason is: the single signal assumption is wrong, i.e. $K > 1$. This section deals with the problem of invalidity of $K = 1$.

6.2.1 Narrower Passing Band

Let us look at the FFT spectrums of the input data shown in Fig.1.2(a)-(g). Our desired signal should be around 2.5 KHz (Section 1.3). From the figures, there are some other peaks in most spectrums. We suspect that these other peaks are due to other signals. One way to eliminate the interferences (such that $K = 1$ becomes valid) is passing the data through a narrower band-limited filter. Currently, we compute $\hat{\boldsymbol{R}}$ from the frequency data from 1.5 KHz to 4 KHz. We suggest computing $\hat{\boldsymbol{R}}$ with a narrower bandwidth of 2 KHz to 3 KHz.

Experiment 6.2: Narrower bandwidth

Objective: To test the DF methods with a narrower bandwidth in forming $\hat{\boldsymbol{R}}$.

Scenario: We test for 2 cases. In (a), cv = 95%. In (b), cv = 90%.

Results: The results are shown in Tables 6.3 and 6.4.

Findings:
(a) MUSIC performs better than when using the original (larger) bandwidth, but dispersive methods give marginally worse results than before.
(b) There is a noticable change in the angles estimated for the iar data. The $\mathrm{E}[\hat{\theta}]/\mathrm{E}[\hat{\bar{\theta}}]$ changes from around 110^0 to around 90^0.

Remarks: One explanation for Finding (a): the side peaks are *not* due to other signals, but are dispersive components of the desired signal. By passing the data through a narrower band-limited filter, such dispersive components are filtered out. Comparing to Table 4.2, $\hat{\alpha}_\theta$ is generally reduced. Thus, MUSIC performs better. Since the dispersive methods are designed for dispersive signals, such change does not give much benefit. In fact, they suffer as less signal energy is collected in $\hat{\boldsymbol{R}}$.

Table 6.3: Narrower bandwidth, cv = 95%

		MUSIC	DISP1	DISP2	MUDI	BFDI
	$E[\hat{\theta}]$ / $E[\hat{\tilde{\theta}}]$	181.2^0	183.6^0	182.5^0	184.1^0	183.6^0
cfh_a/8K	Bias	-0.7^0	1.7^0	0.6^0	2.2^0	1.7^0
$E[\hat{M}_0] = 3.7$	Std. Dev.	3.0^0	3.5^0	4.9^0	4.2^0	$\mathbf{2.2^0}$
$E[\hat{\alpha}_\theta] = 5.5^0$	RMSE	3.1^0	3.9^0	4.9^0	4.7^0	$\mathbf{2.8^0}$
	$E[\hat{\theta}]$ / $E[\hat{\tilde{\theta}}]$	94.9^0	93.9^0	94.8^0	89.8^0	91.8^0
iar_a/8K	Bias	-3.5^0	-4.5^0	-3.6^0	-8.6^0	-6.6^0
$E[\hat{M}_0] = 3.7$	Std. Dev.	$\mathbf{3.6^0}$	4.8^0	5.2^0	7.7^0	7.5^0
$E[\hat{\alpha}_\theta] = 19.2^0$	RMSE	$\mathbf{5.0^0}$	6.5^0	6.3^0	11.5^0	10.0^0
	$E[\hat{\theta}]$ / $E[\hat{\tilde{\theta}}]$	254.3^0	247.4^0	248.8^0	246.7^0	248.6^0
vai_a/8K	Bias	5.2^0	-1.7^0	-0.3^0	-2.4^0	-0.5^0
$E[\hat{M}_0] = 3.6$	Std. Dev.	8.5^0	4.5^0	5.3^0	$\mathbf{2.7^0}$	3.4^0
$E[\hat{\alpha}_\theta] = 9.3^0$	RMSE	9.9^0	4.8^0	5.3^0	3.6^0	$\mathbf{3.5^0}$
	$E[\hat{\theta}]$ / $E[\hat{\tilde{\theta}}]$	177.8^0	171.5^0	172.1^0	163.5^0	166.7^0
vcs_a/8K	Bias	-3.7^0	-10.0^0	-9.4^0	-18.0^0	-14.8^0
$E[\hat{M}_0] = 3.9$	Std. Dev.	18.2^0	$\mathbf{10.4^0}$	10.7^0	11.2^0	11.9^0
$E[\hat{\alpha}_\theta] = 24.7^0$	RMSE	18.6^0	14.4^0	$\mathbf{14.2^0}$	21.2^0	18.9^0
	$E[\hat{\theta}]$ / $E[\hat{\tilde{\theta}}]$	181.3^0	183.9^0	183.4^0	184.6^0	182.1^0
vcs_b/8K	Bias	-0.2^0	2.4^0	1.9^0	3.1^0	0.6^0
$E[\hat{M}_0] = 2.8$	Std. Dev.	8.1^0	2.8^0	$\mathbf{2.6^0}$	9.3^0	3.9^0
$E[\hat{\alpha}_\theta] = 3.6^0$	RMSE	8.1^0	3.7^0	$\mathbf{3.2^0}$	9.8^0	3.9^0
	$E[\hat{\theta}]$ / $E[\hat{\tilde{\theta}}]$	189.9^0	194.1^0	196.9^0	193.0^0	193.4^0
vcs_c/8K	Bias	8.4^0	12.6^0	15.4^0	11.5^0	11.9^0
$E[\hat{M}_0] = 3.9$	Std. Dev.	3.5^0	3.5^0	6.3^0	3.1^0	3.0^0
$E[\hat{\alpha}_\theta] = 8.6^0$	RMSE	$\mathbf{9.1^0}$	13.0^0	16.6^0	11.9^0	12.2^0
	$E[\hat{\theta}]$ / $E[\hat{\tilde{\theta}}]$	181.1^0	182.2^0	182.1^0	184.0^0	178.9^0
vcs_d/8K	Bias	-0.4^0	0.7^0	0.6^0	2.5^0	-2.6^0
$E[\hat{M}_0] = 3.1$	Std. Dev.	4.4^0	4.7^0	6.8^0	7.3^0	3.9^0
$E[\hat{\alpha}_\theta] = 7.1^0$	RMSE	$\mathbf{4.4^0}$	4.7^0	6.8^0	7.7^0	4.7^0
Overall	Std. Dev.	8.6^0	$\mathbf{5.4^0}$	6.4^0	7.2^0	6.0^0
Result	RMSE	9.6^0	$\mathbf{8.4^0}$	9.5^0	11.4^0	9.8^0

Table 6.4: Narrower bandwidth, cv = 90%

		MUSIC	DISP1	DISP2	MUDI	BFDI
	$E[\hat{\theta}]$ / $E[\hat{\bar{\theta}}]$	181.2^0	183.7^0	182.7^0	184.6^0	183.1^0
cfh_a/8K	Bias	-0.7^0	1.8^0	0.8^0	2.7^0	1.2^0
$E[\hat{M}_0] = 2.6$	Std. Dev.	3.0^0	3.3^0	3.6^0	3.1^0	$\mathbf{2.1^0}$
$E[\hat{\alpha}_\theta] = 5.5^0$	RMSE	3.1^0	3.8^0	3.7^0	4.1^0	$\mathbf{2.4^0}$
	$E[\hat{\theta}]$ / $E[\hat{\bar{\theta}}]$	94.9^0	93.2^0	93.5^0	90.4^0	90.5^0
iar_a/8K	Bias	-3.5^0	-5.2^0	-4.9^0	-8.0^0	-7.9^0
$E[\hat{M}_0] = 2.8$	Std. Dev.	$\mathbf{3.6^0}$	5.3^0	6.0^0	4.8^0	5.0^0
$E[\hat{\alpha}_\theta] = 19.2^0$	RMSE	$\mathbf{5.0^0}$	7.4^0	7.8^0	9.3^0	9.4^0
	$E[\hat{\theta}]$ / $E[\hat{\bar{\theta}}]$	254.3^0	249.9^0	251.4^0	248.2^0	249.0^0
vai_a/8K	Bias	5.2^0	0.8^0	2.3^0	-0.9^0	-0.1^0
$E[\hat{M}_0] = 2.8$	Std. Dev.	8.5^0	5.8^0	6.2^0	$\mathbf{4.5^0}$	4.7^0
$E[\hat{\alpha}_\theta] = 9.3^0$	RMSE	9.9^0	5.8^0	6.6^0	$\mathbf{4.6^0}$	4.7^0
	$E[\hat{\theta}]$ / $E[\hat{\bar{\theta}}]$	177.8^0	169.8^0	171.8^0	161.5^0	165.0^0
vcs_a/8K	Bias	-3.7^0	-11.7^0	-9.7^0	-20.0^0	-16.5^0
$E[\hat{M}_0] = 3.1$	Std. Dev.	18.2^0	12.6^0	$\mathbf{10.4^0}$	12.4^0	11.7^0
$E[\hat{\alpha}_\theta] = 24.7^0$	RMSE	18.6^0	17.2^0	$\mathbf{14.2^0}$	23.5^0	20.2^0
	$E[\hat{\theta}]$ / $E[\hat{\bar{\theta}}]$	181.3^0	183.1^0	182.8^0	183.3^0	182.9^0
vcs_b/8K	Bias	-0.2^0	1.6^0	1.3^0	1.8^0	1.4^0
$E[\hat{M}_0] = 1.9$	Std. Dev.	8.1^0	2.6^0	2.1^0	2.5^0	$\mathbf{2.1^0}$
$E[\hat{\alpha}_\theta] = 3.6^0$	RMSE	8.1^0	3.1^0	$\mathbf{2.4^0}$	3.1^0	2.5^0
	$E[\hat{\theta}]$ / $E[\hat{\bar{\theta}}]$	189.9^0	194.5^0	195.3^0	194.6^0	194.2^0
vcs_c/8K	Bias	8.4^0	13.0^0	13.8^0	13.1^0	12.7^0
$E[\hat{M}_0] = 3.0$	Std. Dev.	3.5^0	4.0^0	5.1^0	3.8^0	$\mathbf{3.3^0}$
$E[\hat{\alpha}_\theta] = 8.6^0$	RMSE	$\mathbf{9.1^0}$	13.6^0	14.7^0	13.6^0	13.1^0
	$E[\hat{\theta}]$ / $E[\hat{\bar{\theta}}]$	181.1^0	182.0^0	181.8^0	181.2^0	180.9^0
vcs_d/8K	Bias	-0.4^0	0.5^0	0.3^0	-0.3^0	-0.6^0
$E[\hat{M}_0] = 2.3$	Std. Dev.	4.4^0	4.6^0	4.0^0	4.6^0	$\mathbf{2.7^0}$
$E[\hat{\alpha}_\theta] = 7.1^0$	RMSE	4.4^0	4.6^0	4.0^0	4.6^0	$\mathbf{2.8^0}$
Overall	Std. Dev.	8.6^0	6.3^0	5.9^0	6.0^0	$\mathbf{5.5^0}$
Result	RMSE	9.6^0	9.4^0	$\mathbf{8.9^0}$	11.3^0	10.1^0

6.2.2 Changing K for MUSIC

For MUSIC, using a $K > 1$ is easily implemented. The noise eigenvector matrix $\hat{V}_N$ would then contain $(M-K)$ eigenvectors corresponding to the smallest $(M-K)$ eigenvalues, the noise subspace projector $\hat{P}_N = \hat{V}_N \hat{V}_N^\dagger$ and then one just applies Eq.(2.15).

Experiment 6.3: $K > 1$

Objective: To test MUSIC with various number of sensors and $K > 1$.

Scenario: We repeat Experiment 6.1, but now using $K = 2, 3$ and 4.

Results: The results are shown in Tables 6.5 to 6.7.

Findings:

(a) The best estimates are obtained with $K = 2$ and $M = 10$.

(b) For vcs_a, if $K = 1$, MUSIC fails to yield a consistent $\hat{\theta}$. If $K > 1$, the performance is much better. Besides, the $\mathrm{E}[\hat{\theta}]$ changes from around 200^0 to around 175^0, which is nearer to the $\mathrm{E}[\hat{\theta}]$ found from the dispersive methods (Table 4.2).

(c) The performance improvement by using a larger K is not universally true. For vcs_d, much better estimates are obtained at $K = 1$.

(d) There seems to be an interesting performance trend: by using a small K, a small M would give a better performance; by using a large K, a large M performs better.

Remarks: It is shown by computer simulation in [3] that K should be set to 1 for MUSIC regardless of the dispersiveness. The above results contradict this. One possible reason is that there is actually more than 1 dispersed signal. Another possible explanation is the dispersiveness encountered here is much larger than the simulation tests performed in [3].

Table 6.5: MUSIC, $K = 2$

		$M = 12$	$M = 10$	$M = 8$
cfh_a/8K	$E[\hat{\theta}]$	181.0^0	181.0^0	181.6^0
	Bias	-0.9^0	-0.9^0	-0.3^0
	Std. Dev.	3.2^0	2.5^0	$\mathbf{1.6^0}$
	RMSE	3.3^0	2.7^0	$\mathbf{1.6^0}$
iar_a/8K	$E[\hat{\theta}]$	108.7^0	112.2^0	112.3^0
	Bias	10.3^0	13.8^0	13.9^0
	Std. Dev.	8.7^0	8.9^0	$\mathbf{2.2^0}$
	RMSE	$\mathbf{13.5^0}$	16.4^0	14.1^0
vai_a/8K	$E[\hat{\theta}]$	253.0^0	253.2^0	245.8^0
	Bias	3.9^0	4.1^0	-3.3^0
	Std. Dev.	8.2^0	$\mathbf{7.0^0}$	8.2^0
	RMSE	9.0^0	$\mathbf{8.1^0}$	8.9^0
vcs_a/8K	$E[\hat{\theta}]$	178.9^0	176.0^0	167.7^0
	Bias	-2.6^0	-5.5^0	-13.8^0
	Std. Dev.	16.0^0	$\mathbf{10.8^0}$	16.6^0
	RMSE	16.2^0	$\mathbf{12.1^0}$	21.6^0
vcs_b/8K	$E[\hat{\theta}]$	183.5^0	183.0^0	183.0^0
	Bias	2.0^0	1.5^0	1.5^0
	Std. Dev.	4.2^0	$\mathbf{3.8^0}$	4.9^0
	RMSE	4.7^0	$\mathbf{4.1^0}$	5.1^0
vcs_c/8K	$E[\hat{\theta}]$	189.8^0	190.2^0	190.4^0
	Bias	8.3^0	8.7^0	8.9^0
	Std. Dev.	3.6^0	4.3^0	$\mathbf{3.2^0}$
	RMSE	$\mathbf{9.1^0}$	9.7^0	9.5^0
vcs_d/8K	$E[\hat{\theta}]$	180.5^0	180.3^0	183.0^0
	Bias	-1.0^0	-1.2^0	1.5^0
	Std. Dev.	$\mathbf{4.9^0}$	9.4^0	10.3^0
	RMSE	$\mathbf{5.0^0}$	9.4^0	10.4^0
Overall Result	Std. Dev.	8.1^0	$\mathbf{7.3^0}$	8.4^0
	RMSE	$\mathbf{9.7^0}$	9.9^0	11.8^0

Table 6.6: MUSIC, $K = 3$

		$M = 12$	$M = 10$	$M = 8$
cfh_a/8K	$E[\hat{\theta}]$	183.9^0	183.5^0	180.7^0
	Bias	2.0^0	1.6^0	-1.2^0
	Std. Dev.	4.8^0	5.6^0	$\mathbf{4.4^0}$
	RMSE	5.3^0	5.8^0	$\mathbf{4.6^0}$
iar_a/8K	$E[\hat{\theta}]$	107.8^0	112.4^0	101.6^0
	Bias	9.4^0	14.0^0	3.2^0
	Std. Dev.	8.4^0	5.7^0	$\mathbf{4.1^0}$
	RMSE	12.6^0	15.1^0	$\mathbf{5.2^0}$
vai_a/8K	$E[\hat{\theta}]$	251.6^0	244.3^0	237.4^0
	Bias	2.5^0	-4.8^0	-11.7^0
	Std. Dev.	9.6^0	10.8^0	$\mathbf{3.9^0}$
	RMSE	$\mathbf{9.9^0}$	11.8^0	12.3^0
vcs_a/8K	$E[\hat{\theta}]$	180.8^0	174.1^0	174.5^0
	Bias	-0.7^0	-7.4^0	-7.0^0
	Std. Dev.	17.1^0	$\mathbf{12.3^0}$	13.1^0
	RMSE	17.1^0	$\mathbf{14.3^0}$	14.9^0
vcs_b/8K	$E[\hat{\theta}]$	183.6^0	183.0^0	183.5^0
	Bias	2.1^0	1.5^0	2.0^0
	Std. Dev.	$\mathbf{2.6^0}$	3.7^0	4.3^0
	RMSE	$\mathbf{3.4^0}$	4.0^0	4.7^0
vcs_c/8K	$E[\hat{\theta}]$	190.2^0	192.0^0	197.1^0
	Bias	8.7^0	10.5^0	15.6^0
	Std. Dev.	$\mathbf{4.8^0}$	6.9^0	8.6^0
	RMSE	$\mathbf{10.0^0}$	12.6^0	17.9^0
vcs_d/8K	$E[\hat{\theta}]$	182.8^0	182.5^0	182.2^0
	Bias	1.3^0	1.0^0	0.7^0
	Std. Dev.	$\mathbf{6.2^0}$	9.5^0	11.0^0
	RMSE	$\mathbf{6.3^0}$	9.5^0	11.0^0
Overall Result	Std. Dev.	8.8^0	8.3^0	$\mathbf{7.9^0}$
	RMSE	$\mathbf{10.2^0}$	11.2^0	11.2^0

Table 6.7: MUSIC, $K = 4$

		$M = 12$	$M = 10$	$M = 8$
cfh_a/8K	$E[\hat{\theta}]$	183.4^0	183.9^0	183.3^0
	Bias	1.5^0	2.0^0	1.4^0
	Std. Dev.	**4.8^0**	5.1^0	5.0^0
	RMSE	**5.1^0**	5.5^0	5.2^0
iar_a/8K	$E[\hat{\theta}]$	99.4^0	96.7^0	80.2^0
	Bias	1.0^0	-1.7^0	-18.2^0
	Std. Dev.	**10.7^0**	11.7^0	33.0^0
	RMSE	**10.8^0**	11.8^0	37.6^0
vai_a/8K	$E[\hat{\theta}]$	249.8^0	244.5^0	242.8^0
	Bias	0.7^0	-4.6^0	-6.3^0
	Std. Dev.	**9.3^0**	10.9^0	9.5^0
	RMSE	**9.4^0**	11.9^0	11.4^0
vcs_a/8K	$E[\hat{\theta}]$	177.5^0	171.1^0	177.5^0
	Bias	-4.0^0	-10.4^0	-4.0^0
	Std. Dev.	15.7^0	11.9^0	**5.0^0**
	RMSE	16.2^0	15.8^0	**6.3^0**
vcs_b/8K	$E[\hat{\theta}]$	183.9^0	182.3^0	182.4^0
	Bias	2.4^0	0.8^0	0.9^0
	Std. Dev.	**2.6^0**	6.0^0	4.7^0
	RMSE	**3.6^0**	6.0^0	4.8^0
vcs_c/8K	$E[\hat{\theta}]$	190.1^0	192.8^0	201.2^0
	Bias	8.6^0	11.2^0	19.7^0
	Std. Dev.	**3.5^0**	6.2^0	6.5^0
	RMSE	**9.3^0**	12.9^0	20.7^0
vcs_d/8K	$E[\hat{\theta}]$	186.8^0	180.5^0	182.0^0
	Bias	5.3^0	-1.0^0	0.5^0
	Std. Dev.	**6.9^0**	9.5^0	12.1^0
	RMSE	**8.7^0**	9.5^0	12.1^0
Overall Result	Std. Dev.	**8.8^0**	9.2^0	14.3^0
	RMSE	**9.8^0**	11.0^0	17.8^0

6.2.3 Assume Multiple Signals for Dispersive Methods

By assuming multiple signals, the effective signal dimension m_0 is no longer equal to the total effective signal dimension M_0. Additionally, we cannot use $\{\hat{\lambda}\}$ to estimate $\hat{\alpha}_\theta$ as $\{\hat{\lambda}\}$ are the estimated eigenvalues of the combined signals.

Here, we estimate $\hat{\alpha}_\theta$ from $\hat{m}_0$ by using Approach C discussed in Subsection 5.3.1, where $\hat{m}_0$ is assumed to have some relationship with $\hat{M}_0$. In particular, we test the following two relations.

$$\begin{aligned} \hat{m}_0 &= \hat{M}_0 - 1 \\ \hat{m}_0 &= \frac{\hat{M}_0}{2} \end{aligned}$$

Experiment 6.4: Assume multiple signals

Objective: To test the dispersive methods by assuming multiple signals.

Scenario: We test for 2 cases. In (a), $\hat{m}_0 = \hat{M}_0 - 1$. In (b), $\hat{m}_0 = \frac{\hat{M}_0}{2}$. The MUSIC results are estimated by using $M = 12$, $K = 1$, and act as benchmark.

Results: The results are shown in Tables 6.8 and 6.9.

Findings: The performances are worse than that assuming $K = 1$ (Table 4.2).

Remarks: The result does not mean that there is only 1 dispersed signal. There may be more than 1 signal present but the desired signal may not have the greatest strength. Anyway, we consider it too complicated to further investigate multiple dispersed signals. Up to now, there is *no* published paper about detecting the number of dispersed signals. In fact, single or multiple dispersed signals are hard to differentiate both theoretically and practically. In an extreme example, even a spatially white noise can be treated as a dispersed signal (uniformly distributed, $\bar{\theta} = 0^0$, $\alpha_\theta = 180^0$)! For simplicity, we suggest using the assumption $K = 1$.

Table 6.8: Dispersive Methods, $\hat{m}_0 = \hat{M}_0 - 1$

		MUSIC	DISP1	DISP2	MUDI	BFDI
	$E[\hat{\theta}]$ / $E[\hat{\tilde{\theta}}]$	181.0^0	183.5^0	182.8^0	183.7^0	183.9^0
cfh_a/8K	Bias	-0.9^0	1.6^0	0.9^0	1.8^0	2.0^0
$E[\hat{M}_0] = 3.7$	Std. Dev.	3.2^0	2.1^0	2.4^0	2.0^0	$\mathbf{1.7^0}$
$E[\hat{\alpha}_\theta] = 5.9^0$	RMSE	3.4^0	2.6^0	$\mathbf{2.6^0}$	2.7^0	2.6^0
	$E[\hat{\theta}]$ / $E[\hat{\tilde{\theta}}]$	112.4^0	109.3^0	110.5^0	105.2^0	109.4^0
iar_a/8K	Bias	14.0^0	10.9^0	12.1^0	6.8^0	11.0^0
$E[\hat{M}_0] = 3.6$	Std. Dev.	5.8^0	5.9^0	8.1^0	9.9^0	$\mathbf{4.4^0}$
$E[\hat{\alpha}_\theta] = 15.3^0$	RMSE	15.1^0	12.4^0	14.5^0	12.0^0	$\mathbf{11.8^0}$
	$E[\hat{\theta}]$ / $E[\hat{\tilde{\theta}}]$	254.3^0	246.2^0	247.3^0	245.4^0	248.3^0
vai_a/8K	Bias	5.2^0	-2.9^0	-1.8^0	-3.7^0	-0.8^0
$E[\hat{M}_0] = 4.4$	Std. Dev.	8.4^0	6.3^0	6.7^0	4.6^0	$\mathbf{2.7^0}$
$E[\hat{\alpha}_\theta] = 8.6^0$	RMSE	9.9^0	6.9^0	6.9^0	5.9^0	$\mathbf{2.8^0}$
	$E[\hat{\theta}]$ / $E[\hat{\tilde{\theta}}]$	197.6^0	172.5^0	172.9^0	156.5^0	168.5^0
vcs_a/8K	Bias	16.1^0	-9.0^0	-8.6^0	-25.0^0	-13.0^0
$E[\hat{M}_0] = 4.0$	Std. Dev.	31.2^0	12.5^0	$\mathbf{10.4^0}$	12.5^0	16.5^0
$E[\hat{\alpha}_\theta] = 18.9^0$	RMSE	35.1^0	15.4^0	$\mathbf{13.5^0}$	28.0^0	21.0^0
	$E[\hat{\theta}]$ / $E[\hat{\tilde{\theta}}]$	183.9^0	184.0^0	183.7^0	183.5^0	184.1^0
vcs_b/8K	Bias	2.4^0	2.5^0	2.2^0	2.0^0	2.6^0
$E[\hat{M}_0] = 3.2$	Std. Dev.	5.2^0	3.0^0	3.4^0	$\mathbf{2.5^0}$	5.3^0
$E[\hat{\alpha}_\theta] = 3.8^0$	RMSE	5.7^0	3.9^0	4.0^0	$\mathbf{3.2^0}$	5.9^0
	$E[\hat{\theta}]$ / $E[\hat{\tilde{\theta}}]$	196.3^0	191.8^0	192.7^0	193.7^0	195.2^0
vcs_c/8K	Bias	14.8^0	10.3^0	11.2^0	12.2^0	13.8^0
$E[\hat{M}_0] = 4.0$	Std. Dev.	6.5^0	$\mathbf{2.1^0}$	3.0^0	3.2^0	3.2^0
$E[\hat{\alpha}_\theta] = 6.9^0$	RMSE	16.2^0	$\mathbf{10.6^0}$	11.6^0	12.6^0	14.1^0
	$E[\hat{\theta}]$ / $E[\hat{\tilde{\theta}}]$	181.1^0	181.5^0	181.7^0	182.5^0	180.6^0
vcs_d/8K	Bias	-0.4^0	-0.0^0	0.2^0	1.0^0	-0.9^0
$E[\hat{M}_0] = 3.3$	Std. Dev.	4.4^0	4.7^0	7.1^0	6.0^0	$\mathbf{3.2^0}$
$E[\hat{\alpha}_\theta] = 6.7^0$	RMSE	4.4^0	4.7^0	7.1^0	6.1^0	$\mathbf{3.3^0}$
Overall	Std. Dev.	13.0^0	6.2^0	6.5^0	6.9^0	7.1^0
Result	RMSE	16.4^0	9.2^0	9.6^0	13.0^0	11.0^0

Table 6.9: Dispersive Methods, $\hat{m}_0 = \frac{\hat{M}_0}{2}$

		MUSIC	DISP1	DISP2	MUDI	BFDI
	$E[\hat{\theta}]$ / $E[\hat{\tilde{\theta}}]$	181.0^0	183.9^0	183.9^0	183.5^0	182.1^0
cfh_a/8K	Bias	-0.9^0	2.0^0	2.0^0	1.6^0	0.2^0
$E[\hat{M}_0] = 3.7$	Std. Dev.	3.2^0	4.2^0	4.7^0	3.4^0	$\mathbf{2.4^0}$
$E[\hat{\alpha}_\theta] = 2.4^0$	RMSE	3.4^0	4.7^0	5.1^0	3.7^0	$\mathbf{2.4^0}$
	$E[\hat{\theta}]$ / $E[\hat{\tilde{\theta}}]$	112.4^0	104.2^0	108.5^0	106.1^0	111.8^0
iar_a/8K	Bias	14.0^0	5.8^0	10.1^0	7.7^0	13.4^0
$E[\hat{M}_0] = 3.6$	Std. Dev.	5.8^0	7.7^0	11.4^0	7.9^0	$\mathbf{5.2^0}$
$E[\hat{\alpha}_\theta] = 6.9^0$	RMSE	15.1^0	$\mathbf{9.6^0}$	15.2^0	11.0^0	14.4^0
	$E[\hat{\theta}]$ / $E[\hat{\tilde{\theta}}]$	254.3^0	247.9^0	249.6^0	244.5^0	251.9^0
vai_a/8K	Bias	5.2^0	-1.2^0	0.5^0	-4.6^0	2.8^0
$E[\hat{M}_0] = 4.4$	Std. Dev.	8.4^0	9.0^0	9.2^0	$\mathbf{7.5^0}$	7.7^0
$E[\hat{\alpha}_\theta] = 3.0^0$	RMSE	9.9^0	9.1^0	9.2^0	8.8^0	$\mathbf{8.2^0}$
	$E[\hat{\theta}]$ / $E[\hat{\tilde{\theta}}]$	197.6^0	167.9^0	168.0^0	164.0^0	174.2^0
vcs_a/8K	Bias	16.1^0	-13.6^0	-13.5^0	-17.5^0	-7.3^0
$E[\hat{M}_0] = 4.0$	Std. Dev.	31.2^0	$\mathbf{13.8^0}$	13.9^0	14.3^0	20.5^0
$E[\hat{\alpha}_\theta] = 9.0^0$	RMSE	35.1^0	$\mathbf{19.3^0}$	19.4^0	22.6^0	21.8^0
	$E[\hat{\theta}]$ / $E[\hat{\tilde{\theta}}]$	183.9^0	183.8^0	183.6^0	183.5^0	183.5^0
vcs_b/8K	Bias	2.4^0	2.3^0	2.1^0	2.0^0	2.0^0
$E[\hat{M}_0] = 3.2$	Std. Dev.	5.2^0	2.5^0	2.6^0	$\mathbf{2.4^0}$	4.3^0
$E[\hat{\alpha}_\theta] = 1.5^0$	RMSE	5.7^0	3.4^0	3.3^0	$\mathbf{3.1^0}$	4.8^0
	$E[\hat{\theta}]$ / $E[\hat{\tilde{\theta}}]$	196.3^0	191.0^0	191.5^0	191.6^0	192.9^0
vcs_c/8K	Bias	14.8^0	9.5^0	10.0^0	10.1^0	11.4^0
$E[\hat{M}_0] = 4.0$	Std. Dev.	6.5^0	$\mathbf{3.3^0}$	3.5^0	4.7^0	3.6^0
$E[\hat{\alpha}_\theta] = 2.9^0$	RMSE	16.2^0	$\mathbf{10.1^0}$	10.6^0	11.1^0	12.0^0
	$E[\hat{\theta}]$ / $E[\hat{\tilde{\theta}}]$	181.1^0	183.1^0	182.2^0	182.7^0	180.6^0
vcs_d/8K	Bias	-0.4^0	1.6^0	0.7^0	1.2^0	-0.9^0
$E[\hat{M}_0] = 3.3$	Std. Dev.	4.4^0	6.3^0	6.2^0	5.6^0	$\mathbf{3.8^0}$
$E[\hat{\alpha}_\theta] = 2.3^0$	RMSE	4.4^0	6.5^0	6.3^0	5.8^0	$\mathbf{3.9^0}$
Overall	Std. Dev.	13.0^0	7.6^0	8.3^0	$\mathbf{7.5^0}$	8.9^0
Result	RMSE	16.4^0	$\mathbf{10.2^0}$	11.2^0	11.3^0	11.6^0

Chapter 7

Conclusion

7.1 Achievement

Here is a summary of the work done in this project.

(a) We verified the input data by examining the FFT spectrums (Section 1.4). Among the 216 data sets (each data set contains 8K samples), 4 of them are corrupted.

(b) We developed a general signal model to compute $\tilde{R}$ of a dispersed signal (Section 2.2).

(c) By assuming uniform distribution, we came up with 3 approximated signal models (Section 3.1). Model 2 (multiple points simulation) is the best due to its implementation flexibility.

(d) We suggested 3 approaches to estimate $\hat{\bar{\theta}}$ (Section 3.2). Among them, Approach 3 (estimate $\hat{\alpha}_\theta$ from $\{\hat{\lambda}\}$, and a 1-D search on $\bar{\theta}$) gives the best performance and requires the smallest computation load.

(e) We tried 6 different distribution types to construct $\tilde{R}$ (Section 4.1). Testing results show that the performance is not very sensitive to the distribution type. Type 2 (uniform distribution with square region) was adopted for its relatively simplicity in implementation.

(f) We suggested combining several dispersive methods by summing up the normalized cost function values (Section 4.3). The result was quite promising.

(g) We fine-tuned the parameter settings (Chapter 5). Here are the suggested settings.

(i) Grid density of the multipe points model: The azimuth adjacent distance (aad) should be set to 1^0 and the elevation adjacent distance (ead) should be set to 2^0.

(ii) Total effective signal dimension $\hat{M}_0$: it should be derived from $\{\hat{\lambda}\}$, cp = 6 (or $\frac{1}{2}M$), cv = 95% (or 90%).

(iii) The azimuth spread $\hat{\alpha}_\theta$: the resulting $\hat{\bar{\theta}}$ is not very sensitive to the choice of $\hat{\alpha}_\theta$. If K is assumed equal to 1, $\hat{\alpha}_\theta$ should be found from Approach A (i.e. estimated from $\{\hat{\lambda}\}$). If K is assumed larger than 1, it can be found using Approach C (i.e. estimated from $\hat{m}_0$).

(h) We tried to adjust M and K (Chapter 6). For MUSIC, we suggest using $M = 8$ and $K = 1$. For dispersive methods, we suggest using $M = 12$ and $K = 1$.

(i) We tried to compute $\hat{\boldsymbol{R}}$ by using a narrower passing band (Section 6.2). MUSIC then performs better.

7.2 The Best Achieved Results

We compare the best achieved results from MUSIC and from the dispersive methods. In particular, we choose the following five sets of results, which are listed in Table 7.1.

- MUSIC1: MUSIC with K=1, M=8 (Table 6.2),
- MUSIC2: MUSIC with K=2, M=10 (Table 6.5),
- BFDI1: Distribution Type = 2, cp = 6, cv = 95%, $\hat{\alpha}_\theta$ estimated from $\{\hat{\lambda}\}$ (Table 4.2),
- BFDI2: Distribution Type = 2, cp = 6, cv = 95%, $\hat{\alpha}_\theta = 10^0$ (Table 5.16),
- COMB: Combining DISP 1, MUSIC DISC and BF DISC (Table 4.7).

The estimated $\hat{\theta}$ of MUSIC (i.e. using the data collecting from 12 antennas) and MUSIC1 (i.e. using the data collected from 8 antennas), and $\hat{\tilde{\theta}}$ of BFDI1 are plotted in Fig.7.1(a)-(g). The straight line shows the suggested nominal angle.

Table 7.1: Comparison of the Best Achieved Results

		MUSIC1	MUSIC2	BFDI1	BFDI2	COMB
cfh_a/8K	$E[\hat{\theta}]$ / $E[\hat{\bar{\theta}}]$	182.1^0	181.0^0	185.2^0	186.7^0	184.3^0
	Bias	0.2^0	-0.9^0	3.3^0	4.8^0	2.4^0
	Std. Dev.	2.2^0	2.5^0	3.0^0	2.9^0	$\mathbf{1.7^0}$
	RMSE	$\mathbf{2.2^0}$	2.7^0	4.5^0	5.6^0	3.0^0
iar_a/8K	$E[\hat{\theta}]$ / $E[\hat{\bar{\theta}}]$	111.1^0	112.2^0	109.3^0	110.7^0	108.7^0
	Bias	12.7^0	13.8^0	10.9^0	12.3^0	10.3^0
	Std. Dev.	3.5^0	8.9^0	4.7^0	$\mathbf{3.1^0}$	4.1^0
	RMSE	13.2^0	16.4^0	11.9^0	12.7^0	$\mathbf{11.1^0}$
vai_a/8K	$E[\hat{\theta}]$ / $E[\hat{\bar{\theta}}]$	254.8^0	253.2^0	247.3^0	247.6^0	247.0^0
	Bias	5.7^0	4.1^0	-1.8^0	-1.5^0	-2.1^0
	Std. Dev.	8.9^0	7.0^0	2.1^0	$\mathbf{1.8^0}$	2.3^0
	RMSE	10.6^0	8.1^0	2.8^0	$\mathbf{2.3^0}$	3.1^0
vcs_a/8K	$E[\hat{\theta}]$ / $E[\hat{\bar{\theta}}]$	189.8^0	176.0^0	167.6^0	173.6^0	168.9^0
	Bias	8.3^0	-5.5^0	-13.9^0	-7.9^0	-12.6^0
	Std. Dev.	21.2^0	10.8^0	8.0^0	3.4^0	$\mathbf{3.3^0}$
	RMSE	22.8^0	12.1^0	16.1^0	$\mathbf{8.6^0}$	13.0^0
vcs_b/8K	$E[\hat{\theta}]$ / $E[\hat{\bar{\theta}}]$	183.4^0	183.0^0	186.2^0	190.0^0	185.2^0
	Bias	1.9^0	1.5^0	4.7^0	8.5^0	3.7^0
	Std. Dev.	6.3^0	$\mathbf{3.8^0}$	5.8^0	5.8^0	4.2^0
	RMSE	6.6^0	$\mathbf{4.1^0}$	7.5^0	10.3^0	5.6^0
vcs_c/8K	$E[\hat{\theta}]$ / $E[\hat{\bar{\theta}}]$	197.5^0	190.2^0	196.7^0	196.1^0	195.8^0
	Bias	16.0^0	8.7^0	15.2^0	14.6^0	14.3^0
	Std. Dev.	6.9^0	4.3^0	$\mathbf{2.1^0}$	2.5^0	2.1^0
	RMSE	17.4^0	$\mathbf{9.7^0}$	15.4^0	14.8^0	14.5^0
vcs_d/8K	$E[\hat{\theta}]$ / $E[\hat{\bar{\theta}}]$	181.1^0	180.3^0	178.6^0	178.9^0	181.2^0
	Bias	-0.4^0	-1.2^0	-2.9^0	-2.6^0	-0.3^0
	Std. Dev.	$\mathbf{1.8^0}$	9.4^0	4.2^0	4.9^0	4.5^0
	RMSE	$\mathbf{1.8^0}$	9.4^0	5.1^0	5.6^0	4.5^0
Overall Result	Std. Dev.	9.5^0	7.3^0	4.7^0	3.7^0	$\mathbf{3.3^0}$
	RMSE	12.9^0	9.9^0	10.3^0	9.5^0	$\mathbf{9.0^0}$

Figure 7.1: Plots of the Estimated Azimuth Angles

(a) cfh_a

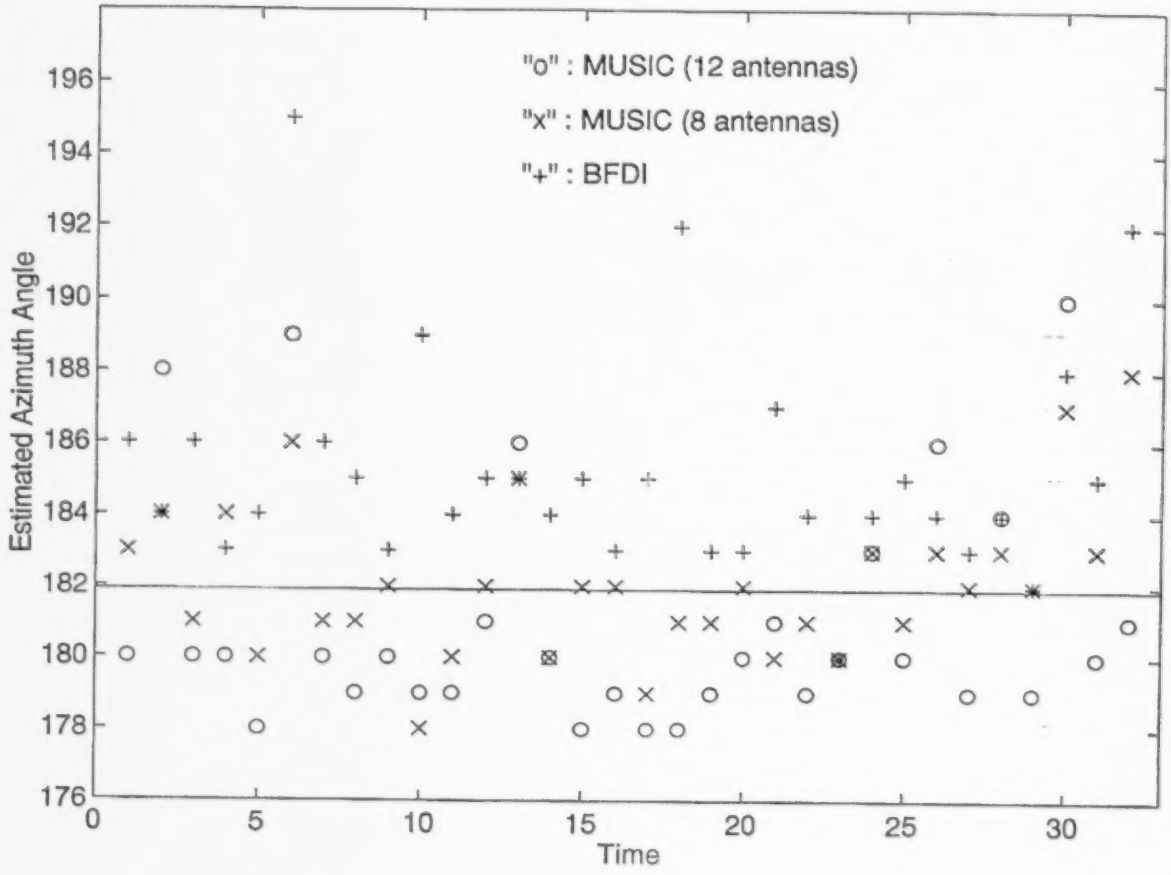

Figure 7.1: Plots of the Estimated Azimuth Angles (Cont'd)

(b) iar_a

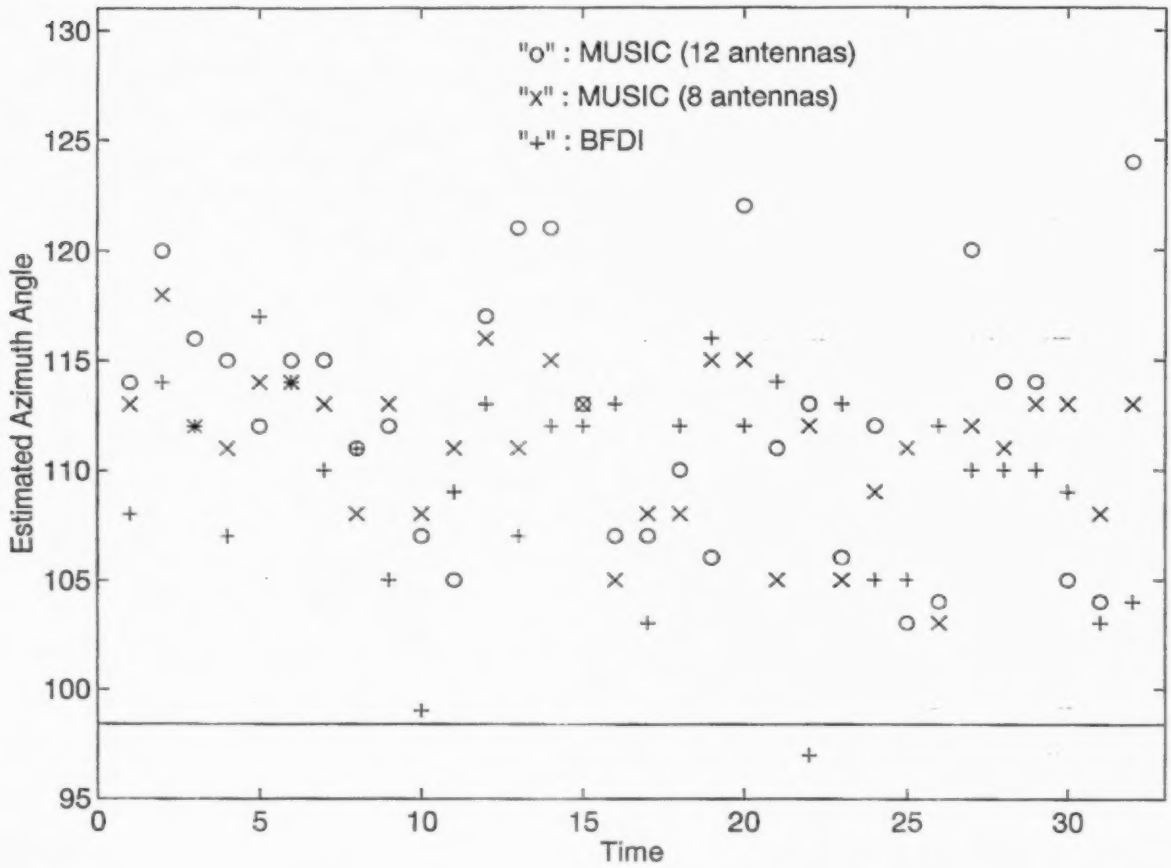

Figure 7.1: Plots of the Estimated Azimuth Angles (Cont'd)

(c) vai_a

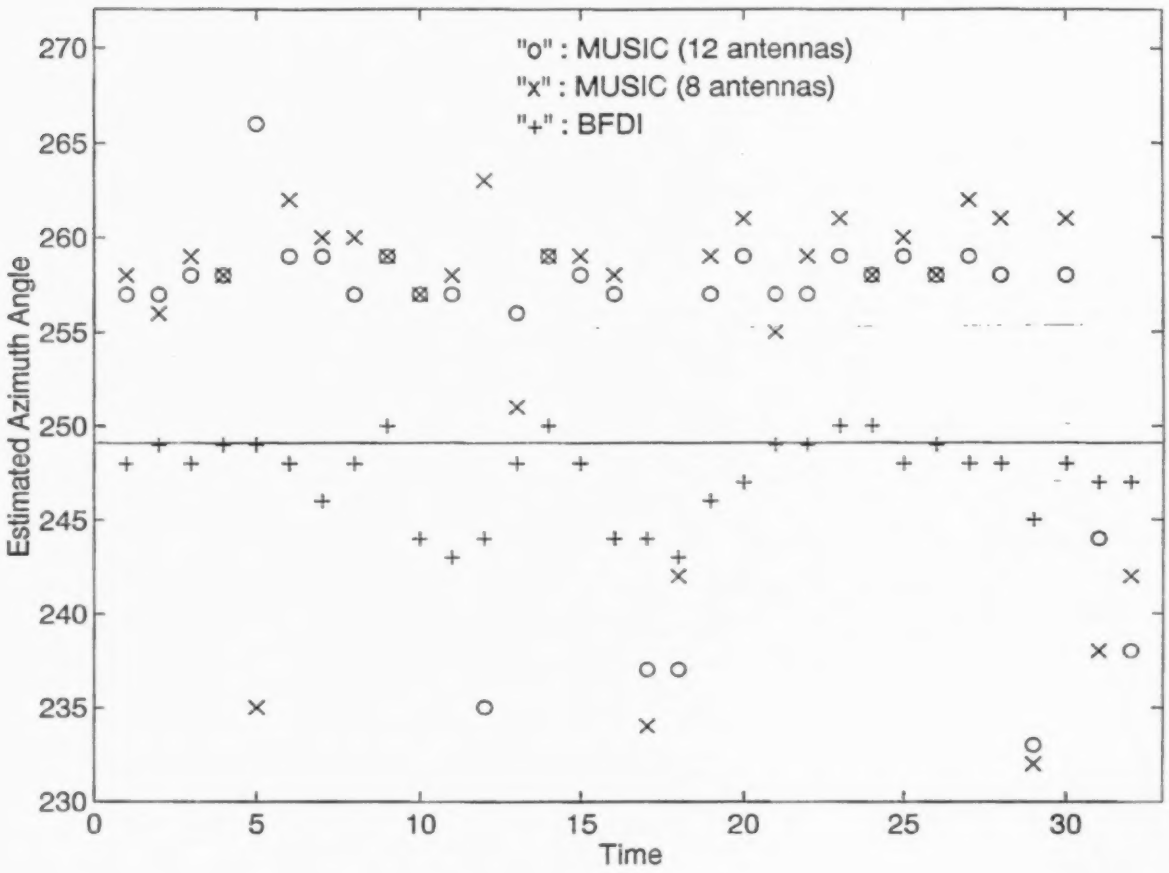

Figure 7.1: Plots of the Estimated Azimuth Angles (Cont'd)

(d) vcs_a

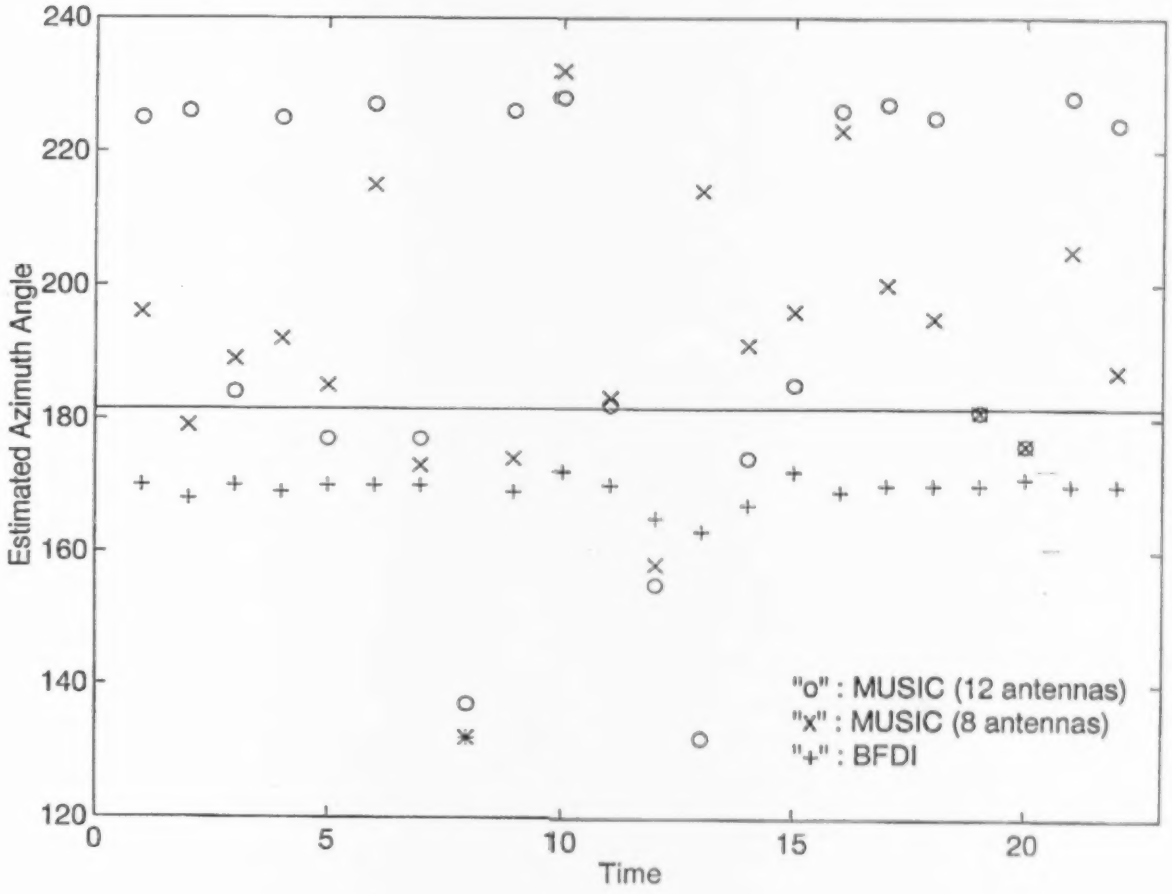

Figure 7.1: Plots of the Estimated Azimuth Angles (Cont'd)

(e) vcs_b

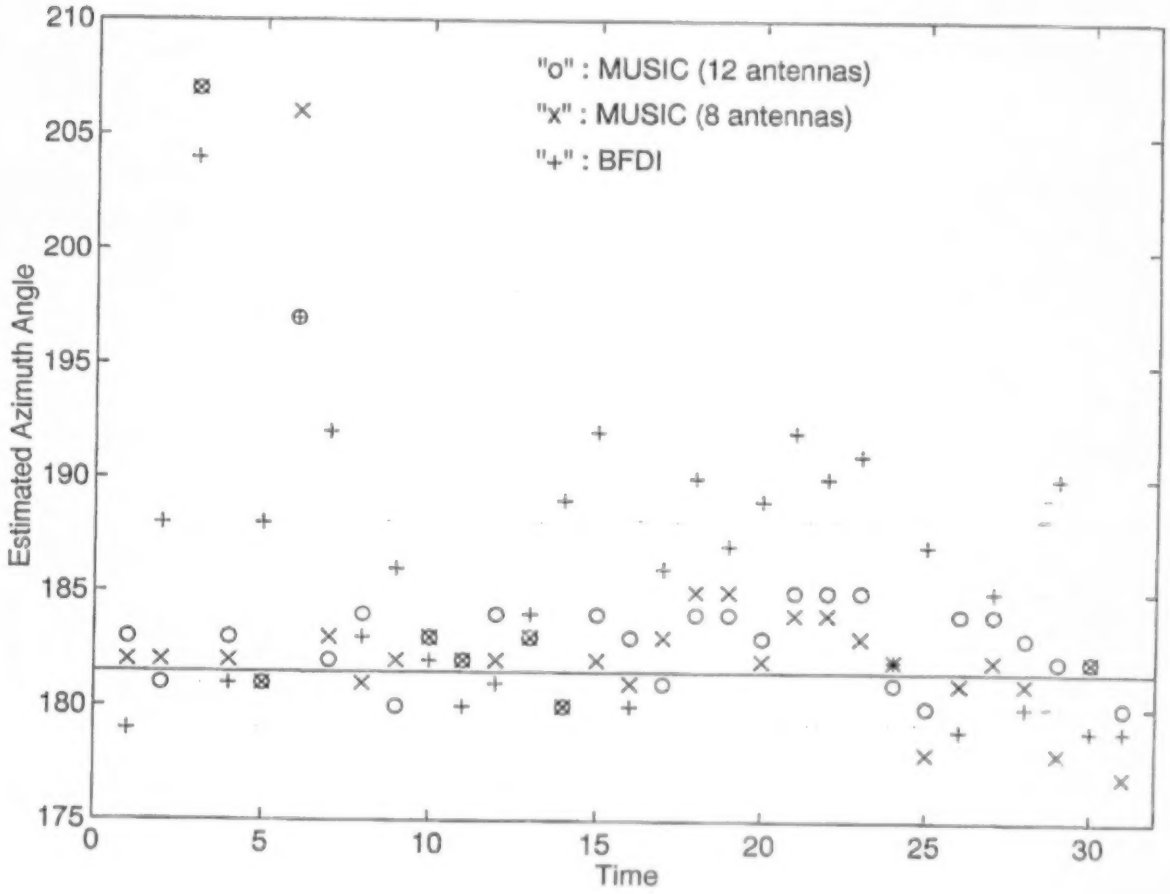

Figure 7.1: Plots of the Estimated Azimuth Angles (Cont'd)

(f) vcs_c

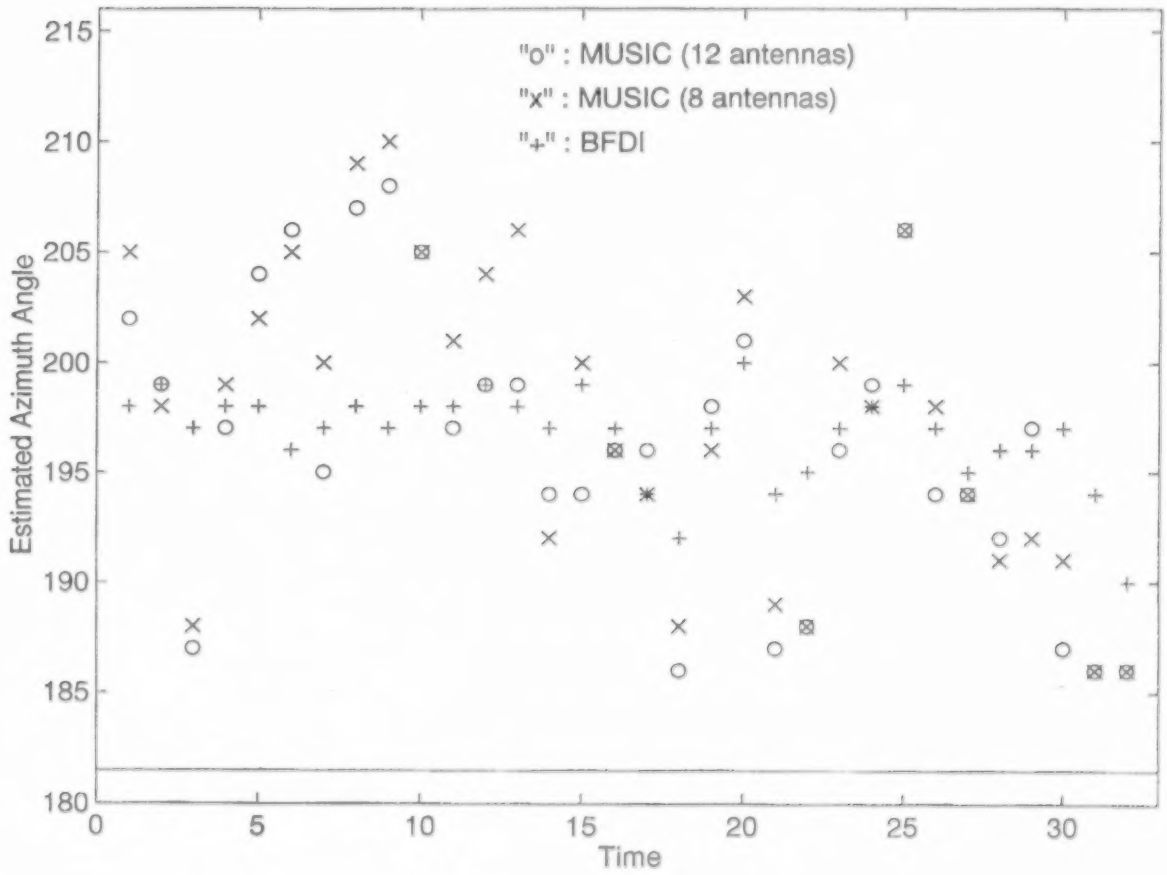

Figure 7.1: Plots of the Estimated Azimuth Angles (Cont'd)

(g) vcs_d

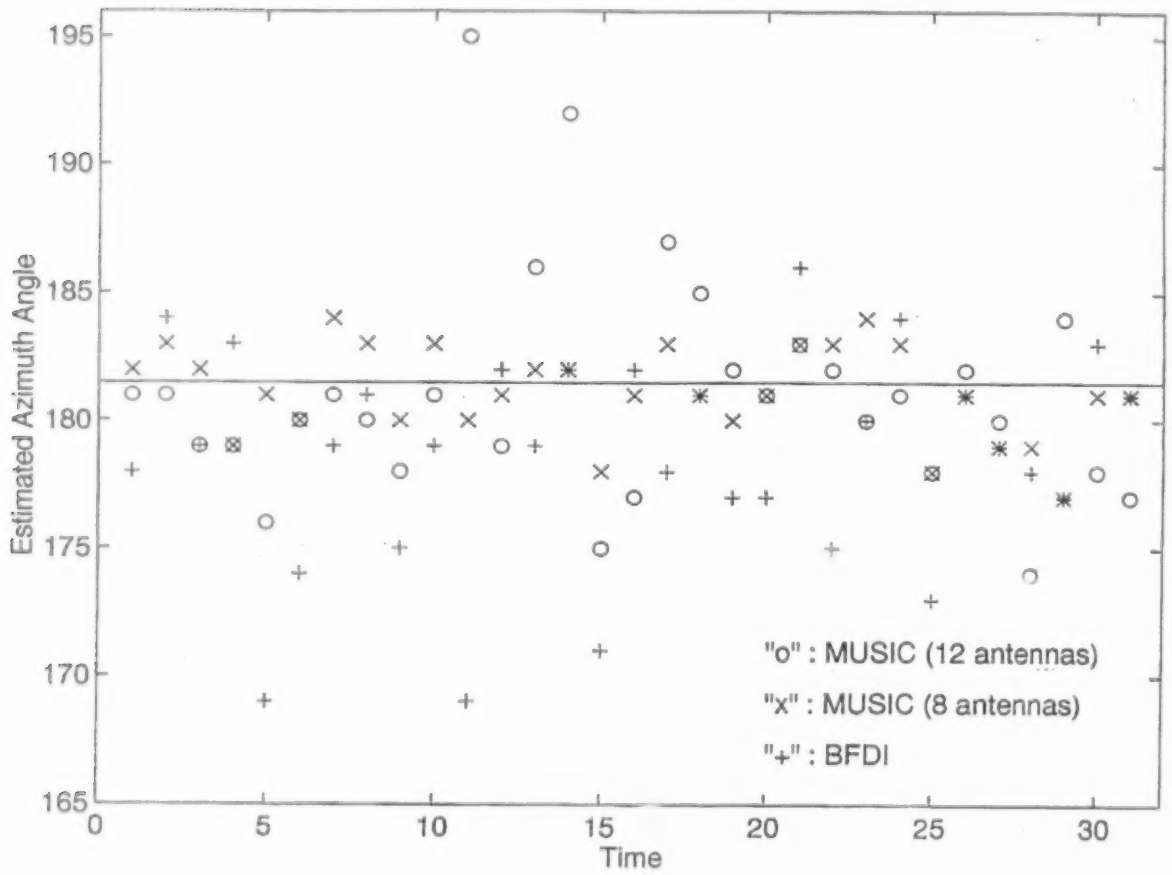

7.3 Conclusion

(a) Comments on the Suggested True Angle

One problem in the comparison process is that the suggested nominal azimuth angle θ_s may not be true due to the random signal scattering in the ionosphere. Thus, we should pay more attention to the "Standard Deviaton" than the "Root Mean Square Error" of the estimated $\hat{\tilde{\theta}}$. From numerous testing results, we believe that the nominal angles should be around 110^0 for iar_a, 170^0 for vcs_a and 195^0 for vcs_c.

(b) Comparison of MUSIC and Dispersive Methods

For small spread α_θ (say, less than 10^0) like that in cfh_a, vcs_b and vcs_d, MUSIC and dispersive methods yield similar performances. Sometimes MUSIC even performs better. Thus, it is not worthwhile to adopt the more complicated dispersive methods in such situations. However, for large α_θ like that in vai_a, vcs_a and vcs_c, dispersive methods perform much better than MUSIC. In fact, for very large spread, MUSIC just cannot give any consistent estimations.

Another observation is that though there is great improvement on the stability of $\hat{\tilde{\theta}}$ by using dispersive methods, the RMSE does not improve by a corresponding amount. We suspect that dispersive methods introduce bias, but it is hard to prove in this project as θ_s are not exact.

(c) Improvement on MUSIC

By using an array with a smaller aperture or a larger K, MUSIC can give a better estimation. For the Vortex system, we believe that K should be set to 1 and use the observed data from the first 8 sensors.

(d) Multiple Signals

We suspected that there were multiple signals present. We tried several methods but were unable to get a better performance for the dispersive methods. For simplicity, we suggest to retaining the assumption that $K = 1$ (thus, $\hat{M}_0 = \hat{m}_0$) for the dispersive methods.

Bibliography

[1] R. O. Schmidt, "Multiple Emitter Location and Signal Parameter Estimation," *IEEE Trans. AP*, vol. 34, pp. 276-280, March, 1986.

[2] Y. Meng, *Estimation of Directions of Arrival of Spatially Dispersed Signals in High Resolution Array Processing*, PhD. thesis, McMaster University, July 1995

[3] A. To, *Estimation of the Directions of Arrival of Spatially Dispersed Signals in Array Signal Processing*, M.Eng. thesis, McMaster University, July 1996